

Title	不均一系触媒を用いた非可食性バイオマス資源からの 化成品原料合成プロセスの開発に関する研究
Author(s)	Jaya, Tuteja
Citation	
Issue Date	2015-06
Type	Thesis or Dissertation
Text version	ETD
URL	http://hdl.handle.net/10119/12983
Rights	
Description	Supervisor:海老谷 幸喜, マテリアルサイエンス研究 科, 博士

***Studies on Development of
Heterogeneous Catalytic System for
Transformations of Inedible Biomass into
Valuable Chemicals***

JAYA TUTEJA

Japan Advanced Institute of Science and Technology

Doctoral Dissertation

***Studies on Development of Heterogeneous
Catalytic System for Transformations of Inedible
Biomass into Valuable Chemicals***

Jaya Tuteja

Supervisor: Prof. Dr. Kohki Ebitani

School of Materials Science

Japan Advanced Institute of Science and Technology

June 2015

Supervisor: Prof. Dr. Kohki Ebitani

Referees: Prof. Dr. Ikko Mikami

Prof. Dr. Noriyoshi Matsumi

Prof. Dr. Kazuaki Matsumura

Prof. Dr. Tatsuo Kaneko

Studies on Development of Heterogeneous Catalytic System for Transformations of Inedible Biomass into Valuable Chemicals

Jaya Tuteja

Ebitani Laboratory, School of Materials Science, JAIST

Introduction

During the last century, the standard of living of our society has been reached to a high level on the cost of utilization of natural fossil resources. Considering the diminishment of these resources, it is imperative to make the transition from non-renewable fossil fuel to renewable biomass resources to meet the future demands. A fundamental challenge in the conversion of biomass into tailor-made fuels is to develop cost effective processes for transformation of the high oxygen content of saccharides. The current biomass conversion methods are dominated by high-temperature pyrolysis and acid-catalyzed dehydration, which leads to difficulty in recovering catalyst from the reaction mixture and pose environmental and health risks. The aforementioned difficulties associated with the previous reports can be alleviated by developing suitable heterogeneous catalytic system for desired chemical transformations.

Results and Discussion

For achieving the goal of shifting the load away from non-renewable sources to biomass resources for sustainable development, the following studies were conducted in this thesis. As sugars comprise the main class of biomass compounds, the selective conversions of sugars to produce furan compounds were carried out over solid acid and base catalysts in one-pot manner in **chapter 2**. The effective synthesis of furans from various saccharides are likely progressed by the aldose-ketose isomerization of sugars over Hydrotalcite (solid base) followed by successive dehydration to furans over Amberlyst-15 (solid acid). Furan compounds are versatile intermediates of biomass based and petroleum based industries. Among them 5-hydroxymethylfurfural (HMF) has received a considerable attention owing to its potential in bio-refinery. Subsequently in **chapter 3**, HMF was selectively transformed into 1,6-hexanediol (HDO) *via* Brønsted acid-catalyzed hydrogenolytic ring opening of HMF by transfer hydrogenation methodology using formic acid (FA). The hydrogenolysis of HMF to HDO supposedly proceeds through 2 key reactions; (1) deoxygenation of furan ring (C-O bond cleavage) (2) hydrogenation of C=O and C=C bond. I found that Pd/ZrP exhibited a significant activity due to the specific Brønsted acidity on ZrP support, which accelerates the cleavage of C-O bond in the furan ring. Further hydrogenation was achieved over Pd metal sites together with the presence of FA as a source of hydrogen instead of high pressured-hydrogen. The produced HDO from renewable resources has immense advantages in polymer industry owing to its terminal hydroxyl groups. The same molecule can be further transformed into other valuable chemicals. One chemical of such immense value is 6-hydroxycaproic acid (HCA) that has potential applications in polycaprolactone production. Accordingly, the selective oxidation of HDO using *N,N*-dimethyldodecylamine *N*-oxide (DDAO) stabilized AuPd bimetallic nanoparticles supported on hydrotalcite as heterogeneous catalyst is demonstrated in basic aqueous media with hydrogen peroxide as oxidizing agent in **chapter 4**. The spectroscopic investigations suggested AuPd interactions to provide negatively charged-Au species, which might be responsible for the excellent catalysis in the selective oxidation of one primary OH group of C6 aliphatic diol, HDO. To substantiate the versatility of Pd/ZrP (catalyst from chapter 2) in catalytic transfer hydrogenation (CTH) reactions, selective hydrogenation of various substituted nitroarenes was investigated over Pd/ZrP in presence of FA as a hydrogen source in **chapter 5**.

Conclusion

In conclusion, new pathways have been developed to produce important industrial commodities directly from inedible biomass-resources employing novel heterogeneous catalytic systems. HDO and HCA like important industrial entities whose synthesis were only dependent on fuel resources can now be produced from biomass in just few steps. Furthermore, a new CTH methodology is developed using bio-based FA as hydrogen source over reusable Pd/ZrP catalyst. The chemoselective, eco-friendly, cost-effective methodology which can work under base-free conditions will lead to a new direction of CTH reactions.

Keywords: Biomass, Heterogeneous Catalysis, Sustainable Chemistry, Analytical Techniques, Organic Transformations.

Preface

During late 18th and early 19th century there was the first “Industrial Revolution” for the transition to new manufacturing process. The transition included the new chemical manufacturing, hand production methods to machines and iron production processes. The second “Industrial Revolution” came in the early 20th century and known as Technological Revolution. The first two “Industrial Revolutions” made people richer, and more urban on the expenses of fossil fuel resources. Now a third “Industrial Revolution” is under way, where the transition is focused on building the future *i.e.* development of “Bio-refineries”. Broadly bio-refineries can be define as: processing industrial material with efficient utilization of renewable products. Concern about the increase in energy demand and non-availability of fossil resources in near future, motivated me to contribute towards the development of bio-refineries.

Catalysis more specifically heterogeneous catalysis is known to play an important role in chemical transformations. This thesis basically focused on investigation of some new strategies for making bio-refineries into commercial reality over novel heterogeneous catalytic systems. The main objective was to make the process practical to large scale, more-economic, sustainable and dependent on renewable energy sources.

This dissertation is submitted for the degree of Doctor of Philosophy at the Japan Advanced Institute of Science and Technology. The research described herein was conducted under the supervision of Prof. Kohki Ebitani in the School of Materials Science. The extent of information derived from the existing literature has been indicated in the dissertation at appropriate places giving the source(s) of information. A brief summary of the doctoral work is appended. It is needless to say that I stand solely responsible for the

errors that might have occurred in this work, despite all precautions taken best to my ability.

Doing PhD research is a challenge, but it also provided opportunities to learn from working with others that would not have been possible otherwise. In particular, there are a number of people without whom this thesis might not have been written, and to whom I am greatly indebted. First, I would like to give all my honors and glory to God, who can sustain me forever and will never abandon me.

Secondly, I would like to express my gratitude to my advisor Prof. Dr. Kohki Ebitani. It has been an honor to be his Ph.D. student. I thank him for his expertise, advice, support, funding and most of all, his patience to make my Ph.D. experience productive and stimulating. He has always been open to my ideas and allowed the freedom for me to try my ideas in the laboratory. I consider it as a great opportunity to do my doctoral research under his guidance and to learn from his research expertise.

In addition to Prof. Ebitani, a special thanks to Asst. Prof. Dr. Shun Nishimura for his valuable guidance and consistent encouragement, I received throughout the research work. This feat was possible only because of the unconditional support provided by him. He has always made himself available to clarify my doubts despite his busy schedules. I am grateful to him for all his help and support.

Next, I would like to say a word of thanks to my colleague and friend Hemant Choudhary, for his valuable input and support throughout the entire doctoral period. I convey my sincere thanks to my lab members Duangta Tongsakul, Pham Anh Son, Kittichai Chaiseeda, Youtarou Ohmi, Naoya Ikeda, Takamasa Takahashi, Saumya Dabraal, Mujahid Mohammad, Jia Jixiang, Ryou Satou, Takuma Shimura, Mahiro Shirotori, Shinpei Fujiwara, Nao Yoshida, Jatin Sharma, Kanishka Gaur, Naoto Ozawa,

Ryosuke Matsuzawa, Kunihiro Mizuhori, Pooja Tomar, Ravi Tomar, Yuuhei Umehara, Syuusuke Miyazaki and Souta Yuuki for their kind cooperation, encouragement, support and especially for their friendly behavior.

Lastly, I would like to thank my family for all their love and encouragement. My mom and dad have played a crucial role in shaping me for who I am today. I would never have gotten as far in my education if it hadn't been for their undying efforts to provide me with the best education possible. I must acknowledge my brothers Amit Tuteja and Joginder Tuteja, Sister in laws Neha Tuli Tuteja and Taruna Mehta Tuteja and nephew Vihaan Tuteja for their unconditional love, support and motivation, I would not have made it this far without them.

June 2015

Jaya Tuteja

Table of Contents

Abstract	III
Preface	V
Chapter 1: General Introduction	1-30
1.1 Renewable energy sources	2
1.2 Availability of Biomass resources	4
1.3 Composition of Biomass	5
1.4 Challenges involved in utilization of biomass	8
1.5 Catalysis for Sustainability	10
1.6 Concept guiding the metal catalysts	12
1.7 Reaction Classes	13
1.8 Outline of this Thesis	19
1.9 References	25
 Chapter 2: One-pot Synthesis of Furans from Various Saccharides using a Combination of Solid Acid and Base Catalysts	 31-54
2.1 Introduction	33
2.2 Experimental section	35
2.2.1 Materials	35
2.2.2 General Procedure for reaction	35
2.3 Results and discussion	37
2.3.1 One-pot synthesis of 2-furaldehyde (furfural) from Arabinose	37
2.3.2 One-pot synthesis of 5-methyl-2-furaldehyde (MF) from rhamnose	41
2.3.3 One-pot synthesis of HMF from lactose	47
2.3.4 One-pot synthesis of furans from sugar mixtures	48
2.4 Conclusions	50
2.5 References	51

Chapter 3: *A Direct and Facile Synthesis of 1,6-Hexanediol from Bio-based HMF over Heterogeneous Pd/ZrP Catalyst using Formic Acid as Hydrogen Source* 55-80

3.1 Introduction	57
3.2 Experimental section	59
3.2.1 Materials	59
3.2.2 Synthesis of ZrP	59
3.2.3 Synthesis of Pd/ZrP	60
3.2.4 Hydrogenolysis of HMF	60
3.2.5 Characterizations	61
3.3 Results and discussion	61
3.3.1 Catalytic Activity	61
3.3.2 XRD of the fresh and used catalyst	71
3.3.3 Proposed Reaction Mechanism	71
3.3.4 Recyclability	73
3.4 Conclusions	75
3.5 References	76

Chapter 4: *Selective Oxidation of Long Chain Aliphatic Diols to mono-Hydroxycarboxylic acid over Reusable Hydrotalcite Supported Capped AuPd Bimetallic Nanoparticle catalysts using H₂O₂ as Oxidant* 81-124

4.1 Introduction	83
4.2 Experimental section	85
4.2.1 Materials	85
4.2.2 Catalyst Preparation	85
4.2.3 Catalyst Testing	86
4.2.4 Isolation of Product	87
4.2.5 Hot Filtration Test	87
4.2.6 Radical Scavenger Test	88
4.2.7 Catalyst Poisoning Test	88
4.2.8 Characterization	88

4.3	Results and discussion	89
4.3.1	Catalytic Activity	89
4.3.2	¹ H- and ¹³ C-NMR of the Product	94
4.3.3	Recyclability	95
4.3.4	UV-Vis Spectroscopy	97
4.3.5	X-ray Photoelectron Spectroscopy	99
4.3.6	X-ray Absorption Spectroscopy	101
4.4	Role of Capping Agent	106
4.4.1	Catalytic Activity	107
4.4.2	Catalyst Characterization	108
4.4.2.1	Transmission Electron Microscopy	108
4.4.2.2	X-ray Diffraction Pattern	109
4.4.2.3	X-ray Absorption Spectroscopy	110
4.5	Proposed Reaction Mechanism	116
4.6	Catalytic Activity of other Aliphatic Diols	118
4.7	Conclusions	118
4.8	References	120

Chapter 5: *Base-free Chemoselective Transfer Hydrogenation of Nitroarenes to Anilines with Formic acid as Hydrogen Source by a Reusable Heterogeneous Pd/ZrP*

Catalyst 125-152

5.1	Introduction	127
5.2	Experimental section	129
5.2.1	Materials	129
5.2.2	Catalyst Preparation	130
5.2.3	Characterizations	131
5.2.4	Catalytic Reactions	131
5.3	Results and discussion	132
5.3.1	Catalytic Activity	132
5.3.2	Time course of the reaction	138
5.3.3	Reusability	138

5.3.4	CTH of substituted nitroarenes	140
5.3.5	Hammett plot	142
5.3.6	XRD and TEM	143
5.3.7	Proposed Reaction Mechanism	145
5.4	Conclusions	147
5.5	References	147
Chapter 6: <i>Summary and Outlook</i>		153-161
6.1	Summary	154
6.2	Contribution to Current Science and Technology	159
6.3	Scope from Thesis	161
<i>Accomplishments</i>		163-166

Chapter 1

General Introduction

1.1 Renewable energy sources

In the last 2-3 decades the use of renewable resources have gained a remarkable attention,^{1,2} in view of the fact that the fossil fuel resources are continuously depleting in the fulfillment of high energy demand^{3,4}. Renewable resource are the natural resources that can renew itself in a sufficient time-frame as compared to its consumption. Biomass, wind energy, hydroelectricity, solar energy, wave power and geothermal energy are some of the popular renewable sources of energy. Gasoline, coal and other things that come from fossil fuels cannot be stated as renewable, as millions of years are required for its production while its consumption rate is quite high. Another problem associated with the usage of fossil sources is global warming, while the renewable resources are very clean. Earlier it was assumed that implication of renewable resources costs higher than the fossil resources for energy production, however recently developed new technology for the renewable sources made the process cheaper. In addition to that the limited resources of fossil fuels makes their use more expensive in today's era.

The concept of utilizing renewable sources is not new, people have been using these from centuries for various purposes, for example wood for construction, building houses and for heat production. Among renewable energy resources, biomass is the only resource that possesses carbon-containing compounds. Carbon is an essential element of our life, it is the fourth element found most abundantly in the universe.^{5,6} If we look around our self the fuels, polymers and all day to day life things are made-up of carbon. Thus, it would not be wrong to say that our lives revolve around carbon.

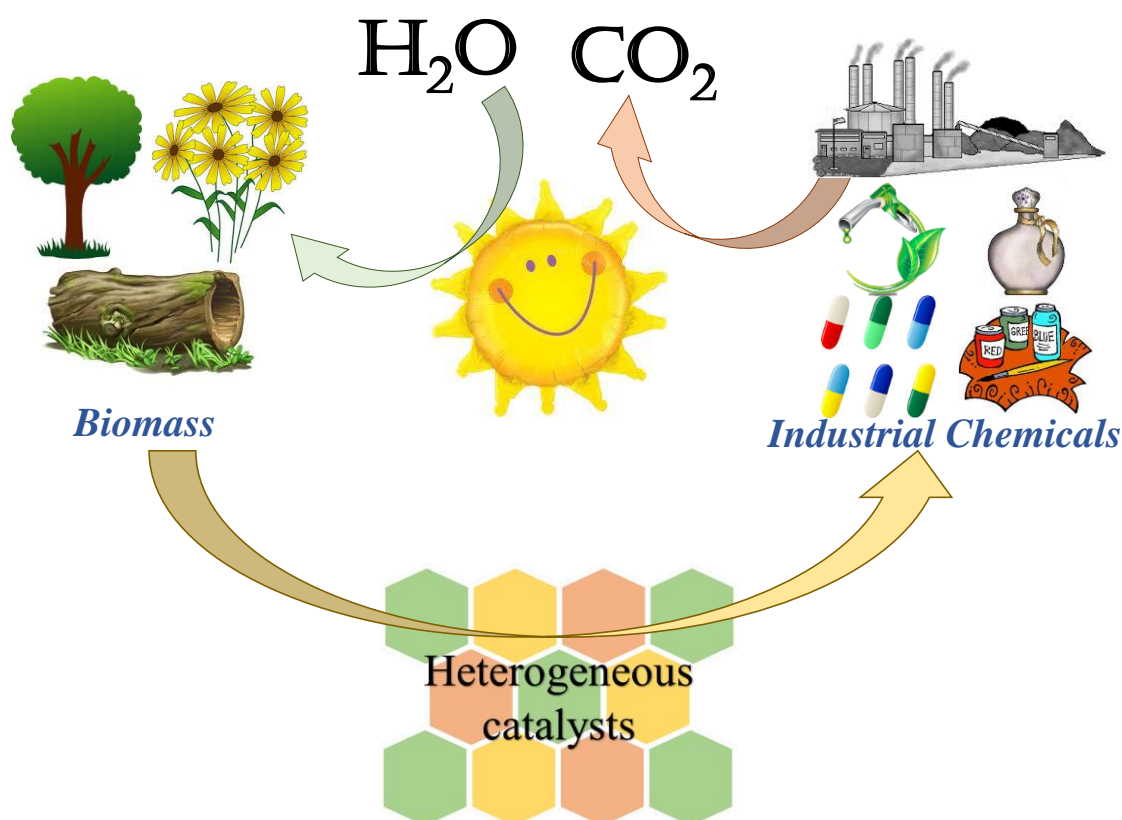


Figure 1: Conversion of biomass resources to Industrial chemicals over heterogeneous catalysts.

Biomass differentiates itself from other resources in terms of chemical bond energy stored in them, and this energy can be used for production of liquid fuels, chemicals along with the generation of heat and electricity.⁷⁻⁹ Biomass can either be directly burn to produce heat and electricity and can be converted chemically to produce biofuels and chemicals. The same biomass if left in nature or buried under earth can be transformed into fossil fuels by anaerobic decomposition of dead trees. The time required for these process in ~650 million years, on the other hand biomass itself is annually renewable.¹⁰ In addition of being renewable, biomass presents a carbon-neutral concept. Burning coal and other fossil fuels in the main cause of CO_2 emission and other pollutants. In contrast plant burning also produce CO_2 , but during biomass regrowth the CO_2 from atmosphere is converted into nutrition and energy *via* photosynthesis (Figure 1).^{11,12}

From the above discussion it is clear that the biomass has the potential to serve as an alternate energy resources to replace fossil fuels. Of the leading alternative energy sources biomass is the most cost-effective, reliable and practical strategy. Thus the sustainable development is the need of an hour and a great challenge for mankind nowadays and, the most efficient way for the utilization of these biomass resources is to produce petroleum compounds. It is strongly desirable to utilize inedible biomass (lignocellulosic) to avoid conflict with food supply chain for human and animals.

1.2 Availability of Biomass resources

Throughout the world, bio-energy (burning wood, fuel from crop residues) is the biggest source of renewable energy. It can be cultivated or produce anywhere on small or large area. In recent years various researchers have demonstrated processes to produce fuels and chemicals from inedible-biomass.¹³⁻¹⁵ Before considering the potential of biomass to substitute fossil fuel, it is important to know about the availability of these resources. It is estimated that worldwide forests constitutes 30% of land area¹⁶ or the earth has 1800 billion tons of the biomass on ground¹⁷. However, all these cannot be utilized for energy production as some part is used as food and other things which are essential for living being. Therefore, it is important to estimate the amount of biomass resources (waste biomass) that can be utilized. The major contribution in waste biomass is of forestry residues, which is approximately 22 EJ (Exa Joules, 10^{18} Joules) on worldwide basis. 15 EJ is obtained from agricultural waste biomass and livestock biomass contributes 5.4 EJ.

Biomass currently represents 14% the world's final energy consumption.⁹ United States (US) alone can produce one third of its total energy consumption from lignocellulosic biomass.^{18,19} In 2000, in the US almost 50% of the total energy provided

by renewable sources, was produced from the biomass, and now biomass is providing more than twice of any other renewable source.

1.3 Composition of Biomass

Broadly lignocellulosic biomass can be classified into five main categories, which are cellulose, hemicellulose, lignin, starch and others (**Figure 2**).²⁰⁻²² The composition of biomass is very vast, a wide variety of biomass is available composing of wood from forestry residues, dead trees and branches, other sources include plant and animal materials, animal wastes, municipality solid waste, agricultural residues, food processing wastes etc.²³ From the perspective of energy lignocellulosic biomass consisting of cellulose and hemicellulose represents the great potential. Because of the diversity in the chemical structure of the components the reactivity is also different. The detailed description about the chemical structure of lignocellulose components is described here:

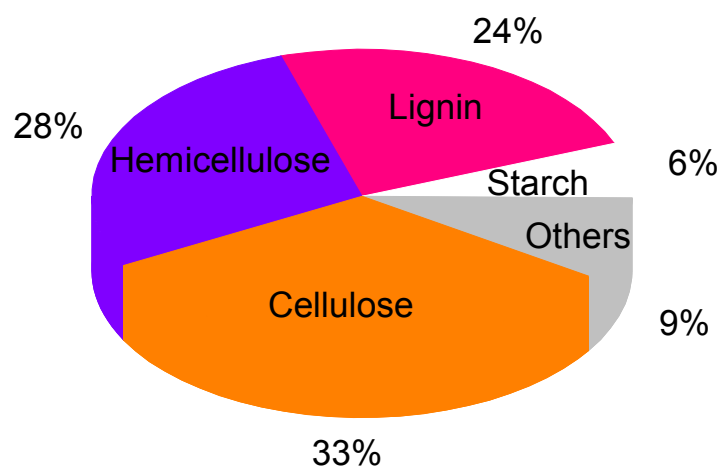


Figure 2: Composition of Biomass.

Typical Components of lignocellulosic Biomass:

- (a) **Cellulose:** It is the major component of rigid cell walls in plants. It contains a long chain of linked glucose units firmly bound by β -glycosidic linkage (**Figure 3**).

Cellulose is a polysaccharide consisting 30,000 glucose units, very crystalline and resistant to acid and alkali reagents.

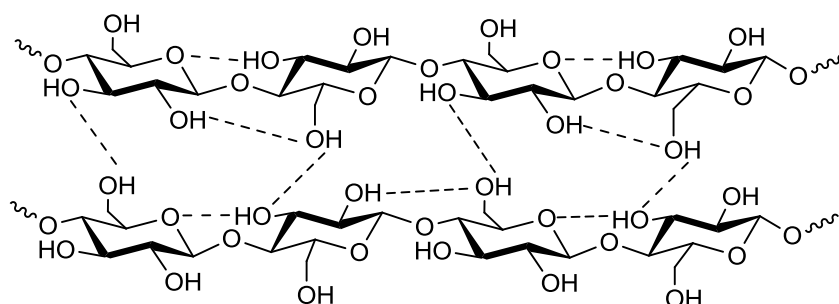


Figure 3: Molecular structure of cellulose.

(b) Hemicellulose: Polysaccharide of 5-carbon unit such as xylose, arabinose and 6-carbon unit including glucose, mannose and galactose is called as hemicellulose. It is easier to break hemicellulose unit than cellulose because its degree of polymerization is less than that of cellulose. Hemicellulose is also known as polyose and found in plant cell walls. A very common hemicellulose is xylan consisting of β 1-4 linkage of 5-carbon sugars xylose and arabinose (**Figure 4**).

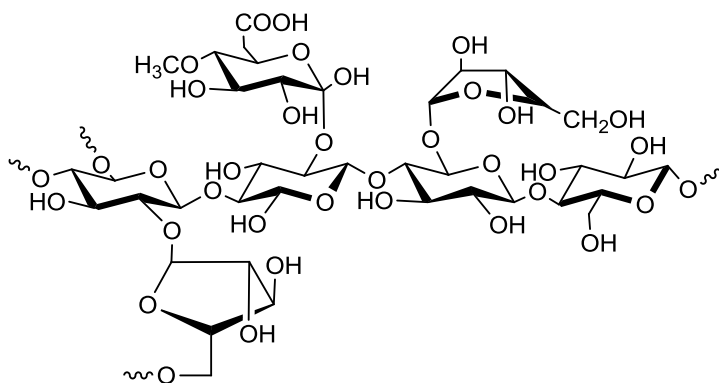


Figure 4: Molecular structure of hemicellulose.

(c) Lignin: Lignin is a complex polymer whose units are phenylpropane and its derivatives bonded 3-dimensionally (**Figure 5**). It is the most abundant and naturally found polymer which do not consist any carbohydrate unit. Lignin

is the only source of aromatic compounds from biomass. It is found in secondary cell walls of plant or in algae.

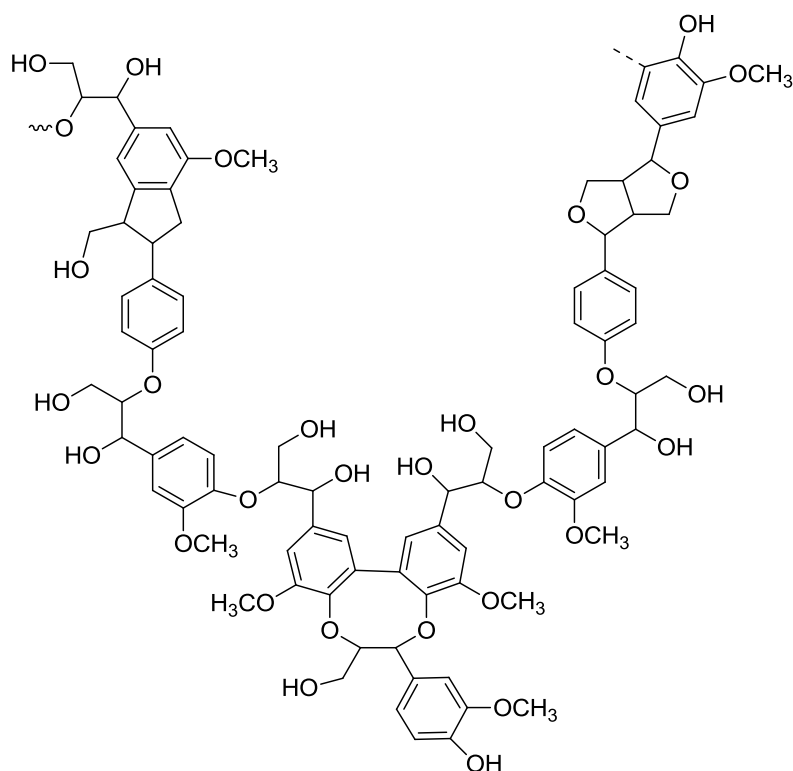


Figure 5: Molecular structure of lignin.

- (d) **Starch:** A naturally abundant polymer obtained from biomass consisting of large number of glucose units like cellulose. In starch the glucose units are bound by α -glycosidic bonds unlike to cellulose (**Figure 6**). Starch is important, as it has a very high value as food and found in potatoes, roots, stems, corn and wheat etc.

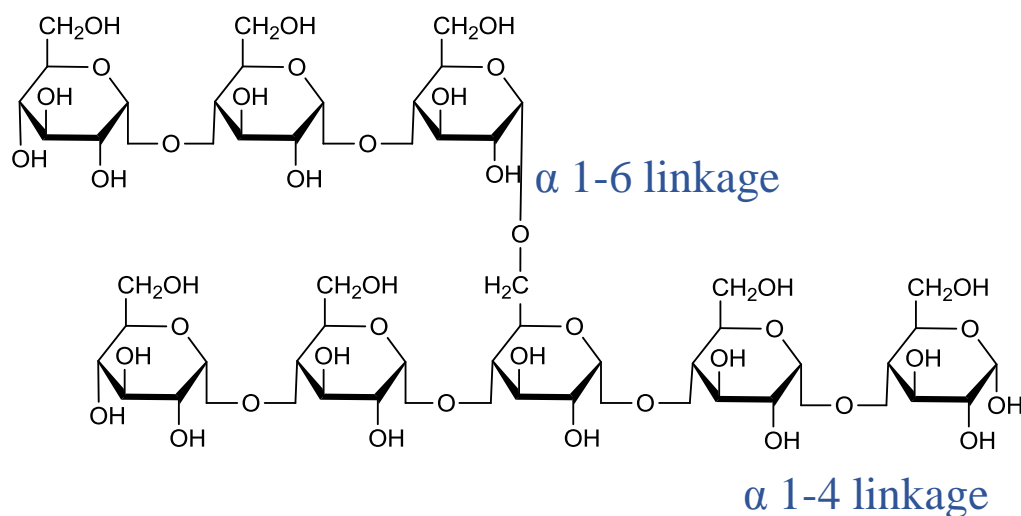


Figure 6: Molecular structure of starch.

(e) **Others:** Valuable organic and inorganic components present in biomass can be broadly classified as others. The organic component with high value includes glycerides, alkaloids, terpenes and waxes. Biomass also comprises inorganic substances in trace amounts including Ca, K, P, Mg, Si, Al, Ni, Fe and Na.

1.4 Challenges involved in utilization of biomass

The substitution of biomass in replacement of petroleum, demands development of number of approaches as both opposed each other in terms of chemical structure. Petroleum is comprised of hydrocarbons while biomass feedstock possess highly oxygenated compounds embedded in polymeric structure (**Figure 7**). Thus, some of the catalytic approaches that were previously developed for petroleum resources cannot be applied for biomass resources. For instance the conversion of biomass into fuels requires intense chemical changes and processing, on other side petrochemical industry involves separation of hydrocarbons by fractional distillation.

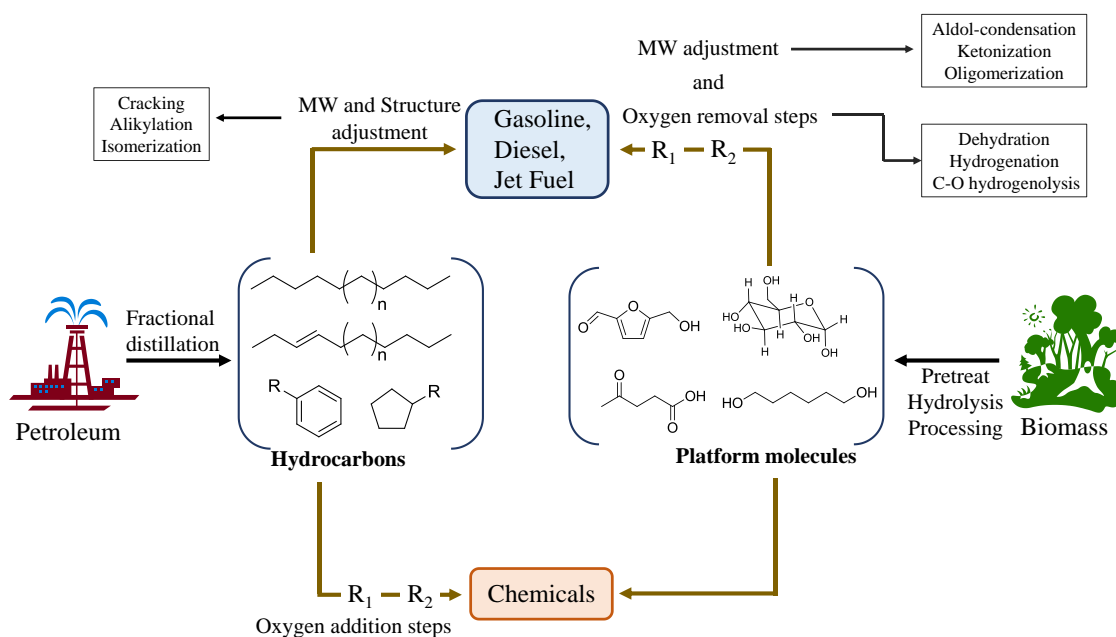


Figure 7: Divergence between biomass and petroleum resources.

The difficulty in the effective utilization of inedible lignocellulosic biomass is its structural and chemical complexities that can be resolved by converting them into smaller fractions. In other words the decomposition of complex polymers to its monomer (sugars) units employing various physical techniques such as milling, grinding, separation etc. The choice of material depending on its demand, availability and cost of transformation also plays a significant role. For example, the high crystallinity and rigidity of cellulose makes its depolymerization difficult and costlier than that of hemicellulose. As owing to heterogeneity in structure of hemicellulose, it can easily undergo chemical treatment comprising of hydrolysis, hydrogenation, deoxygenation, combustion, hydrothermal reaction and pyrolysis to construct new platform molecule. Cellulose can also undergo depolymerization over cellulase enzyme with high yield but high cost of enzyme comes in a way to low value glucose production.

1.5 Catalysis for Sustainability

Catalysis or more precisely heterogeneous catalysis serves as the best solution to effectively transform biomass (raw materials) to desirable fuels and chemicals (valuable products) (**Figure 8**). Designing heterogeneous catalysts for chemical production from carbohydrates offers new challenges in development of catalyst technology. Till date fine and specialty chemical market is dependent on homogeneous or biocatalyst system for conversion of substrates having multiple reactive groups. However the cost, separation issues and limitation with temperature constrain their use in production of chemicals from biorenewable feedstock.



Figure 8: The importance of catalysis.

There are well established heterogeneous catalytic system for hydrocarbon feedstock such as selective hydrogenation, isomerization, reforming etc. However, solid catalysts for dehydration, hydrogenolysis, decarboxylation etc. are not yet developed for converting bio-based product to desirable products. On account of having a range of functionality in biorenewable feedstock, controlled reactivity is a difficult task to achieve. Thus, for the sustainable development new approaches for designing of catalysts are required for the controlled transformation of biomass-derived molecules to direct desired products.

The other challenge involves with the use of biomass-derived compounds is the low volatility at relative low reaction temperatures. This particular property necessitates the development of condensed phase system in comparison to current gas-phase system which is currently used for hydrocarbon processing. Thus, these liquid-solid phase system offered new opportunities for designing new catalytic material with stability and high transport properties.

Synthesis of chemicals rather hydrocarbons from biomass has gained considerable attention, as it reduces the efforts involved in lengthy process of deoxygenation. High oxygenated bio-based products such as acetic acid, glyceric acid, glycerol etc. are the chemicals which can be produced more efficiently from biomass than fossil fuels. Recently, a small group of biomass-derived molecules has been identified as platform molecule or building block, they contains multiple functionality and are suitable for a range of chemical transformation. The molecules are sugars (glucose, xylose), furans (5-hydroxymethyl furfural, furfural), acids (levulinic acid, lactic acid) and alcohols (ethanol, 1,6-hexanediol) etc.

The production of these chemicals *via* catalytic conversion of biomass and its derivatives has been a subject of interest in recent years. A variety of review articles has been published during last decade focusing carbohydrates,^{24,25} cellulose,²⁶⁻²⁸ 5-hydroxymethylfurfural,²⁹⁻³¹ glycerol,³²⁻³⁵ hemicellulose^{36,37} as feedstock. The catalytic reactions for conversion of these feedstock are hydrogenation,³⁸ dehydrogenation,³⁹ oxidation,⁴⁰ dehydroxylation,^{41,42} and reforming as well as acid/base catalysts for dehydration,^{43,44} reactions. The choice of feedstock, catalyst design and type of reaction can be made by targeting which chemical we want to produce.

1.6 Concept guiding the metal catalysts

For sustainable industrial production of chemicals over metal supported catalyst, it is imperative that metal should not leach into the solution due to chelating properties of reactants or products. Achieving high selectivity of desired product is also most important criteria to be considered from the viewpoint of atom economy of the reaction. The selectivity can be tuned by introducing another metal: the second metal can be alloyed or can be ad-atoms on the surface of preliminary metal. The use of bimetallic catalyst can also boost up the activity to very high in addition of high selectivity.

In hydrogenolysis reactions, metal catalyzed reactions can lead to rupturing of C-C bond with C-O at various positions. That will ultimately result in multiple of by-products formation. From the literature view it can be judged that control reactivity or selectivity is attained by the choice of metal and support. Efficient catalysts must meet the requirements of high activity, selectivity and stability. Lots of studies have been conducted on achieving high activity and selectivity but long term stability, which is very important for industrial use of these catalyst is still neglected. For example oxidation reactions generally resulted in the deactivation of catalysts by over oxidation of metal surface or deposition of reactant or product molecule on the active sites of catalyst. These are the serious issues which should be considered during oxidation reactions. The improvement which have been done to solve this issue is: the incorporation of non-active oxophilic metal (e.g.: Bi, Pb) as co-promoter. Still the influence of second metal, internal structure of bimetal etc. are the facts which are needed to be considered.

1.7 Reaction Classes

From the above discussion, it can be seen that biomass derived compounds can take many forms, thus it will be worth to define the range of chemicals to be discussed in the subsequent chapters and the main reactions that would be required in these strategies.

- 1. Hydrolysis:** Lignocellulosic biomass being renewable, abundance in nature and non-competitiveness with food crops presents an attractive and sustainable resource for chemical production. The chemical process for converting these biopolymers into sugars is known as hydrolysis (**Figure 9**). The hydrolysis can be carried out using acid or base catalysts depending on the polysaccharide's nature. Acid hydrolysis is preferred over base hydrolysis as it leads to lower yields due to side reactions. The acid hydrolysis have the advantage of breaking down the cellulose and hemicellulose into individual sugar units. Variety of concentrated and dilute acids have been used previously among which H_2SO_4 and HCl were noticed to be typical acids for this reaction.⁴⁵ However, use of these acid catalysts in large amount suffers from reactor corrosion, waste generation and catalyst recovery.^{46,47}

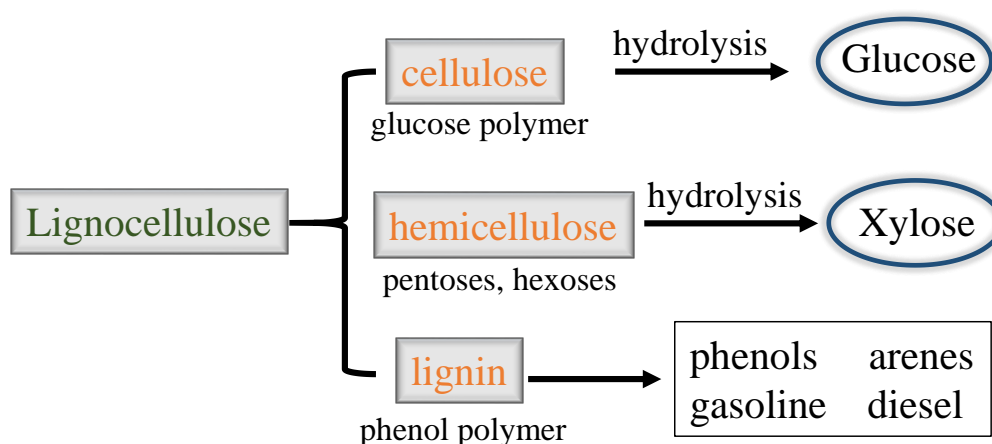


Figure 9: Scheme of hydrolysis of lignocellulose.

In this regard, the area of interest shifted to develop solid catalysts owing to its advantages with recyclability, product separation and less damage to reactor system. Numerous reports have been published since then on the transformation of cellulose over solid acid catalysts.⁴⁸⁻⁵² Similarly, hydrolysis of hemicellulose can be achieved over same solid acid catalyst with moderate temperature to obtain xylose. The obtained sugars molecule can now be subjected to the formation of desired chemicals *via* further chemical treatments.

- 2. Dehydration:** The well-known as well as an important reaction which sugars are likely to undergo is the dehydration or cyclodehydration to form furan compounds. For instance, 5-hydroxymethylfurfural (HMF) from glucose, galactose, lactose and furfural from xylose and arabinose etc. These furan compounds have immense importance in themselves and can be upgraded to various other molecules to obtain liquid fuel additives (by aqueous phase hydrogenation and aldol condensation reactions) (**Figure 10**). Other applications include, industrial solvent *via* hydrogenation of furan compounds (tetrahydrofuran, tetrahydrofurfuryl alcohol, furfural), polymer precursor *via* oxidation of HMF to 2,5-furandicarboxylic acid (FDCA) (**Figure 4**).

One could have think that the synthesis of furans is very simple, but it has been reported by many individual scientists that chemistry of furans from sugars is very complex. For example, HMF decomposes to give levulinic acid and polymerizes to produce humin, which ultimately leads to decrease in HMF yield. Generally four groups of products formed during the course of this reaction, the groups are isomerization, dehydration, fragmentation and condensation. Van Dam⁵³ and Cottier⁵⁴ have demonstrated that total of 37 products formed from

sugar decomposition in aqueous and non-aqueous solvents. It was also noticed that the polymerization can be occurred in both aqueous and non-aqueous media, while degradation is more favored in aqueous medium. The furans synthesis is more efficient and faster from ketoses as compared to aldose sugars. Despite, glucose is the first choice of industry for HMF due to its low price.

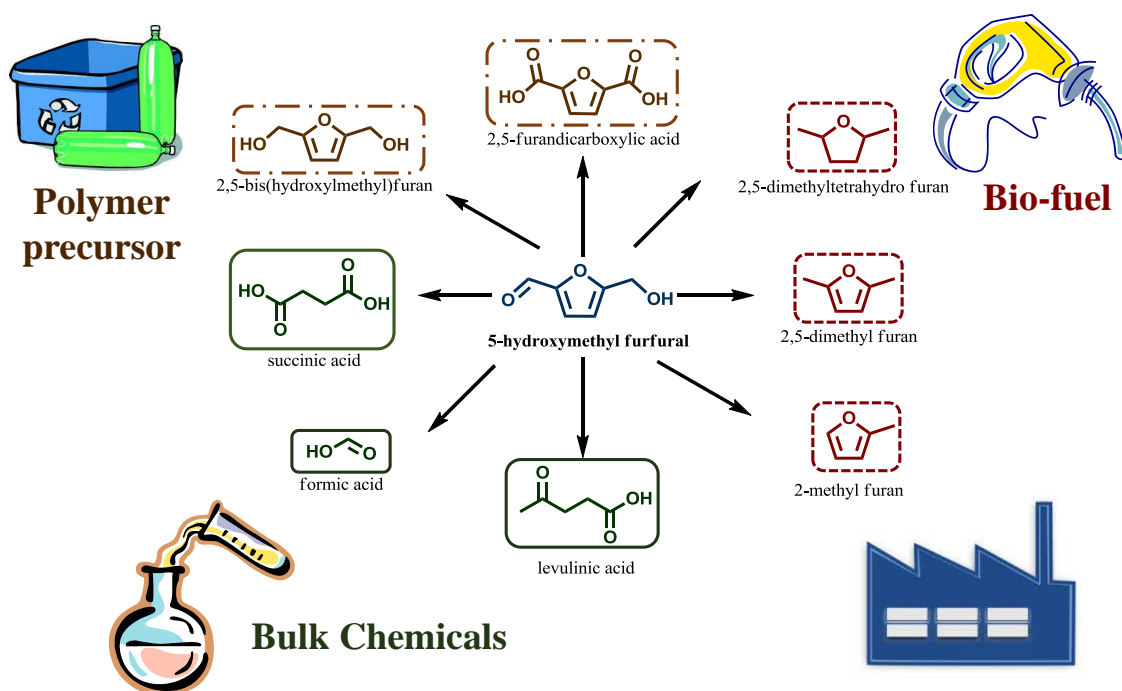


Figure 10: HMF a platform molecule.

Direct transformation of glucose to HMF is difficult because the isomerization of glucose to fructose is hard over acid catalysis and leads to the formation of oligomers. Dehydration of sugars has been reported in water, organic solvents, bi-phasic solvents^{55,56} and ionic liquids⁵⁷⁻⁵⁹ over a different range of catalysts including mineral acids, oxalic acid, solid acids, zeolites and ion-exchange catalysts.

3. Hydrogenolysis: The cleavage of C-C and C-O bond in the presence of hydrogen is called as hydrogenolysis. It is generally carried out at high temperatures around 400-500 K with high pressure of hydrogen gas (14-300 bar) over transitional metal based supported catalysts under basic conditions.⁶⁰⁻⁶³ The purpose of hydrogenolysis or cleavage of C-C and C-O bond is to remove oxygen from highly oxygenated species to produce polyols or diols, which have tremendous importance in polymer industries.

Hydrogenolysis of glycerol (by-product of biodiesel) has gained a considerable attention. Depending on the choice of metal catalysts and reaction conditions, the hydrogenolysis of glycerol can lead to formation of one among multiple precursors, such as acetaldehyde, acetol, 1,3-propanediol, 1,2-propanediol, ethylene glycol, propanol, ethanol, 3-hydroxypropionaldehyde etc as shown in **Figure 11**. In addition to glycerol the hydrogenolysis reaction plays an important role for the direct production of polyol or diol from furan compounds. For example hydrogenolysis followed by hydrogenation can form 1,5- or 1,2-pentanediol from furfural^{64,65} (**Figure 12**).

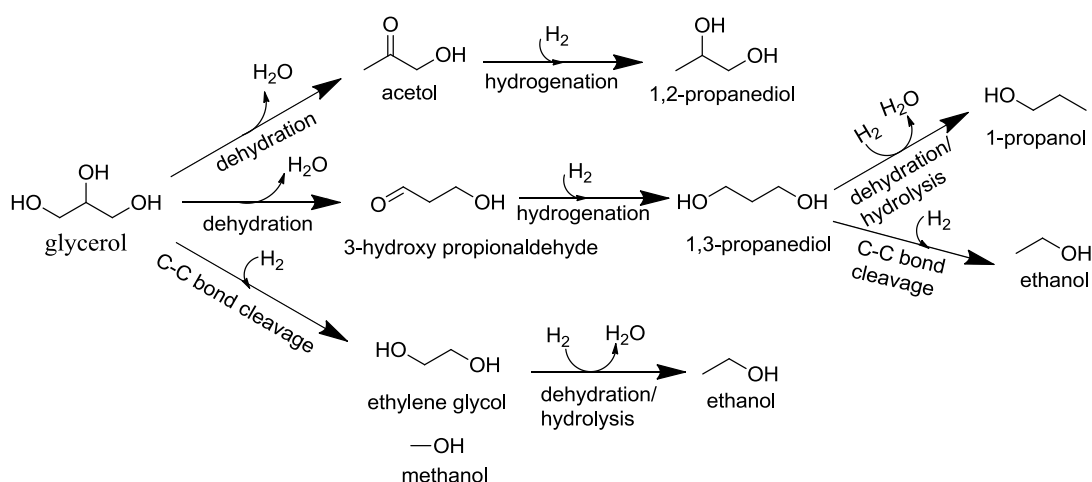


Figure 11: Reaction pathways for glycerol hydrogenolysis.

4. Hydrogenation: To saturate C-O-C, C=C and C=O bonds with hydrogen over catalysts is termed as hydrogenation reactions. Hydrogenation occurs in the presence of metal catalysts (Pt, Pd, Ru, Ni, Cu) with pressure of hydrogen gas at moderate temperature range of 370-420 K. The hydrogenation of C=C bond can transform the biomass obtained from furan compounds to important chemical entities such as tetrahydrofuran (**Figure 12**) which further can be transformed by aldol condensation to produce diesel fuel component. Further the C=O bond hydrogenation of furans leads to furfuryl alcohol⁶⁶, 2,5-bis-hydroxymethyl furan⁶⁷, 2,5-dimethylfuran⁶⁸.

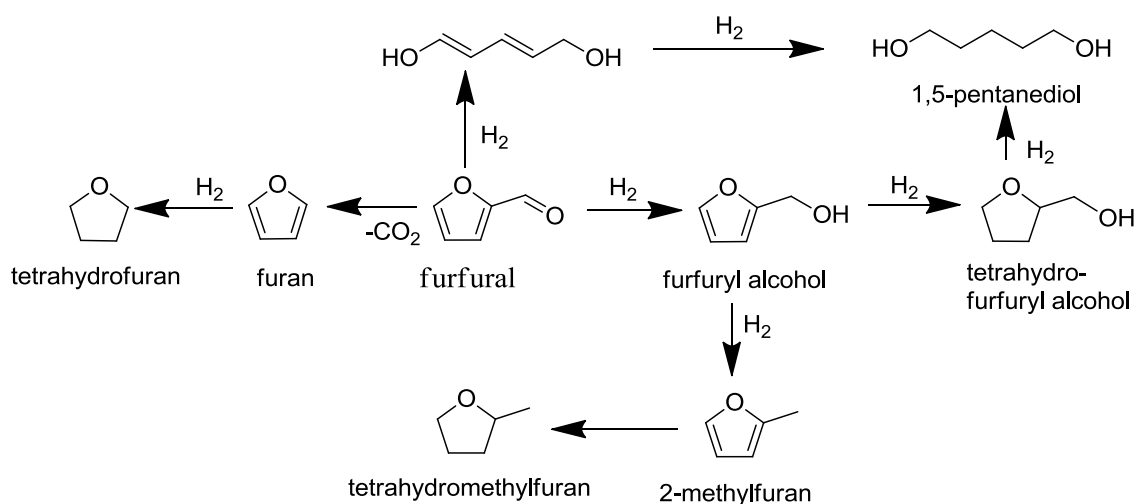


Figure 12: Hydrogenation of furfural.

Currently, the research has been aimed to produce furfuryl alcohol from selective conversion of furfural. The particular reaction has been carried out over copper chromite catalyst previously, but now there is a need to find effect and environmentally benign catalyst to selectively hydrogenate C=O bond retaining C=C bond. Variety of factors are there which decides the selectivity of hydrogenation, some of these factors are: nature of catalyst, solvent, pressure of hydrogen gas,

temperature. Solvent can influence the adsorption-desorption properties of substrate to the catalyst.

5. Selective oxidation: The selective oxidation of biomass is the reaction which is generally conducted to produce chemical intermediates possessing specific functionalities (**Figure 13**). The challenge for the selective oxidation reaction is to control the oxidation or direct the reaction pathways towards desired product as the oxidation reaction can lead to multiple products. The reaction is carried out in the presence of metal oxides, metal hydroxides, transition metal supported catalysts and metal derivatives such as potassium dichromate, vanadyl phosphate etc. using aqueous or organic solvents with either in the presence of oxygen pressure or oxygen flow at 330-420 K. The nature of catalyst, type of solvent, pH, oxygen pressure and temperature influences the formation of product in oxidation reaction.

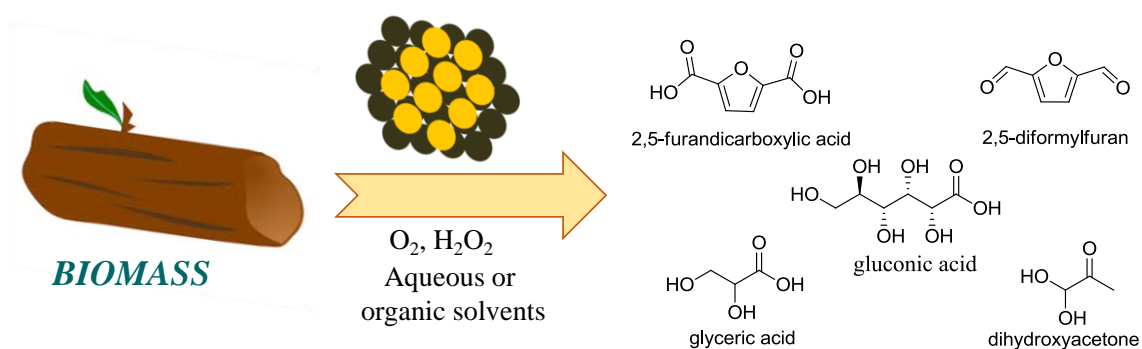


Figure 13: Selective oxidation of biomass to produce special chemicals.

For example basic condition and low temperature leads to the formation of 2,5-furandicarboxylic acid (FDCA) from the oxidation of HMF^{69,70} while neutral pH and high temperature forms 2,5-diformylfuran (DFF)⁷¹. Similarly oxidation of primary or secondary alcohol group of glycerol can be controlled by

maintaining *pH*. Acidic conditions favors the oxidation of secondary alcohol group leading to dihydroxyacetone (DHA)^{72,73} while basic conditions selectively oxidizes primary alcohol group and forms glyceric acid⁷⁴⁻⁷⁶ as main product. Recently, bimetallic catalysts such as Au-Pd and Au-Pt are experienced to be more active than monometallic (Au, Pd and Pt) catalysts for glycerol oxidation reactions.⁷⁷ It was seen that synergism between bimetals was crucial to achieve high catalysis.

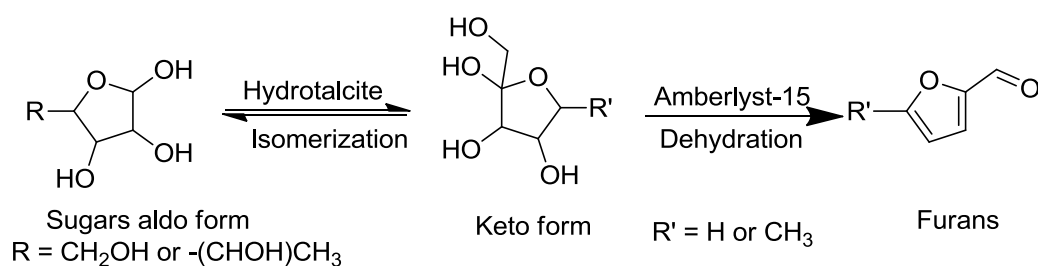
Another important oxidation reaction of biomass is oxidation of sugars to corresponding sugar acids over Au metal nanoparticles (NPs) based heterogeneous catalysts. Au NPs based catalysts were chosen over Pd or Pt NPs based catalysts due to their high activity and selectivity for synthesis of sugar acids. The particle size effect, influence of preparation method and stability has been studied intensively.⁷⁸

1.8 Outline of this Thesis

In this section, I will be discussing on the process development and catalytic concepts for the selective transformation of biomass-derived carbohydrates into value-added commodities. Comprehensively, I would like to show that the fundamental concepts on chemical and controlled process conditions can lead to strategies for desired reaction pathways for production of special chemicals from highly-oxygenated biomass feedstock in good yields.

- 1. Conversion of Saccharides into furans:** Although numerous combinations of catalysts and solvent are there to produce furan derivatives from renewable feedstock, however a single system having ability to efficiently convert aldo-

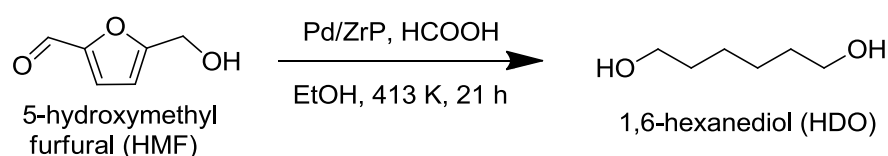
hexose, pentoses, disaccharides and multiple of sugars together in a single pot to produce furan derivatives is still lacking. Here, in Chapter 2 synthesis of furan derivatives such as furfural, 5-hydroxymethylfurfural (HMF), 5-methylfurfural (MF) was carried out from direct conversion of aldo-sugars using Mg-Al Hydrotalcite (HT) and Amberlyst-15 as solid base and acid catalysts respectively in one-pot (**Scheme 1**). Survey of previous reports have demonstrated the furans formation from the acid catalyzed derivation of ketoses is much more selective than from aldoses. Thus furans from aldoses which are component of lignocellulosic biomass seems much more difficult. In the present case HT acts as a solid base catalysts for isomerization of aldoses to ketoses followed by dehydration with Amberlyst-15 as solid acid catalyst. For the realization of the system for all kinds of saccharides, conversion of disachharides and mixture of aldo-hexoses, aldo-pentoses and disaccharides were also carried out to achieve appreciable yields of furans.



Scheme 1: Synthesis of Furans from sugars.

2. Hydrogenolysis of HMF to HDO: 5-Hydroxymethylfurfural (HMF), dehydration product of hexoses, is one of the most promising platform chemicals in the biorefinery, and it is called as “*sleeping giant*” in the field of intermediate chemicals derived from renewable sources. Herein Chapter 3, I reported the new

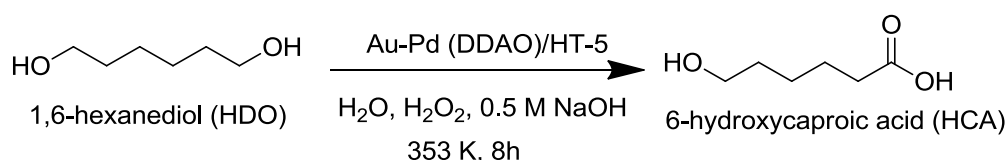
approach for the production of 1,6-hexanediol (HDO, a linear-diol with two primary hydroxyl groups) by a hydrogenolytic ring opening reaction of HMF (**Scheme 2**).⁷⁹ HDO is extensively used in the production of polyesters for polyurethane elastomers, coatings, adhesives and polymeric plasticizers. For the transformation of HMF to HDO what I need to do is: a) the ring hydrogenolysis to obtain open chain compound followed by b) hydrogenation of open chain unsaturated compound. Literature survey highlighted the role of Brønsted acid sites for C-O bond hydrogenolysis. Thus, various Brønsted and/or Lewis acidic supports were screened for the efficient ring opening of HMF to HDO among which Pd/ZrP exhibited a significant activity due to the specific Brønsted acidity on ZrP support, which accelerates the cleavage of C-O bond in the furan ring. For hydrogenation, formic acid (FA, HCOOH) was used as a cheap, safe and high potential hydrogen donor in comparison with high-pressured H₂, the latter is difficult to handle and requires an expensive facility.



Scheme 2: Hydrogenolysis of HMF to HDO.

- 3. Selective oxidation of HDO to HCA:** After the successful completion of HDO synthesis from renewable feedstock, the studies were further carried out for the selectively oxidation of HDO to 6-hydroxycaproic acid (HCA, **Scheme 3**) in Chapter 4. Poly-condensation of HCA under reduced pressure can leads to the synthesis of industrially valuable polycaprolactone (PCL). This particular method is not generally used for PCL production as HCA is scarcely available and

expensive and is generally synthesized from caprolactone *via* ring opening polymerization (ROP). Disadvantage of using ROP is: it requires catalyst and harsh conditions while production of PCL from 6-HCA is quite simple and requires only reduced pressure.



Scheme 3: Selective oxidation of HDO to HCA.

The obstacle of HCA synthesis can be removed by its production from selective oxidation of bio-HDO. If we look in the literature for selective oxidation of aliphatic diol system, we will find that there are multiple publications on selective oxidation of C2-C5- diol system, but hardly any report could be found on C6 system. So the question arises why? It is because as the carbon chain length increases between two primary hydroxyl groups the selective oxidation becomes difficult and chances of formation of diacid product is major. Therefore to solve this problem, a novel heterogeneous catalyst is developed based on AuPd bimetallic nanoparticles (NPs) using *N,N*-dodecyltrimethylamine *N*-oxide as capping agent. For controlled oxidation aqueous hydrogen peroxide was used as greener oxidant in basic aqueous medium. The details of catalyst characterization and optimization of reaction conditions have been discussed in detail in Chapter 4.

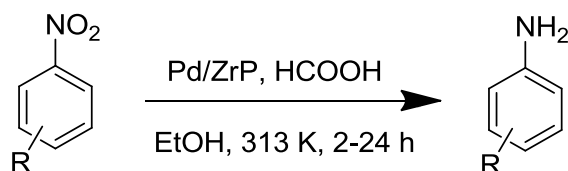
4. Catalytic transfer hydrogenation using biomass-based formic acid: Amines are of immense importance; as the amine group serves as a site for further

derivatization. Specially the aromatic amines *i.e.* anilines which have found their immense importance in synthesis of dyes, pigments, agrochemicals, pharmaceuticals and fine chemicals. Till date the hydrogenation of nitro aromatic compounds to anilines is either dependent on high pressure H_2 or the base promoted transfer hydrogenation using liquid hydrogen sources.

Catalytic transfer hydrogenation (CTH) reactions have tremendous importance over traditional hydrogenations using molecular hydrogen. As they requires special gas handling auxiliaries under pressurized conditions, moreover the highly diffusible gas is easily ignited and presents considerable hazard. In this point of view, formic acid (FA, $HCOOH$), which is known as safe, cheap and high potential hydrogen donor for CTH, is an inexpensive and practical alternative for high-pressured H_2 . FA can be traditionally obtained from biomass processing and it produces only CO_2 as co-product. Since, no special venting, elaborate apparatus are required; these advantages bring significant cost savings and flexibility of operations. Transition metals such as Pd are most often used for transfer hydrogenation reactions.

Literature survey and my own experience with Pd/ZrP catalyst suggested that presence of Brønsted acid played a crucial role for hydrogenation reactions. It was seen that Pd/ZrP catalyzes the transition hydrogenation under base-free conditions. Thus to further investigate the ability of Pd supported ZrP in CTH reactions the well-known industrially important CTH of nitro aromatic compounds was studied in Chapter 5 (**Scheme 4**). In addition selective hydrogenation of nitro group was achieved in the presence of other reducing groups such as $-C=C$, $-C\equiv N$ and $-COOCH_3$. To investigate the reaction

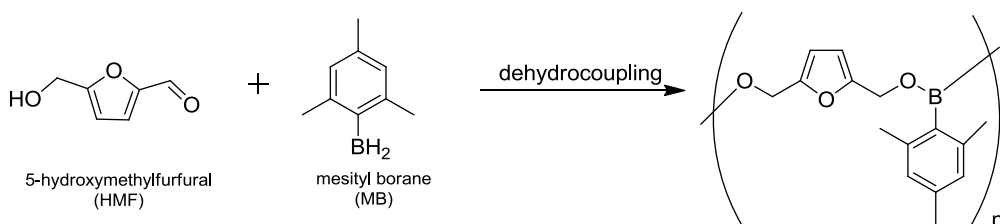
mechanism, Hammett plot was obtained for CTH of *p*-substituted nitroarenes. A negative ρ value in the Hammett plot indicates that this reaction proceeded via cationic intermediate.



Scheme 4: Reduction of various nitroarenes to anilines.

In last chapter *i.e.* Chapter 6, some concluding remarks have been given based on the preceding chapter's achievements. This chapter also includes possible contributions of this work to catalytic science and technology and scope from the present thesis.

In appendix (minor research theme), a series of novel organoboron polymer electrolytes are prepared by dehydrocoupling of 5-hydroxymethylfurfural (HMF) with mesitylborane (MB) and subsequent anion exchange reaction with LiTFSI [lithium bis(trifluoromethylsulfonyl)imide]. The ion conductive properties and lithium ion transference number of various polymer unit compositions have been studied in detail to check its applicability as solid polymer electrolyte in lithium ion secondary batteries.



Scheme 5: Dehydrocoupling of HMF with mesitylborane.

1.9 References

1. A. J. Ragauskas, C. K. Williams, B. H. Davison, G. Britovsek, J. Cairney, C. A. Eckert, W. J. Frederick Jr., J. P. Hallett, D. J. Leak, C. L. Liotta, J. R. Mielenz, R. Murphy, R. Templer and T. Tschaplinski, *Science*, **2006**, *311*, 484-489.
2. C. H. Christensen, J. Rass-Hansen, C. C. Marsden, E. Taarning and K. Egeblad, *ChemSusChem*, **2008**, *1*, 283-289.
3. G. A. Olah, G. K. S. Prakash and A. Goepfert, *J. Am. Chem. Soc.*, **2011**, *133*, 12881-12898.
4. G. A. Olah, *Angew. Chem. Int. Ed.*, **2013**, *52*, 104-107.
5. P. Levi, *The Periodic Table*, Schocken Books, New York, **1984**.
6. E. Roston, *The Carbon Age: How Life's Core Element Has Become Civilization's Greatest Threat*, Walker & Company, New York, **2008**.
7. A. Corma, S. Iborra and A. Velty, *Chem. Rev.*, **2007**, *107*, 2411-2502.
8. Y. Romàn-Leshkov, C. J. Barret, Z. Y. Liu and J. A. Dumesic, *Nature*, **2007**, *447*, 982-986.
9. G.W. Huber, J. N. Chheda, C. J. Barret and J. A. Dumesic, *Science*, **2005**, *308*, 1446-1450. (d) M. Stöcker, *Angew. Chem. Int. Ed.*, **2008**, *47*, 9200-9211.
10. P. N. R. Vennestørn, C. M. Osmundsen, C. H. Christensen and E. Taarning, *Angew Chem. Int. Ed.*, **2011**, *50*, 10502-10509.
11. O. Inderwildi and D. King, *Energy Environ. Sci.*, **2009**, *2*, 343-346.
12. A. M. Ruppert, K. Weinberg and R. Palkovits, *Angew. Chem. Int. Ed.*, **2012**, *51*, 2564-2601.
13. G. W. Huber, S. Iborra and A. Corma, *Chem. Rev.*, **2006**, *106*, 4044-4098.

14. J. N. Chheda, G. W. Huber and J. A. Dumesic, *Angew. Chem. Int. Ed.*, **2007**, *46*, 7164-7183.
15. J.-P. Lange, R. Price, P. M. Ayoub, J. Louis, L. Petrus, L. Clarke and H. Gosselink, *Angew. Chem. Int. Ed.*, **2010**, *49*, 4479-4483.
16. Asian Biomass Handbook; Part 2: Biomass Resources.
17. M. Parikka, *Biomass and Bioenergy*, **2004**, *27*, 613-620.
18. Special issue on Sustainability and Energy, *Science*, **2007**, *315*, 781.
19. F. W. Lichtenthaler, *Acc. Chem. Res.*, **2002**, *35*, 728-737.
20. R. Rinaldi and F. Schuth, *ChemSusChem*, **2009**, *2*, 1096-1107.
21. J. C. Serrano-Ruiz and J. A. Dumesic, *Energy Environ. Sci.*, **2011**, *4*, 83-99.
22. M. Stöcker, *Angew. Chem. Int. Ed.*, **2008**, *47*, 9200-9211.
23. A. E. Farrell, R. J. Plevin, B. T. Turner, A. D. Jones, M. O'Hare and D. M. Kammen, *Science*, **2006**, *311*, 506-508.
24. D. De Oliveira-Vigier and F. Jérôme, *Top. Curr. Chem.*, **2010**, *295*, 63-92.
25. M. J. Climent, A. Corma and S. Iborra, *Green Chem.*, **2011**, *13*, 520-540.
26. R. Palkovits, K. Tajvidi, J. Procelewska, R. Rinaldi and A. Ruppert, *Green Chem.*, **2010**, *12*, 972-978.
27. J. A. Geboers, S. Van de Vyver, R. Ooms, B. Op de Beeck, P. Jacobs and B. F. Sels, *Catal. Sci. Technol.*, **2011**, *1*, 714-726.
28. H. Kobayashi, H. Ohta and A. Fukuoka, *Catal. Sci. Technol.*, **2012**, *2*, 869-883.
29. A. A. Rosatella, S. P. Simenov, R. F. M. Frade and C. A. M. Alfonso, *Green Chem.*, **2011**, *13*, 754-793.
30. L. Hu, G. Zhao, W. Hao, X. Tang, Y. Sun, L. Lin and S. Liu, *RSC Adv.*, **2012**, *2*, 11184-11206.

31. R.-J. van Putten, J. C. van der Waal, E. de Jong, C. B. Rasrendra, H. J. Heeres and J. G. de Vries, *Chem. Rev.*, **2013**, *113*, 1499-1597.
32. C. H. Zhou, J. N. Beltramini, Y. X. Fan and G. Q. Lu, *Chem. Soc. Rev.*, **2008**, *37*, 527-549.
33. A. Behr, J. Eilting, K. Irawadi, J. Leschinski and F. Lindner, *Green Chem.*, **2008**, *10*, 13-30.
34. A. Brandner, K. Lehnert, A. Bienholz, M. Lucas and P. Claus, *Top. Catal.*, **2009**, *52*, 278-287.
35. B. Katryniok, H. Kimura, E. Skrzynski, J. S. Girardon, P. Fongarland, M. Capron, R. Ducoulombier, N. Mimura, S. Paul and F. Dumeignil, *Green Chem.*, **2011**, *13*, 1960-1979.
36. C.-H. Zhou, X. Xia, C.-X. Lin, D.-S. Tong and J. Beltramini, *Chem. Soc. Rev.*, **2011**, *40*, 5588-5617.
37. G. Centi, P. Lanzafranco and S. Perathoner, *Catal. Today*, **2011**, *167*, 14-30.
38. R. Alamillo, M. Tucker, M. Chia, Y. Pagán-Torres and J. Dumesic, *Green Chem.*, **2012**, *14*, 1413-1419.
39. O. A. Simakova, E. V. Murzina, P. Mäki-Arvela, A.-R. Leino, B. C. Campo, K. Kordás, S. M. Willför, T. Salmi and D. Y. Murzin, *J. Catal.*, **2011**, *282*, 54-64.
40. S. E. Davis, M. S. Ide, and R. J. Davis, *Green Chem.*, **2013**, *15*, 17-45.
41. J. Ten Dam and U. Hanefeld, *ChemSusChem*, **2011**, *4*, 1017-1034.
42. A. M. Ruppert, K. Weinberg, and R. Palkovits, *Angew. Chem., Int. Ed.*, **2012**, *51*, 2564-2601.
43. A. Takagaki, M. Ohara S. Nishimura and K. Ebitani, *Chem. Commun.*, **2009**, 6276-6278.

44. J. Tuteja, S. Nishimura and K. Ebitani, *Bull. Chem. Soc. Jpn.*, **2012**, 85, 275-281.
45. Y.-B. Huang and Y. Fu, *Green Chem.*, **2013**, 15, 1095-1111.
46. J. F. Saeman, *Ind. Eng. Chem.*, **1945**, 37, 43-52.
47. R. W. Torget, J. S. Kim and Y. Y. Lee, *Ind. Eng. Chem. Res.*, **2000**, 39, 2817-2825.
48. F. Guo, Z. Fang, C. C. Xu and R. L. Smith Jr., *Prog. Energy Combust. Sci.*, **2012**, 38, 672-690.
49. K. D. O. Vigier and F. Jérôme, *Top. Curr. Chem.*, **2010**, 295, 63-92.
50. K. Shimizu and A. Satsum, *Energy Environ. Sci.*, **2011**, 4, 3140-3153.
51. P. L. Dhepe and A. Fukuoka, *ChemSusChem*, **2008**, 1, 969-975.
52. A. Takagaki, M. Nishimura, S. Nishimura and K. Ebitani, *Chem. Lett.*, **2011**, 40, 1195-1197.
53. H. E. Van Dam, A. P. G. Kieboom and H. Van Bekkum, *Starch/Stärke*, **1986**, 38, 95-101.
54. L. Cottier, G. Descotes, C. Neyret and H. Nigay, *Industries Aliment. Agricol.*, **1989**, 567-560.
55. Y. Román-Leshkov, J. N. Chheda and J. A. Dumesic, *Science*, **2006**, 312, 1933-1937.
56. J. N. Chheda, Y. Román-Leshkov and J. A. Dumesic, *Green Chem.*, **2007**, 9, 342-350.
57. H. Zhao, J. E. Holladay, H. Brown and Z. C. Zhang, *Science*, **2007**, 316, 1597-1600.
58. Y. Su, H. M. Brown, X. Huang, X.-D. Zhou, J. E. Amonette and Z. C. Zhang, *Appl. Catal. A*, **2009**, 361, 117-127.

59. J. B. Binder and R. T. Raines, *J. Am. Chem. Soc.*, **2009**, *131*, 1979-1985.
60. J. Chaminand, L. Djakovitch, P. Gallezot, P. Marion, C. Pinel and C. Rosier, *Green Chem.*, **2004**, *6*, 359-361.
61. D. G. Lahr and B. H. Shanks, *Ind. Eng. Chem. Res.*, **2003**, *42*, 5467-5472.
62. T. Miyazawa, Y. Kusunoki, K. Kunimori and K. Tomishige, *J. Catal.*, **2006**, *240*, 213-221.
63. E. Tronconi, N. Ferlazzo, P. Forzatti, I. Pasquon, B. Casale and L. Marini, *Chem. Eng. Sci.*, **1992**, *47*, 2451-2456.
64. W. Xu, H. Wang, X. Liu, J. Ren, Y. Wang and G. Lu, *Chem. Commun.*, **2011**, *47*, 3924-3926.
65. T. Mizugaki, T. Yamakawa, Y. Nagatsu, Z. Maeno, T. Mitsudome, K. Jitsukawa and K. Kaneda, *ACS Sustainable Chem. Eng.*, **2014**, *2*, 2243-2247.
66. A. B. Merlo, V. Vetere, J. F. Ruggera and M. L. Casella, *Catal. Commun.*, **2009**, *10*, 1665-1669.
67. M. Chatterjee, T. Ishizaka and H. Kawanami, *Green Chem.*, **2014**, *16*, 4734-4739.
68. S. Nishimura, N. Ikeda and K. Ebitani, *Catal. Today*, **2014**, *232*, 29-98.
69. N. K. Gupta, S. Nishimura, A. Takagaki and K. Ebitani, *Green Chem.*, **2011**, *13*, 824-827.
70. C. Carlini, P. Patrono, A. M. Raspolli Galletti, G. Sbrana and V. Zima, *Appl. Catal. A: Gen*, **2005**, *289*, 197-204.
71. A. Takagaki, M. Takahashi, S. Nishimura and K. Ebitani, *ACS Catal.*, **2011**, *1*, 1562-1565.
72. W. Hu, D. Knight, B. Lowry and A. Varma, *Ind. Eng. Chem. Res.*, **2010**, *49*, 10876-10882.

73. R. M. Painter, D. M. Pearson and R. M. Waymouth, *Angew. Chem. Int. Ed.*, **2010**, *49*, 9456-9459.
74. D. Tongsakul, S. Nishimura and K. Ebitani, *ACS Catal.*, **2013**, *3*, 2199-2207.
75. D. Tongsakul, S. Nishimura, C. Thammacharoen, S. Ekgasit and K. Ebitani, *Ind. Eng. Chem. Res.*, **2012**, *51*, 16182-16187.
76. D. Tongsakul, S. Nishimura and K. Ebitani, *J. Phys. Chem. C*, **2014**, *118*, 11723-11730.
77. C. L. Bianchi, P. Canton, N. Dimitratos, F. Porta and L. Prati, *Catal. Today*, **2005**, *102*, 203-212.
78. S. E. Davis, M. S. Ide and R. J. Davis, *Green Chem.*, **2013**, *15*, 17-45.
79. J. Tuteja, H. Choudhary, S. Nishimura and K. Ebitani, *ChemSusChem*, **2014**, *7*, 96-100.

Chapter 2

*One-pot synthesis of furans from various
saccharides using a combination of solid
acid and base catalysts*

One-pot synthesis of furans from various saccharides using a combination of solid acid and base catalysts

Abstract

Herein, I have studied the one-pot synthesis of furans from various saccharides such as D-arabinose, L-rhamnose and lactose monohydrate with combination of solid acid and base catalysts under mild reaction conditions. The effective synthesis of furans from various saccharides are likely progressed by the aldose-ketose isomerization of sugars over solid base followed by successive dehydration to furans over solid acid.

Combination of solid acid Amberlyst-15 and solid base Hydrotalcite (HT, Mg/Al = 3) catalysts was found to display the best activity for synthesis of furans from various sugars. The yield of furfural, MF and HMF from arabinose, rhamnose and lactose was observed to be 26, 39 and 34%, respectively. Only Amberlyst-15 or HT shows low activity in all cases (0-5 % yields of furans). The one-pot conversion of mixed-sugars was also demonstrated, and which serves the yields of 31% furfural, 32% HMF and 29% MF from the mixture of arabinose, rhamnose and lactose respectively. I found that the one-pot conversion of single or mixed carbohydrates over the acid-base pair catalysts provided the novel process for the synthesis of furans.

Introduction

Bio-refinery has gained so much attention due to its potential to serve as a source of carbon-based fuels and chemicals with carbon-neutral concept,¹⁻³ the CO₂ released during energy conversion is consumed during subsequent biomass regrowth. Lignocellulosic biomass encompassing municipal and animal wastes, forestry residues and others is special interest resource on account of the most abundant, inedible and inexpensive biomass. The challenge for the effective utilization of lignocellulosic biomass is to develop cost effective processes for transformation of huge built carbohydrates into value-added chemical compounds. Furan derivatives such as 2-furaldehyde (furfural), 5-(hydroxymethyl)furfural (HMF) and 5-methylfurfural (MF) have the potential to be substitutes of the building blocks derived from petrochemicals in the production of fine chemicals, pharmaceuticals and polymers.⁴⁻⁸ For instance, HMF can be converted to 2,5-diformylfuran, 2,5-furandicarboxylic acid, 2,5-dimethylfuran and levulinic acid.⁹⁻¹³ MF is a useful intermediate for the production of agricultural chemicals (pesticides), fragrance industry, a common flavoring component in food industry and considered as a potential anti-tumor agent.¹⁴⁻¹⁷ Industrial solvents like 1,5-pentanediol, 1,4-butanediol and building block such as succinic acid, maleic acid are the main products derived from furfural.¹⁸⁻²¹

Recently, Lam *et al.*²² and Binder *et al.*²³ have reported the synthesis of furfural from xylose in good yield using Nafion 117 and chromium halide with ionic liquid, respectively. Dehydration of xylose to furfural is investigated using various solid acid catalysts like sulfonic acid appended porous silicas,²⁴ metal oxide nanosheets,²⁵ ion-exchange resins²⁶ and zeolites²⁷. Besides, the inorganic acids with sub critical water at 403 K²⁸, organic acids such as oxalic, levulinic, *p*-toluenesulfonic acids²⁹⁻³² were also examined for dehydration of D-fructose. From the view point of reaction system

activation, dehydration in water-methyl isobutyl ketone or water-toluene biphasic system were also investigated with H-mordenite and H-faujasite by Moreau *et al.*³³ Although the yield obtained is significant in the above mentioned process but most of them involves use of high temperature, severe reaction conditions, difficulty in recovery and reusability of catalyst.

The industrial method for the preparation of MF uses 2-methylfuran, phosphorous oxychloride and *N,N*-dimethylformamide (DMF) in dichloroethane.³⁴ Although good yield is obtained, but the process involves the use of 2-methylfuran synthesized from furfural^{35,36} and a highly poisonous and hazardous reagent phosphorus oxychloride. It is also reported for the synthesis of MF that two steps of dehydration of carbohydrates in high concentration of chloride ion at high temperature to form 5-chloromethylfurfural (CMF) followed by its hydrogenation.^{37,38} Recently, Yang *et al.*³⁹ reported the synthesis of MF from fructose by using RuCl₃, HI and Pd/C under the hydrogen flow at high pressure in water-benzene biphasic system with high yields. Here the use of homogeneous catalyst and benzene as solvent screens the process to be applied in practice.

Despite these advances in the synthesis of the furfurals, the conversion of many other sugars from lignocellulosic biomass has not been studied extensively. One-pot synthesis is one of attractive methodologies for the environmentally-friendly chemical process because it enables to reduce the processes for isolation and purification of intermediates in multistage reaction, which saves energy, solvent and time. One most important advantage of the one-pot synthesis is that the unstable intermediate can be easily converted into the product immediately with minimum loss. The one-pot reaction with heterogeneous catalysts also has the advantages of easy separation of catalyst and product. The previous finding of our research group in the conversion of glucose, sucrose,

cellobiose and xylose to 5-hydroxymethylfurfural (HMF) and furfural, which involves base catalyzed isomerisation of aldoses followed by dehydration using acid catalyst, came handy in the present study.⁴⁰⁻⁴² In this work, I studied a direct catalytic method for the production of furfurals from hemicellulose derivatives such as arabinose, rhamnose and lactose using combination of acid and base catalysts under mild conditions (**Scheme 1** (b, c, d)), and further investigated the conversion of mix sugars to corresponding furans.

Experimental section

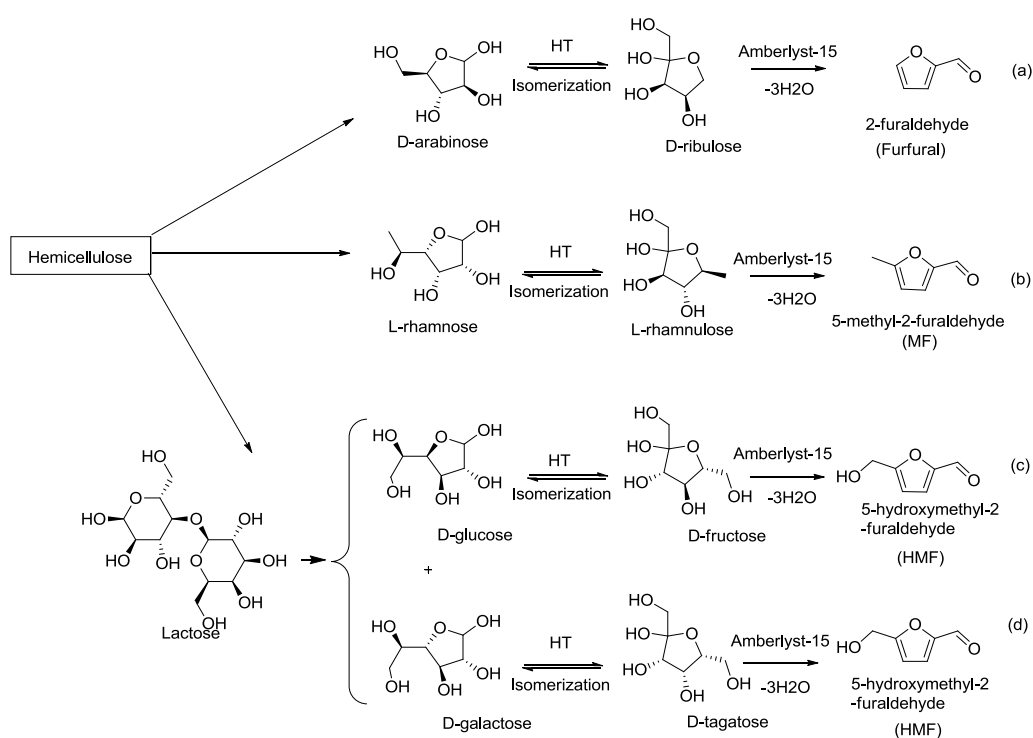
Materials

L-(-)-rhamnose, D-(+)-galactose, D-(-)-glucose, D-(-)-fructose, *N,N*-dimethylformamide (DMF), dimethyl sulfoxide (DMSO), *N,N*-dimethylacetamide (DMA) and acetonitrile (AN) were bought from Kanto Chemicals Co. Inc. D-(-)-arabinose was provided by Acros Organics. D-(-)-Tagatose, Amberlyst-15, Amberlyst A 26, Amberlyst A 21, Nafion SAC 13 and Nafion NR 50 were purchased from Sigma-Aldrich, Inc. Hydrotalcite (HT, Mg/Al=3) was supplied by Tomita Pharmaceuticals Co. Ltd. Lactose monohydrate and D-(-)-ribulose was obtained from Wako Chemicals and MP Biomedicals, respectively. All solvents were purified before use.

General Procedure for reaction

One-pot reaction procedure as finally adopted for conversion of various carbohydrates was performed in a Schlenk glass tube attached to a reflux condenser under N₂ atmosphere. The experiments were carried out with 0.1 g of carbohydrate, 0.1 g of Amberlyst-15, 0.2 g of HT and 3 ml of DMF in oil bath at 373 K for 3 h. After the reaction, the resultant mixture was diluted 30 times with water and filtered off the catalyst using Millex-LG 0.20

μm , then analysed using a high performance liquid chromatography (HPLC, WATERS 600 Pump) with Aminex HPX-87H column (Bio-rad laboratories). The mobile phase was 10 mM sulfuric acid in water at a flow rate of 0.5 ml min^{-1} at 323 K. The products were analyzed using a refractive index detector (WATERS 2414). Authentic samples were used as standards, and a calibration curve method was used for the quantification.



Scheme 1: Reaction schemes for the conversion of various sugars to the corresponding furans.

Results and discussion

One-pot synthesis of 2-furaldehyde (furfural) from Arabinose

Isomerisation of arabinose, a C-3 epimer of xylose, to ribulose and successive dehydration of ribulose to furfural are tried using the combined catalysts with base HT and various acids.

Table 1: One-pot synthesis of furfural from arabinose using acid and base catalysts^a

	D-arabinose		D-ribulose	2-furfuraldehyde
Entry	Acid catalyst	Base catalyst	Conv./% arabinose	Yield (sel.)/% furfural
1	Amberlyst-15	HT	87.6, 89.7 ^b	21.1 (24.0), 26.5 (29.5) ^b
2 ^c			> 99	17.3 (17.3)
3	Nafion NR 50	HT	65.8	8.6 (13.0)
4	Nafion SAC 13	HT	62.6	4.9 (7.8)
5	Amberlyst-15	-	72.7	3.9 (5.3)
6	Nafion NR 50	-	70.1	3.9 (5.5)
7	Nafion SAC 13	-	33.1	3.7 (11.1)
8	-	HT	77.8	4.0 (5.1)

^a**Reaction conditions:** Arabinose (0.66 mmol), Acid catalyst (0.1 g), Base catalyst (0.2 g), DMF(3 ml), 373 K, 3 h, 500 rpm. ^b393 K. ^cTwo-step reaction without catalyst separation. After 4.5 h with HT, Amberlyst-15 was added to the reaction mixture and further stirred for 2 h.

Utilization of only solid acid or base HT catalyst showed low activity for the synthesis of furfural (**Table 1**, entries 5-8). Combination of Amberlyst-15 as solid acid catalyst and HT as solid base catalyst was found to display the best activity for furfural (21.1% yield, 24.0% sel.) among other solid catalysts, and highest yield and selectivity (26.5% yield, 29.5% sel.) was observed at 393 K (entry 1), whereas HT paired with other solid acid catalysts such as Nafion NR 50 and Nafion SAC 13 showed very less activity

(< 9% yield) for the formation of furfural (entries 3 and 4). Although high conversions (> 60%) were observed in all cases, no other products were detected by HPLC.

Table 2: Conversion of Arabinose to Ribulose using HT^a

Entry	Time/ h	Conv./%	Yield/%	
		arabinose	ribulose	furfural
1	0	0	0	0
2	1	36.8	20.5	0
3	2	41.2	23.7	0
4	2.5	56.4	26.4	0
5	3.5	71.5	27.2	0
6	4.5	87.9	27.8	0
7	5	93.2	26.3	0

^a**Reaction Conditions:** Arabinose (0.55 mmol), HT (0.2 g), DMF (3 ml), 373 K, 500 rpm.

Considering on the basis of acidity, Nafion NR 50 and Nafion SAC 13 exhibit strong acid ($H_o = -12$), which leads to the formation of undesired brown colored insoluble by-product such as humins from arabinose, ribulose and furfural as well. The formation of insoluble humins and polymers increases at higher sugar concentration and longer residence time. The moderate acidity of Amberlyst-15 ($H_o = -2.2$) is found to be enough to obtain furfural in good yields with inhibition of the side reaction.

In order to ascertain the efficiency of the one-pot synthesis, two-step reaction without catalyst separation was also examined. The reaction times for isomerization with HT and dehydration with Amberlyst-15 were selected for 4.5 h and 2 h, respectively, which indicated the maximum performance for individual reactions (**Table 2 and 3**). Although the furfural was also formed with the two-step reaction (17.3% yield, **Table 1**, entry 2), the yield and selectivity were lower than that of the one-pot reaction. The isomerization is known as an equilibrium reaction where the dehydration is as a forward reaction. Therefore, the sequential dehydration will enhance the front isomerization under

the one-pot reaction. As these results, I confirmed the one-pot synthesis is superior to the two-step reaction in this type of reaction.

Table 3: Conversion of Ribulose to 2-furaldehyde using Amberlyst-15^a

Entry	Time/ h	Conv./%	Yield (sel.)/%
		ribulose	furfural
1	1	100	21.6 (21.6)
2	2	100	22.0 (22.0)
3	2.5	100	18.4 (18.4)

^a**Reaction Conditions:** Ribulose (0.55 mmol), Amberlyst-15 (0.1 g), DMF (3 ml), 373 K, 500 rpm.

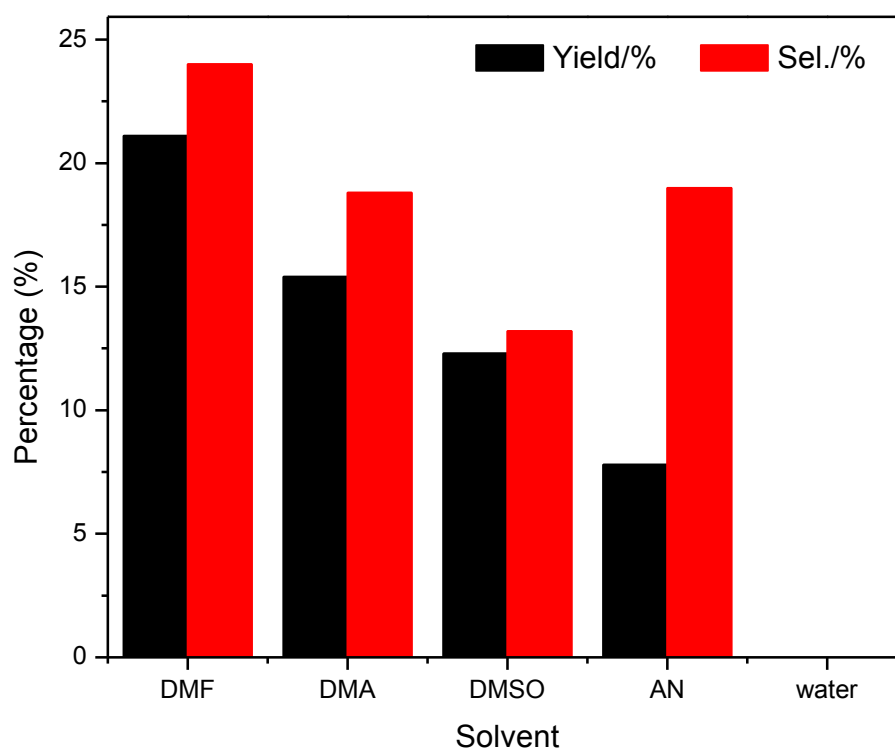


Figure 1: Effect of solvent over the one-pot synthesis of furfural from arabinose.

Reaction conditions: Arabinose (0.66 mmol), Amberlyst-15 (0.1 g), HT (0.2 g), solvent (3 ml), 373 K, 3 h, 500 rpm.

Figure 1 shows the effect of solvent for the one-pot conversion of arabinose. Water and some organic solvents such as DMF, DMA, DMSO and AN were tested in the presence of Amberlyst-15 and HT catalysts. It was observed that aprotic solvent had

activity for the formation of furfural, where the highest yield and selectivity was obtained with DMF.

The time course in the one-pot formation of furfural from arabinose with Amberlyst-15 and HT is shown in **Figure 2**. The conversion of arabinose shows a high value even in the initial stage of the reaction. The yield of ribulose was increased till 25.6% yield during 3 h reaction, and then it started decreasing, whereas the formation of furfural gradually progressed with time.

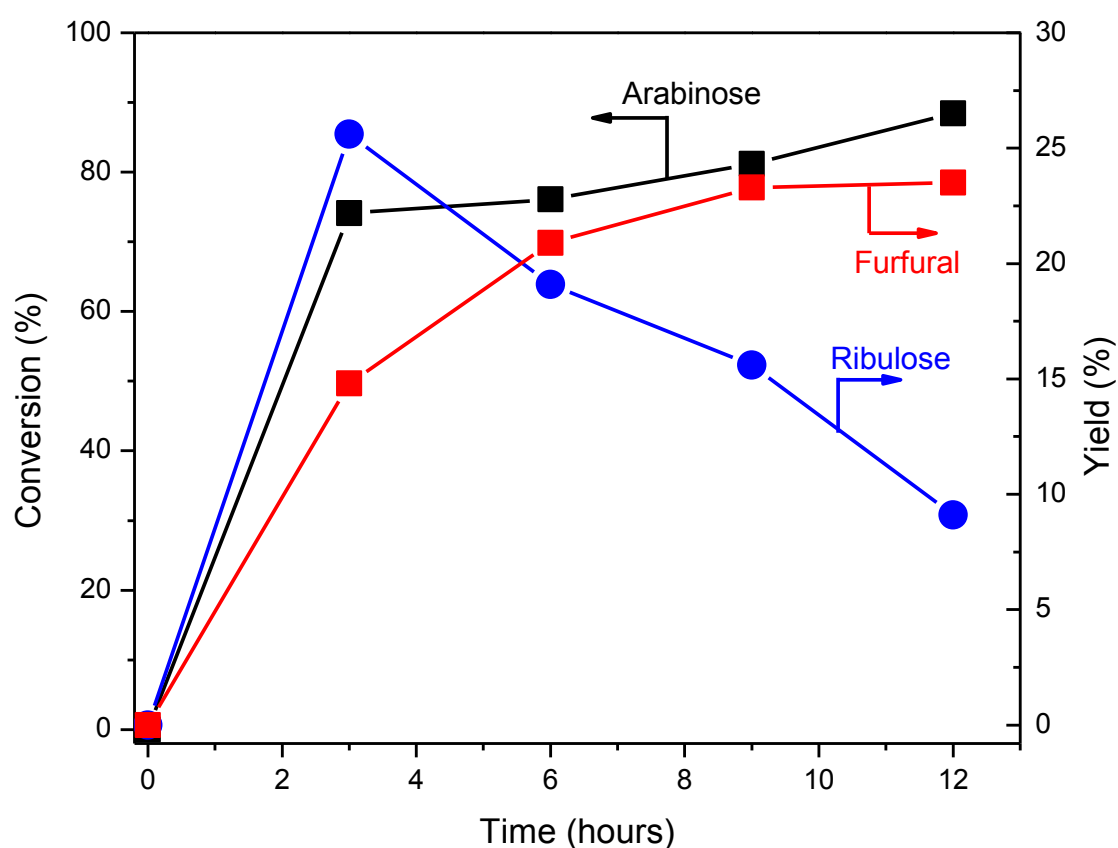


Figure 2: Time course in the one-pot synthesis of furfural from arabinose using Amberlyst-15 and HT.

Reaction conditions: Arabinose (0.66 mmol), Amberlyst-15 (0.1 g), HT (0.2 g), DMF (3 ml), 373 K, 500 rpm.

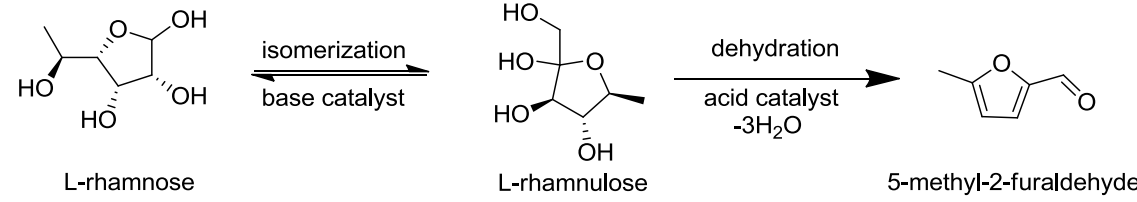
These evaluations suggested that the ribulose was formed as an intermediate during the one-pot formation of furfural from arabinose. In accordance with previous reports,⁴⁰⁻⁴² this reaction is also a one-pot reaction through the isomerization from arabinose to ribulose over HT catalyst and successive dehydration of ribulose to furfural over Amberlyst-15 catalyst. The small difference between conversion of arabinose and yield of furfural can be because of two major possibilities, first one is the reaction of furfural with itself called furfural resinification and other one is the reaction of furfural with an intermediate of the sugar-to-furfural conversion known as furfural condensation.⁴³ These condensations of two furfurals or furfural with arabinose formed some polymers and decreased the yield of furfural.

One-pot synthesis of 5-methyl-2-furaldehyde (MF) from rhamnose

L-(-)-rhamnose is methyl pentose or a deoxy hexose carbohydrate, and is the cheapest deoxy sugar. The isomerization using base catalyst will give L-rhamnulose and following dehydration will form MF (**Scheme 1** (d)). Various acids and base catalysts were examined for the one-pot synthesis of MF from rhamnose as shown in **Table 4**. It was observed that Amberlyst-15 and HT were the best combination of acid and base pair catalysts with 38.6% yield and 51.7% selectivity in this reaction (entry 1). Nafion SAC 13 and Nafion NR 50 in combination with HT shows very poor activity (< 7% yield, entry 2, 3) whereas only HT base or acid catalyst showed no activity, although only Amberlyst-15 indicated a slight activity (5.3% yield) (entry 5-7). Use of less amount of Amberlyst-15 in combination of HT also gave a good yield of MF (33.1%) with high turnover number (TON) of 1.5 for both Amberlyst-15 and HT (entry 1b).

The three acid catalysts including Amberlyst-15, Nafion SAC 13 and Nafion NR 50 have same sulphonic functionality, but Nafion catalysts have perfluorinated group along with sulphonic group. The perfluorinated group increases the cross linking which leads to decrease in swelling capacity of Nafion, which in turns decreases the reactants accessibility to the acid sites buried within the Nafion beads and responsible for the lowering of the activity of catalyst. For improving this point, to entrap the nanosized Nafion resin onto a highly porous silica such as Nafion SAC 13 had investigated.^{44,45}

Table 4: One-pot synthesis of MF from rhamnose using acid and base catalysts^a

				
			Conv./%	Yield (sel.)/%
Entry	Acid catalyst	Base catalyst	Rhamnose	MF
1	Amberlyst-15	HT	74.6, 63.8 ^b	38.6 (51.7), 33.1 (48.1) ^b
2	Nafion SAC 13	HT	62.5	2.1 (3.3)
3	Nafion NR 50	HT	49.5	6.5 (13.1)
4	Amberlyst 15	-	46.4	5.3 (11.4)
5	Nafion SAC 13	-	10.1	0 (0)
6	Nafion NR 50	-	12.5	0 (0)
7	-	HT	23	0 (0)

^a**Reaction conditions:** Rhamnose (0.55 mmol), Acid catalyst (0.1 g), Base catalyst (0.2 g), DMF (3 ml), 383 K, 6 h, 500 rpm, N₂ flow (3 ml min⁻¹). ^bAmberlyst-15 (25 mg).

To further understand their differences, the physical properties of these three solid acid catalysts were listed in **Table 5** by the N₂ adsorption-desorption method (**Figure 3 and 4**). From the view point of pore size, the conversion of rhamnose in the one-pot synthesis of 2-furaldehyde were in order, large pore size induced high conversion. Although the conversion is not directly related to the yield of MF, the accessibility for substrates and/or intermediates also seems to be important factor for the reaction.

Therefore, the high activity of Amberlyst-15 catalyst for synthesis of MF and 2-furaldehyde is attributed to both the medium acidity and better accessibility (larger pore size) for reactants.

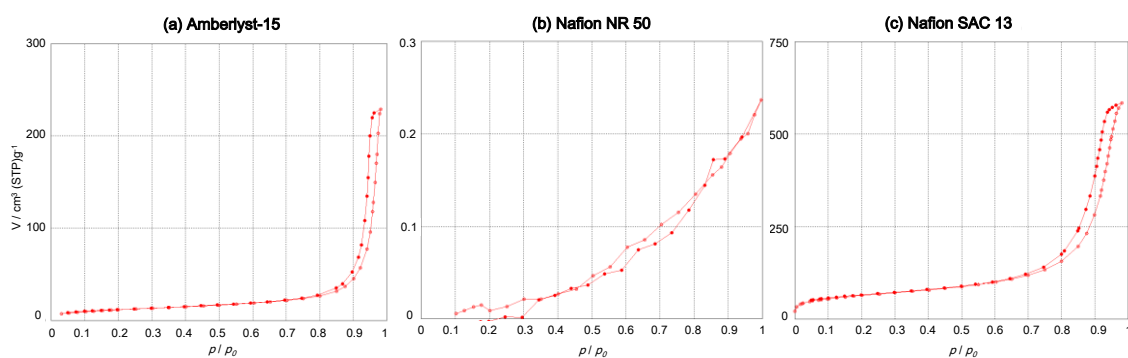


Figure 3: Nitrogen adsorption-desorption isotherms of (a) Amberlyst-15, (b) Nafion NR50 and (c) Nafion SAC 13.

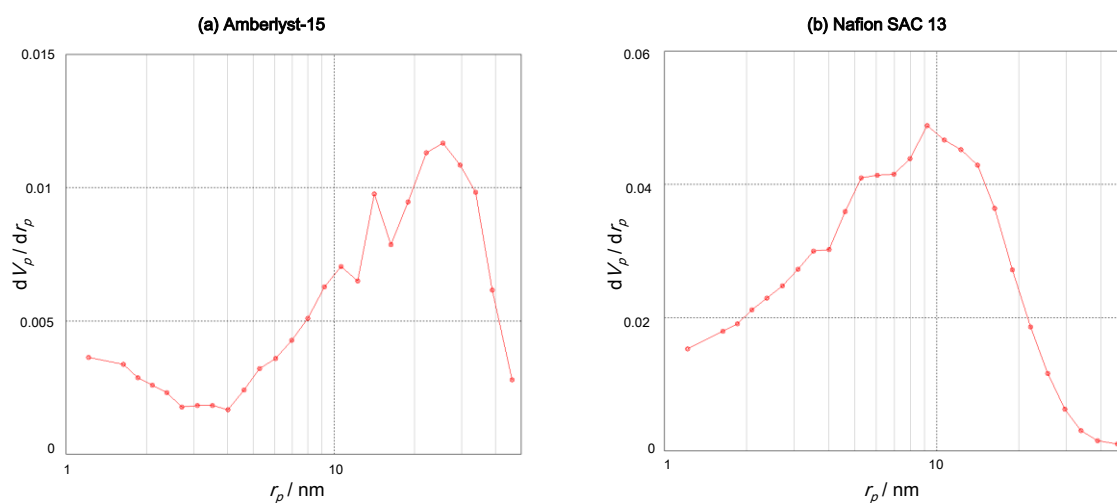
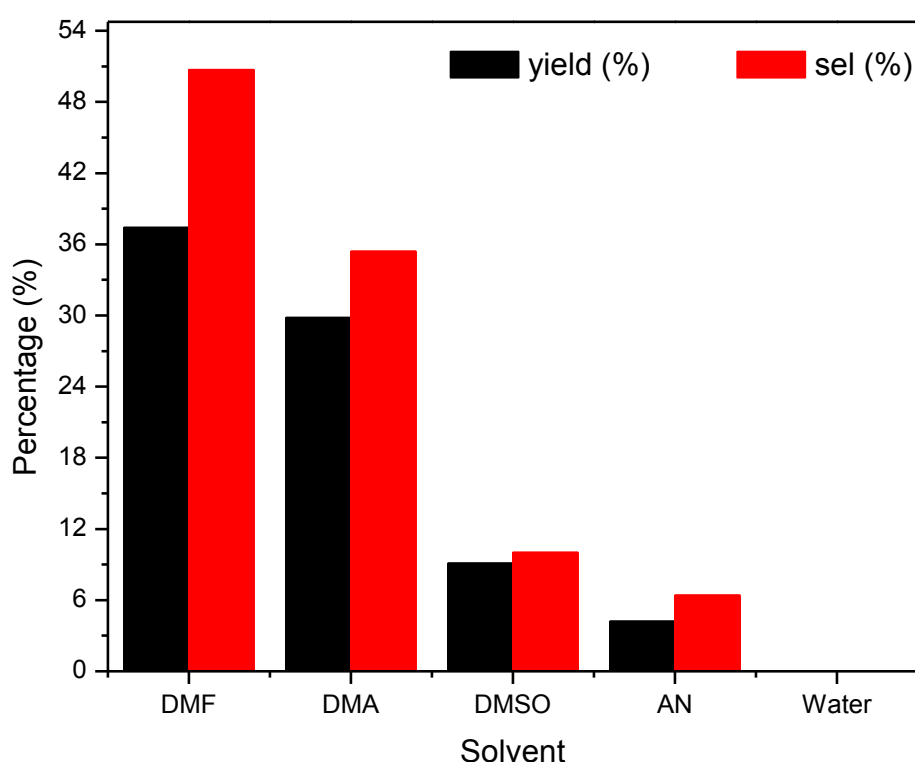


Figure 4: Pore size distribution of Amberlyst-15 and Nafion SAC 13 estimated by nitrogen adsorption-desorption isotherms with BJH method.

Table 5: Physical properties among Amberlyst-15, Nafion NR 50 and Nafion SAC 13

Entry	Samples	Surface area / m^2g^{-1} ^a	Pore volume / cm^3g^{-1} ^b	Average pore size / nm ^b
1	Amberlyst-15	41.5	0.35	25.6
2	Nafion NR 50	< 1 ^c	-	-
3	Nafion SAC 13	226.7	0.88	9.23

^aBET surface area calculated by the N_2 adsorption isotherm under 77 K. ^bCalculated by a BJH method. ^cThis value was estimated by the measurement limitation in the case of the N_2 adsorption.

**Figure. 5:** Effect of solvent for the one-pot synthesis of MF from rhamnose.

Reaction conditions: Rhamnose (0.55 mmol), Amberlyst-15 (0.1 g), HT (0.2 g), Solvent (3 ml), 383, 6 h, 500 rpm, N_2 flow (3 ml min^{-1}).

Figure 5 shows yield and selectivity for the formation of MF from rhamnose in different solvents. Similarly to furfural formation, water shows no activity for MF synthesis and DMF showed highest activity with 37.4% yield of MF. DMA, DMSO and AN also produce MF but in very less quantity as compared to DMF.

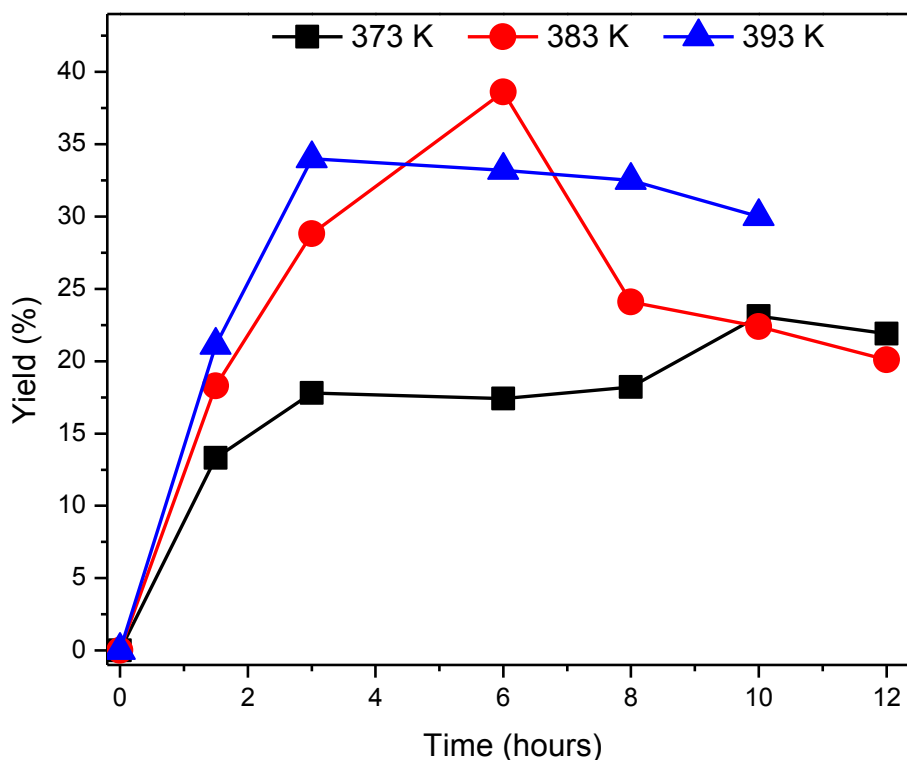


Figure 6: Time course in the one-pot synthesis of MF from rhamnose at different temperatures.

Reaction conditions: Rhamnose (0.55 mmol), Amberlyst-15 (0.1 g), HT (0.2 g), DMF (3 ml), 500 rpm, N₂ flow (3 ml min⁻¹).

Figure 6 shows time course for the one-pot formation of MF from L-rhamnose at different temperature range of 373-393 K. The yield of MF increases with increase in temperature for 3 h, but long time reaction shows quite interesting behavior. The yield increases up to a maximum yield of 24.0% MF in 10 h, thereafter it started decreasing in case of 373 K. While the same tendency with the maximum yield 38.6% in 6 h reaction and following decreasing was obtained at 383 K. The reaction progress at 393 K is different from 373 K and 383 K, and a gradual decrease in yield was observed from 3 h reaction. Accordingly, appearances of the peak tops were shifted to shorter time with increase of the reaction temperature. In system of the one-pot synthesis including isomerization and successive dehydration, increasing of the activity of dehydration

enhances the yield of product owing to the enhancement of isomerization.⁴¹ From the view point of thermodynamics, the dehydration reaction is an exothermic reaction. Therefore, long-time reaction at high temperature leads to good yield of the product. Whereas, the side reactions for undesired by-products like humins, oligomers etc. and decomposition of the product are also enhanced by the high temperature and/or long-time reaction. According to these aspects, I considered that the condition for 6 h at 383 K showed the highest activity for the one-pot synthesis of MF from rhamnose.

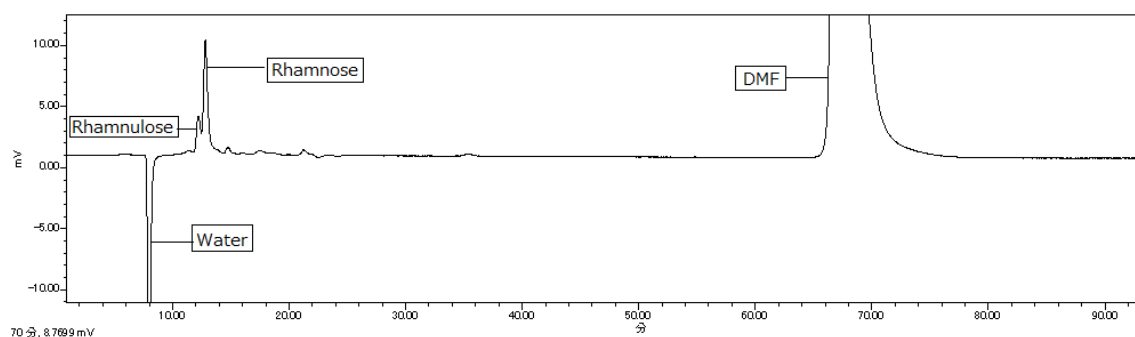


Figure. 7: HPLC chromatogram for the conversion of Rhamnose with only HT.

Reaction conditions: Rhamnose (0.55 mmol), Amberlyst-15 (0.1 g), HT (0.2 g), DMF (3 ml), 500 rpm, N₂ flow (3 ml min⁻¹).

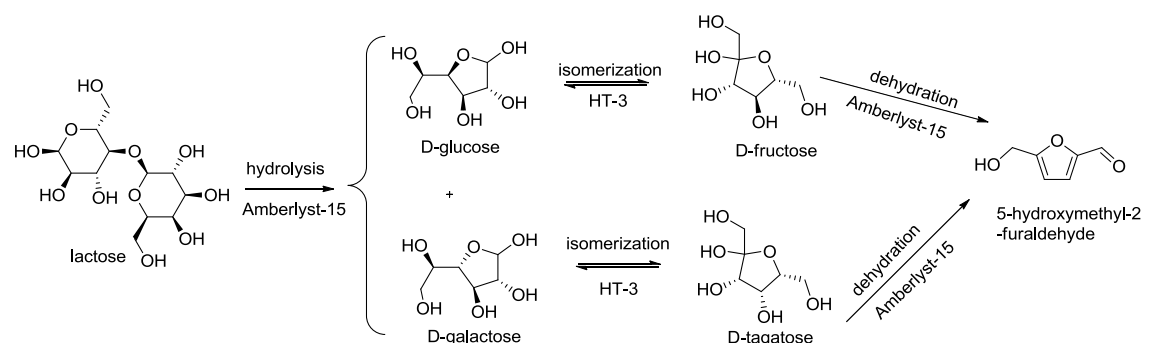
The aldo-sugars have been reported earlier to isomerise to keto-sugars in the presence of solid base for instance glucose to fructose. These isomerization's were detected as twin peaks in the HPLC chromatogram with the retention time as: glucose (11.4) and fructose (12.3); arabinose (13.2) and ribulose (13.6); galactose (12.1) and tagatose (11.8 min).⁴⁰⁻⁴² Similarly, a twin peak is observed in case of rhamnose at 12.3 and 12.8 min (**Figure 7**), where the former is likely attributed to rhamnulose, a keto isomer of rhamnose, while the latter is observed for rhamnose. Rhamnulose is commonly known as 6-deoxyfructose, hence it was supposed that the retention time for fructose and rhamnulose are found to be almost similar.⁴⁶ According to these results, I believed that

the one-pot synthesis of MF from rhamnose was also enhanced the pathway via the isomerization of rhamnose to rhamulose over base catalyst and successive dehydration from rhamulose to MF over acid catalyst.

One-pot synthesis of HMF from lactose

Lactose has poor digestibility, therefore it is widely utilized in the dairy industry and it has much potential to serve as a chemical or energy feedstock.⁴⁷ The lactose is a disaccharide of glucose and galactose. These aldohexoses give fructose and tagatose respectively on isomerization with base catalyst, followed by dehydration with acid catalyst to give HMF (**Scheme 1** (a) and (b)). **Table 6** shows the results in one-pot conversion of lactose, glucose and galactose using Amberlyst-15 and HT catalysts.

Table 6: One-pot synthesis of HMF from lactose, glucose and galactose^a



Entry	Temp / K	Substrate	Conv./% substrate	Yield (Sel.)/% HMF
1	373	Lactose	76.3	13.1 (17.2)
2		Glucose	73	42.3 (58.0)
3		Galactose	89.6	15.1 (16.7)
4	383	Lactose	97.2	30.5 (31.3)
5		Glucose	75.8	39.4 (52.0)
6		Galactose	91.1	21.3 (23.5)
7	393	Lactose	100	25.0 (25.0)
8		Glucose	82	37.0 (43.2)
9		Galactose	100	20.5 (20.5)

^a**Reaction conditions:** Substrate (0.1 g), Amberlyst-15 (0.1 g), HT (0.2 g), DMF (3 ml), 3 h, 500 rpm.

It is clear that HMF obtained from glucose is much higher than that from galactose in all reaction temperatures. The reason behind this can be explained from the stereochemical configuration of galactose. The keto isomer of galactose is tagatose which is a C-4 epimer of fructose and there is an inefficient dehydration of tagatose into HMF. Comparing to the reaction temperatures, glucose shows the maximum yield at 373 K while galactose and lactose produces HMF in good yield at 383 K. Additionally, both hydrolysis of lactose and formation of HMF were enhanced with increasing temperature. These results indicate that the sequential reaction as hydrolysis of lactose by acid, isomerization of galactose and glucose by base, and then dehydration by acid was taken place in the reaction. Moreover, I can easily figure out (**Table 7**), that amount of galactose and tagatose left in the reaction mixture is more than the amount left of glucose and fructose that clearly indicates that under same reaction conditions galactose and tagatose are less reactive than glucose and fructose.

Table 7: One pot conversion of lactose using Amberlyst-15 and HT at different temperatures^a

Entry	Temp/K	Conv./%	Sel./%	Yield/%				
		Lactose	HMF	HMF	Glucose	Fructose	Galactose	Tagatose
1	373	76.3	17.2	13.1	6.8	12.7	21.5	19.7
2	383	97.4	31.3	30.5	7.9	6.2	14.8	12
3	393	100	25	25	6.5	0	11.5	9

^a**Reaction Conditions:** Lactose (0.291 mmol), Amberlyst-15 (0.1 g), HT (0.2 g), DMF (3 ml), 3 h, 500 rpm.

One-pot synthesis of furans from sugar mixtures

Natural biomass contains mixture of sugars like arabinose, galactose, xylose and many other mono and di-saccharides.^{48,49} For example, Rhamnose is commonly bound to other sugars in nature,⁵⁰ therefore it is necessary to develop a method for the conversion of rhamnose to MF in the presence of other sugars, therefore conversion of mixture of sugars

was also carried out and was observed that this method is applicable for the formation of different furans in a single pot.

Table 8: One-pot synthesis of furans from mix sugars using Amberlyst-15 and HT catalysts^a

Entry	Substrate	Yield (sel.)% of furans		
		Furfural	MF	HMF
1 ^b	arabinose+ rhamnose	33.1 (38.5)	32.5 (40.6)	-
2 ^c	arabinose + rhamnose + lactose	30.5 (31.6)	29.1 (38.0)	32.2 (32.2)

^a**Reaction conditions:** Amberlyst-15 (0.1 g), HT (0.2 g), DMF (3 ml), 383 K, 6 h, 500 rpm, N₂ flow (3 ml min⁻¹), b arabinose (0.05 g) and rhamnose (0.05 g), c arabinose (0.04 g), rhamnose (0.03 g) and lactose (0.03 g).

Firstly, one-pot conversion of mixture of arabinose and rhamnose was tested (Table 8, entry 1) with the same acid-base catalyst pair Amberlyst-15 and HT in DMF at the optimum time and temperature for both the sugars i.e. at 383 K for 6 h to obtain 33.1 and 32.5% yield of furfural and MF respectively. Thereafter the conversion of mixture of all three sugars (arabinose, rhamnose and lactose) were examined (entry 2), with near about 29-33% yield of furfural, HMF and MF. The yield of furans obtained from mixture of sugars is slightly less than the yield obtained one-pot conversion of particular single sugar. This is proved from these results that this system can be used for conversion of monosaccharides, disaccharides and for mixture of mono and di-saccharides.

Thereafter the next step was to check the recyclability of the catalysts for conversion of mixture of sugars, the acid and base catalysts were simply recovered by decantation, washed with DMF (10-12 ml), dried *in vacuo* for overnight, and recycled for further reactions. It was found that the catalysts could be reused at least three times (shown in Figure 8) for the synthesis of 2 or 3 furans simultaneously, without any significant loss in the catalytic activity.

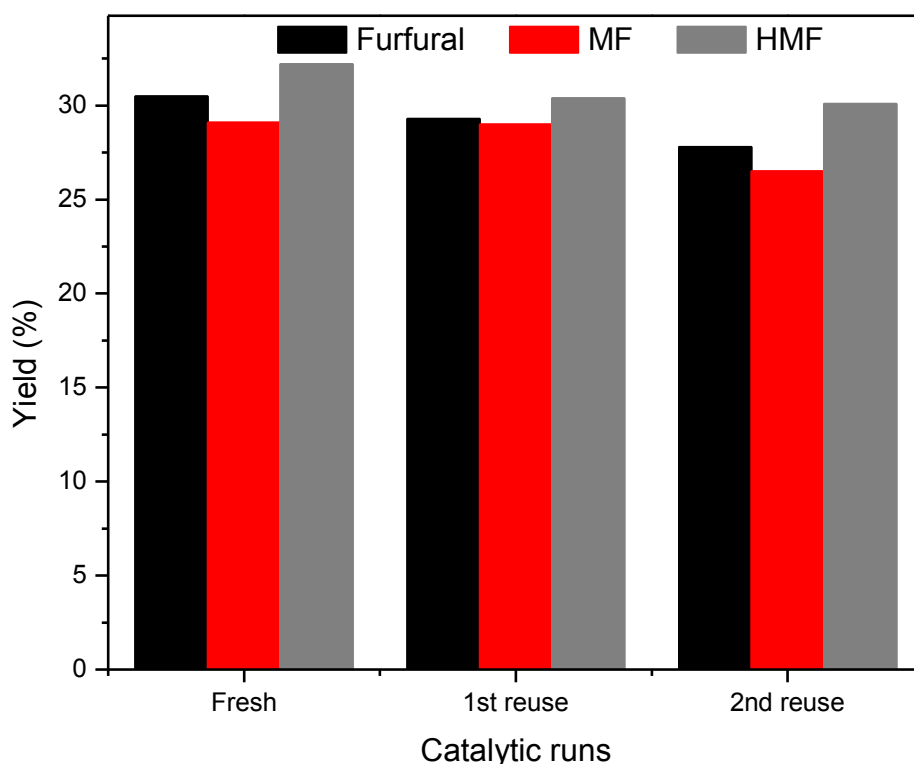


Figure 8: Recyclability of the acid and base catalysts over the synthesis of furans from mix-sugars.

Reaction conditions: Arabinose (0.04 g), rhamnose (0.03 g), lactose (0.03 g), Amberlyst-15 (0.1 g), HT (0.2 g), DMF (3 ml), 383 K, 6 h, 500 rpm, N₂ flow (3 ml min⁻¹).

Conclusions

In conclusion, I successfully showed a method for the one-pot formation of furans from single carbohydrate and mixture of carbohydrates using combination of solid acid Amberlyst-15 and solid base Hydrotalcite catalysts. The acid-base pair catalysts were found to display good activity for the formation of furans and could be reused three times without significant loss of the catalytic activity under the mild reaction conditions.

References

1. A. E. Farrell, R. J. Plevin, B. T. Turner, A. D. Jones, M. O'Hare and D. M. Kammen, *Science*, **2006**, *311*, 506-508.
2. D. R. Dodds and R. A. Gross, *Science*, **2007**, *318*, 1250-1251.
3. J. N. Chheda, C. H. Barrett and J. A. Dumesic, *Science*, **2005**, *308*, 1421-1422.
4. J. N. Chheda, G. W. Huber and J. A. Dumesic, *Angew. Chem. Int. Ed.*, **2007**, *46*, 7164-7183.
5. H. Zhao, J. E. Holladay, H. Brown and Z. C. Zhang, *Science*, **2007**, *316*, 1597-1600.
6. G. W. Huber, S. Iborra and A. Corma, *Chem. Rev.*, **2006**, *106*, 4044-4098.
7. L. Tradrantip, N. D. Sonawane, W. Namkung and A. S. Verkman, *J. Med. Chem.*, **2009**, *52*, 6447-6455.
8. R. Storbeck and M. Ballauff, *Polymer*, **1993**, *34*, 5003-5006.
9. X. Tong, Y. Ma and Y. Li, *Appl. Catal. A.*, **2010**, *385*, 1-13.
10. N. K. Gupta, S. Nishimura, A. Takagaki and K. Ebitani, *Green Chem.*, **2011**, *13*, 824-827.
11. T. Todsapon and T. B. Rauchfuss, *Angew. Chem. Int. Ed.*, **2010**, *49*, 6616-6618.
12. M. Chidambaram and A. T. Bell, *Green Chem.*, **2010**, *12*, 1253-1262.
13. G. W. Huber and A. Corma, *Angew. Chem. Int. Ed.*, **2007**, *46*, 7164-7183.
14. M. E. Jung and G-Y. J. Im, *J. Org. Chem.*, **2009**, *74*, 8739-8753.
15. H. Geneste, D. Sauer, W. Braje, W. Amberg, M. Mezler, M. Bakker and M. Henrica, IPN WO 2008/148790.
16. J. M. De Man, Principles of Food Chemistry, 3rd Ed., Springer, Heidelberg, 1999.

17. K. Michail, V. Matzi, A. Maier, R. Herwig, J. Greilberger, H. Jaun, O. Kunert and R. Wintersteiger, *Anal. Bioanal. Chem.*, **2007**, 387, 2801-2814.
18. W. Xu, H. Wang, X. Liu, J. Ren, Y. Wang and G. Lu, *Chem. Comm.*, **2011**, 47, 3924-3926.
19. Y. Tachibana, T. Masuda, M. Funabashi and M. Kunioko, *Biomacromolecules*, **2010**, 11, 2760-2765.
20. C. Delhomme, D. W. Botz and F. E. Kuhn, *Green Chem.*, **2009**, 11, 13-26.
21. S. Shi, H. Guo and G. Yin, *Catal. Commun.*, **2011**, 12, 731-733.
22. E. Lam, M. Ehsan, A. C. W. Leung, J. H. Chong, A. K. Mahmoud and J. H. T. Luong, *ChemSusChem*, **2011**, 4, 535-541.
23. J. B. Binder, J. J. Blank, A. V. Cefali and R. T. Raines, *ChemSusChem*, **2010**, 3, 1268-1272.
24. A. S. Das, M. Pillinger and A. A. Valente, *J. Catal.*, **2005**, 229, 414-423.
25. A. S. Das, S. Lima, D. Carriazo, V. Rives, M. Pillinger and A. A. Valente, *J. Catal.*, **2006**, 244, 230-237.
26. D. Mercadier, L. Rigal, A. Gaset and J. P. Gorrichon, *J. Chem. Technol. Biotechnol.*, **1981**, 31, 489-496.
27. C. Moreau, R. Durand, S. Razigade, J. Duhamet, P. Faugeras, P. Rivalier, P. Ros and G. Avignon, *Appl. Catal. A: Gen.*, **1996**, 145, 211-224.
28. F. S. Asghari and H. Yoshida, *Ind. Eng. Chem. Res.*, **2006**, 45, 2163-2173.
29. M. L. Mendnick, *J. Org. Chem.* **1962**, 67, 398-403.
30. H. H. Szmant and D. D. Chundury, *J. Chem. Technol. Biotechnol.*, **1981**, 31, 135-145.

31. J. D. Chen, B. F. M. Kuster and K. V. D. Wiele, *Biomass Bioenergy*, **1991**, *1*, 217-223.
32. J. Jow, G.L. Rorrer and M. C. Howley, *Biomass*, **1987**, *14*, 185-194.
33. C. Moreau, R. Durand, D. Peyron, J. Duhamet and P. Rivalier, *Ind. Crops Prod.*, **1998**, *7*, 95-99.
34. J. J. Miller and P. L. De Benneville, *J. Org. Chem.*, **1957**, *22*, 1268-1269.
35. Y-L. Zhu, H-W. Xiang, Y-W. Li, H. Jiao, G-S. Wu, B. Zhong and G-Q. Guo, *New J. Chem.*, **2003**, *27*, 208-210.
36. Z-N. Liu, W-G. Jin, Q. Shin, M-B. Hou and D-B. Jhu, *Shiyou Huagong*, **1999**, *28*, 39-49.
37. K. Hamada, H. Yoshihara and G. Suzukamo, *J. Oleo Sci.*, **2001**, *50*, 533-541.
38. H. H. Harry and D. D. Chundury, *J. Tech. Biotech.*, **1981**, *31*, 205-212.
39. W. Yang and A. Sen, *ChemSusChem*, **2011**, *4*, 349-352.
40. A. Takagaki, M. Ohara, S. Nishimura and K. Ebitani, *Chem. Lett.*, **2010**, *39*, 838-840.
41. A. Takagaki, M. Ohara, S. Nishimura and K. Ebitani, *Chem. Comm.*, **2009**, 6276-6278.
42. M. Ohara, A. Takagaki, S. Nishimura and K. Ebitani, *Appl. Catal. A: Gen.*, **2010**, *383*, 149-155.
43. K. J. Zeitsch, *The Chemistry and Technology of Furfural and its many by-products*, Elsevier Sciences B. V., First Ed. 2000.
44. M. A. Harmer, W. E. Farneth and Q. Sun, *J. Am. Chem. Soc.*, **1996**, *118*, 7708-7715.
45. M. A. Harmer and Q. Sun, *Appl. Catal. A: Gen.*, **2001**, *221*, 45-62.

46. It was hard to get the rhamnulose with both an isolation method and material order to the supplier.
47. P. G. Hobman, *J. Dairy Sci.*, **1984**, 67, 2630-2653.
48. K. Yamaguchi, T. Sakurada, Y. Ogasawara, and N. Mizuno, *Chem. Lett.*, **2011**, 40, 542-543.
49. Y. Ogasawara, S. Itagaki, K. Yamaguchi and N. Mizuno, *ChemSusChem*, **2011**, 4, 519-525.
50. A. H. Tashijan, E. J. Armstrong, J. N. Galanter, A. W. Armstrong, R. A. Arnaout, H. S. Rose, *The PathoPhysiologic Basis of Drug Therapy* ; Chapter 35 – Pharmacology of the Bacterial Cell Wall. *Principles of Pharmacology*. ed. by E. G. David, Lippincott Williams and Wilkins, 2005, pp. 569.

Chapter 3

*A Direct and Facile Synthesis of 1,6-Hexanediol
from Bio-based HMF over Heterogeneous Pd/ZrP
Catalyst using Formic Acid as Hydrogen Source*

A Direct and Facile Synthesis of 1,6-Hexanediol from Bio-based HMF over Heterogeneous Pd/ZrP Catalyst using Formic Acid as Hydrogen Source

Abstract

5-hydroxymethylfurfural (HMF), dehydration product of hexoses, is one of the most promising platform chemicals in the bio-refinery, and it is called as “*sleeping giant*” in the field of intermediate chemicals derived from renewable sources. In this research, hydrogenolytic ring opening of HMF to 1,6-hexanediol (HDO) by a transfer hydrogenation is examined over various Pd/Zirconium phosphate (ZrP) catalyst under milder reaction conditions in the presence of formic acid as a hydrogen source as. Various Brønsted and/or Lewis acidic supports were screened for the efficient ring opening of HMF to HDO among which Pd/ZrP exhibited a significant activity due to the specific Brønsted acidity on ZrP support, which accelerates the cleavage of C-O bond in the furan ring. The 7 wt% Pd/ZrP catalyst (50 mg) afforded 43% yield of HDO from HMF (1 mmol) in ethanol solvent (3 mL) using FA (22 mmol) at 413 K for 21 h. The Pd/ZrP catalyst was easily separated from the reaction mixture and reusable at least 5 times without any significant loss of activity and selectivity. To the best of our knowledge, such a high yield of HDO from HMF is reported for the first time without using high pressure H₂ gas.

3.1 Introduction

Nowadays concern about global warming effect due to increased CO₂ generation and depletion of fossil fuel resources fascinated the society to substitute current energy system (coal, petroleum) with new renewable energy sources. The concept of producing materials from renewable natural sources is well known from generations. People have been wearing woolen clothing and building wooden houses for thousands of years. Lignocellulosic biomass is a promising feedstock, which is abundant, cheaper and potentially more sustainable than conventional fossil resources¹⁻³ together with it has the inherent property to displace petroleum feedstock to produce transportation fuel and polymer precursors. In this respect, the development and implementation of novel and realizable strategies for production of commodity chemicals from renewable bio-resources is the prime target for researchers these days.

5-hydroxymethylfurfural (HMF), which can be synthesized by dehydration of hexoses using various homogeneous and heterogeneous catalysts, is one of the most promising platform chemicals in the bio-refinery process and is regarded as “sleeping giant” in the field of intermediate chemicals from renewable sources.⁴⁻¹⁰ HMF has been successfully transformed into various useful chemicals like 2,5-furandicarboxylic acid,^{11,12} levulinic acid,¹³⁻¹⁶ 2,5-diformylfuran,^{17,18} succinic acid¹⁹ and 2,5-dimethylfuran^{20,21} which may serve as building blocks in advanced polymers.

Ring opening hydrolysis followed by hydrogenation of furan compounds is a major process to obtain linear alkane from biomass conversion. A large number of studies on production of fuel and chemicals has been conducted in petroleum industry for more than a century, thus provide us with enormous knowledge on the processes. On the other

hand the understanding on production of saturated hydrocarbon from biomass conversion is very limited.

Herein, I report a new approach for the production of 1,6-hexanediol (HDO, a linear-diol with two primary hydroxyl groups) from inedible biomass. HDO is extensively used in the production of polyesters for polyurethane elastomers, coatings, adhesives and polymeric plasticizers.²² The major route for HDO synthesis involves the hydrogenation of adipic acid or its esters using various homogeneous or heterogeneous catalysts.^{23,24} Very recently, Buntara *et al.* employed a novel methodology for converting HMF to HDO over 2 to 5 steps process under high pressure H₂ (10-80 bar) using ReO_x-modified Rh based catalyst. The 5 steps process leads to high selectivity of HDO but it shows low yield (4%). Moreover, the large number of steps and purification of product in each step makes the overall process environmentally and economically unbenign. An effort of one-step hydrogenation of HMF employing severe conditions (543 K, 150 bar H₂) afforded less than 4% yield of HDO, whereas the two step process coupled with Nafion SAC 13 gave overall yield of 86% HDO in water.²⁵⁻²⁷ Two other research groups of Chen *et al.*²⁸ and Chia *et al.*²⁹ produce HDO by utilizing tetrahydro-2H-pyran-2-ylmethanol (THPM) as a substrate (HMF derivative), using same catalyst at 393 K with 34 bar H₂. Employment of high pressure H₂ is difficult to handle and require an expensive facility. Thus, an inexpensive and more viable alternative of pressured H₂ is the need of the hour.

Formic acid (FA, HCOOH), has been identified as a safe, convenient and economic hydrogen carrier among other organic compounds such as tetrahydroquinoline, methylpyrrolidine and cyclohexene³⁰. Moreover, FA can be traditionally obtained from biomass processing and produces no waste products.³³⁻³³ FA has been employed by many researchers for various organic transformations.^{20,34-37} In spite of tremendous research

efforts in the field of FA dissociation to produce H₂, the number of catalysts that have prominent activity under practical conditions are limited.

The hydrogenolysis of HMF to HDO may proceed through 2 key reactions, (1) deoxygenation of furan ring (C-O bond cleavage) by Brønsted-acid catalytic sites and (2) hydrogenation of C=O and C=C bond by the metal catalytic sites. In this study, I attempted to use zirconium phosphate (ZrP) as acidic supports which have attracted considerable attention as potential solid acid catalysts³⁸⁻⁴⁰ for dehydration of alcohols,^{41,42} isomerization of olefins,^{43,44} hydrogenation⁴⁵ and hydrodeoxygenation reactions.^{46,47} Transition metals such as Pd are most frequently used for transfer hydrogenation reactions.^{48,49} On the basis of literatures,^{25,48,49} I surveyed acid-based supports for ring cleavage and Pd as metal for hydrogenation.

3.2 Experimental Section

3.2.1 Materials

Zirconium chloride oxide octahydrate (ZrOCl₂·8H₂O), sodium dihydrogen phosphate (NaH₂PO₄·2H₂O), nitric acid, silica gel, hexane, ethylacetate, ethanol and naphthalene were purchased from Kanto Chemicals Co. Inc. 5-hydroxymethyl-2-furfural (HMF) was provided by Aldrich. Formic acid, Niobic acid, SO₄/ZrO₂, Pd(NO₃)₂, Pd/C, Pd/Al₂O₃, PdO and Pd standard were supplied by Wako Chemicals. JRC-Z-HY-5.5 was bought from Tosoh Co. Ltd. JRC-Z5-90H(1) and JRC-SAH-1 was obtained from Totori University and Catalysts and Chemicals Industries Co. Ltd respectively.

3.2.2 Synthesis of ZrP

Zirconium phosphate (ZrP) with a molar ration of P/Zr=2 has been prepared by mixing aqueous solution of 0.1 M ZrOCl₂·8H₂O (100 mL) and 0.2 M sodium dihydrogen

phosphate (100 mL) at pH 1-2, dropwise with continuous stirring at 343 K. Gelatinous precipitates obtained was digested for 1 h at 343 K, filtered, washed with water and dried at room temperature. Material was converted to acid form by treating material (5 g) with 1 M HNO₃ (50 mL) for 30 min, with occasional shaking. Sample was then separated from acid by decantation and washed with distilled water for removal of adhering acid. Acid treatment was repeated at least five times. After final washing the material was dried at room temperature, was characterized with XRD, BET and used for further studies.

3.2.3 Synthesis of Pd/ZrP

Pd/ZrP was prepared by an adsorption method. Pd(NO₃)₂ (7 wt%) was taken in 50 mL of water ZrP (1 g, BET surface area 140 m²g⁻¹, pore volume 0.34 cm³g⁻¹) and stirred for 2 h at room temperature. The solid was filtered, washed with water and dried at room temperature for overnight under vacuum. Calcination in air at 773 K for 6 h gave a material with 7 wt% Pd/ZrP.

3.2.4 Hydrogenolysis of HMF

The hydrogenolysis of HMF was carried out in capped glass pressure tube containing (126 mg, 1mmol) of HMF, 3 mL Ethanol, 50 mg of Pd/ZrP as a catalyst and 1 ml of HCOOH as a source of hydrogen at the reaction condition of T = 413 K under magnetic stirring of 500 rpm. After 24 h the reaction was cooled at room temperature. Then, it was diluted with acetone and naphthalene (130.7 mg, 1 mmol) was added as an internal standard. The catalyst was separated by centrifugation, and the liquid was analyzed by a Shimadzu GC-17A Gas Chromatography with Aglient DB-1 column and a flame ionization detector.

The reaction mixture was evaporated in a rotary evaporator to remove ethanol and was concentrated in *vacuo*, the residue was purified by a silica gel (60 N, Kanto Chemicals) column, eluted with hexane-ethyl acetate solvent system (8:2-2:8) to give HDO (0.467 g, 39.5% from 10 mmol of reactant, in a set of 5 batch reactions of 2 mmol each) as a white to pale yellow solid product. The ^1H and ^{13}C -NMR were recorded in CDCl_3 using TMS as internal standard and was compared with the authentic sample.

3.2.5 Characterizations

Characterization of the catalyst was conducted using several techniques. X-ray diffraction pattern (XRD) was recorded with a Rigaku Smart Lab diffractometer using $\text{Cu K}\alpha$ radiation within $2\theta = 2\text{--}80$ range. Transmission Electron Microscopy (TEM) study was carried out in a Hitachi H-7100 instrument operating at an accelerating voltage at 100 kV. TEM samples were prepared by dispersing the catalyst powder in ethanol under ultrasonic radiation for 1-2 min, and then the resulted solution was dropped on a copper grid followed by slow evaporation of solvent under vacuum at room temperature. Nuclear Magnetic Resonance (NMR) spectroscopy was executed on Brücker advance 400 MHz instrument using CDCl_3 as a solvent.

3.3 Results and discussion

3.3.1 Catalytic Activity

Various Brønsted and/or Lewis acidic supports were screened for the hydrogenolytic ring opening of HMF to HDO in the presence of FA as a hydrogen source as shown in **Table 1**. The products obtained from the hydrogenolysis of HMF with Pd/ZrP catalyst in the presence of FA includes 5-methylfurfural (MF), 2,5-hexanedione (HDN), HDO,

tetrahydrofuran-2,5-dimethanol (THFDM) and 2,5-dimethylfuran (DMF). The selectivity for the formation of HDO considerably varied for the different acidic supports and Pd/ZrP exhibited the best catalytic activity for HDO in high yield (42.5%) (entries 1-10). The Brønsted:Lewis acid site ratio for different solid acid catalysts was compared by Huber *et al.*⁵⁰ Among them, ZrP had the highest ratio. Accordingly the reason for high activity of ZrP is its high Brønsted:Lewis acid site ratio as compared to zeolites, Al₂O₃ and SiO₂-Al₂O₃, thus decreasing the carbon mass balance for these catalysts.

Post synthetic treatment of ZrP with dilute nitric acid enhanced the activity, showing an increase in the carbon mass balance than the non-treated ZrP (entries 1-2). This is because the Brønsted-site can be increased by the acid treatment of material with dilute acid.⁵¹ The loss of framework SiAlOH units with increase of Si/Al molar ratio was attributed to decrease of densities of the acid site (Brønsted + Lewis) for ZSM-5 (Si/Al= 90 or 12), HY zeolite (Si/Al= 5.5), SiO₂-Al₂O₃, (Si/Al=1), and it disfavored HDO formation (entries 4, 6-7, 10). Nb₂O₅ and sulphated ZrO₂ showed lower activity than ZrP for hydrogenolysis and/or hydrogenation, thereby the carbon mass balances were very low (entries 5 and 9). On the contrary, Pd/Al₂O₃ catalyzed the ring hydrogenation reaction over ring hydrogenolysis to afford THFDM as the major product, which in turn increased the carbon mass balance (entry 8).

TEM image and particle size distribution (**Figure 1**) showed that the various supports such as HY zeolite, ZSM-5, SiO₂-Al₂O₃ and sulphated ZrO₂ could afford small sized Pd NPs (mean diameter 3.1-3.3 nm), however, the activities of these catalysts were not so high. Accordingly, I found that the present activity has no correlation with the particle size of Pd NPs. It is well known that hydrogenation reactions do not depend on the size of the metal particles.⁵²⁻⁵⁴

Table 1: Hydrogenolysis of HMF over various palladium catalysts^a

Entry	Catalyst	Conv./%	Yield/ %				Mean Particle		C Mass balance ^c
		HMF	HDO	HDN	THFDM	MF	DMF	size/nm ^b	
1	Pd/ZrP	92.5	37.8	15.2	12.1	4.6	2.4	4	77.9
2	Pd/ZrP ^d	96.9	42.5	16.2	15.6	4.8	2.5	11.9	84.2
3	Pd/ZrP ^e	72	26.9	12.7	0	4.3	1.6	-	63.2
4	Pd/HY zeolite ^f	70.4	27.4	0	5.1	0	0	4.3	46.2
5	Pd/Nb ₂ O ₅	93.3	20.7	12.3	0	0	0	- ^k	35.4
6	Pd/ZSM-5 ^g	90.4	17.3	10.3	38.2	4.5	0	- ^k	77.8
7	Pd/SiO ₂ -Al ₂ O ₃ ^h	90.9	15.8	17.5	30.1	2.3	1.9	3.3	74.4
8	Pd/Al ₂ O ₃	>99	13.3	25.5	30.6	0	16	10.4	85.5
9	Pd/SO ₄ /ZrO ₂	39.1	5.1	0	0	0	0	3.1	13
10	Pd/ZSM-5 ⁱ	54.1	3.2	1.8	0	0	0	3.5	9.2
11	ZrP	50.4	0	0	0	0	0	-	0
12	Pd(NO ₃) ₂	61.6	trace	0	0	0	0	-	0.2
13	PdO	86.2	14.3	7.5	0	trace	trace	-	25.4
14	Blank	78.7	0	0	0	0	0	-	0
15 ^j	Pd/ZrP	84.3	7.5	33.7	0	0	0	-	48.9
16 ^j	Blank	79.6	0	0	0	0	0	-	0

^a**Reaction conditions:** HMF (1 mmol), EtOH (3 mL), FA (22 mmol), 413 K, 21 h, 5 wt% Pd catalyst (50 mg). ^bDetermined by TEM observation.^cDetermined on the basis of observed HDO, HDN, THFDM, MF and DMF products. ^d7 wt% Pd catalyst. ^eWithout post acid treatment. ^fJRC-Z-HY5.5 (Si/Al=2.8). ^gSi/Al=12. ^hJRC-SAH-1 (Si/Al=2.1). ⁱJRC-Z5-90H(1) (Si/Al=45). ^jWithout FA. ^kParticles and support were hardly distinguished.

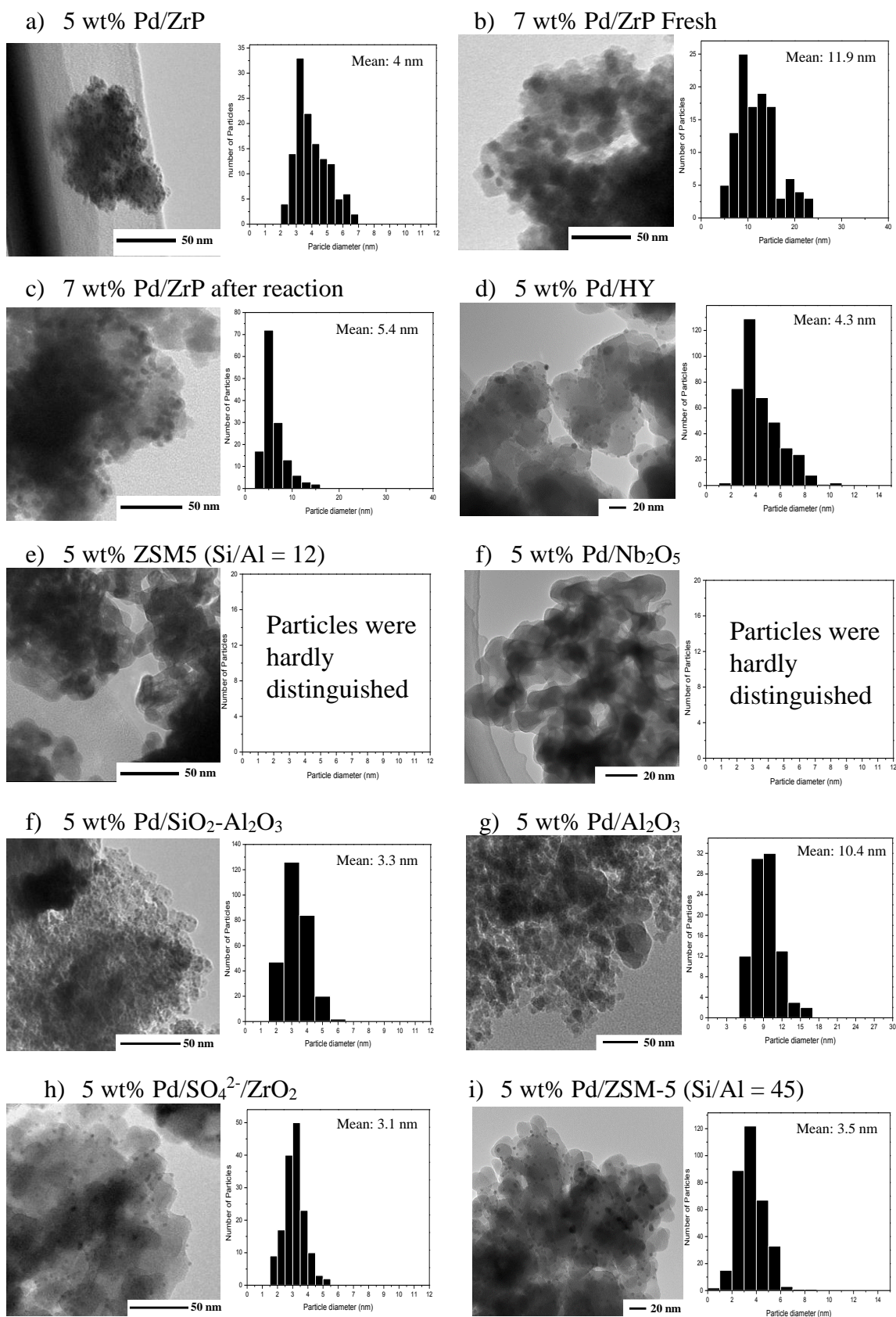


Figure 1: TEM images and particle size distribution of various Pd supported catalysts.

The hydrogenolytic ring opening of HMF demands a high Brønsted:Lewis acid ratio, whereas the role of palladium is to dissociate formic acid, leading to the hydrogenation reaction. The activity of the Pd/ZrP catalyst was studied by further experiments as discussed hereafter. Almost half of the HMF could be converted with no yield of HDO in the presence of only support (ZrP, **Table 1**, entry 11) probably by cause of the adsorption of the substrate on the support. Pd(NO₃)₂, metal source used for preparation of the active catalyst, was itself inactive (**Table 1**, entry 12). PdO exhibited activity on a high conversion of HMF but no yield of HDO because of the levulinate ethyl ester formation in the presence of FA (**Table 1**, entries 13). A control experiment without Pd catalyst afforded high HMF conversion and humin formation in the presence of FA only (**Table 1**, entry 14). In HMF conversion in the absence of FA, the acidic proton on Pd/ZrP managed to yield HDO in 7.5% yield. On the other hand, the absence of both catalyst and FA failed to achieve the hydrogenolysis of HMF to HDO (**Table 1**, entries 15-16). These results clarified the significance of both Pd/ZrP and FA for an efficient single step synthesis of HDO from HMF.⁵⁵

In order to understand the reaction pathway, the time course of the HMF hydrogenolysis was monitored. The conversion of HMF and yields of various products are plotted as a function of time in **Figure 2**. At a reaction time of 3 h, 85% conversion of HMF was achieved, and the primary products (HDO and HDN) were formed. The competitive products like MF and THFDM were produced at 6 h of reaction progress, whereas DMF was obtained in the reaction mixture above 9 h. The yield of HDO reached maxima of 42.5% (HMF conv. 96.9%) after 21 h. These phenomena were also observed in recycling runs. A conversion of 45% was observed even at 0.5 h of reaction progress, demonstrating the facile adsorption of HMF on the catalyst surface. Subsequently,

adsorbed HMF is converted into products. A significant effect on conversion rate of HMF and HDO was noticed with additional experiments.

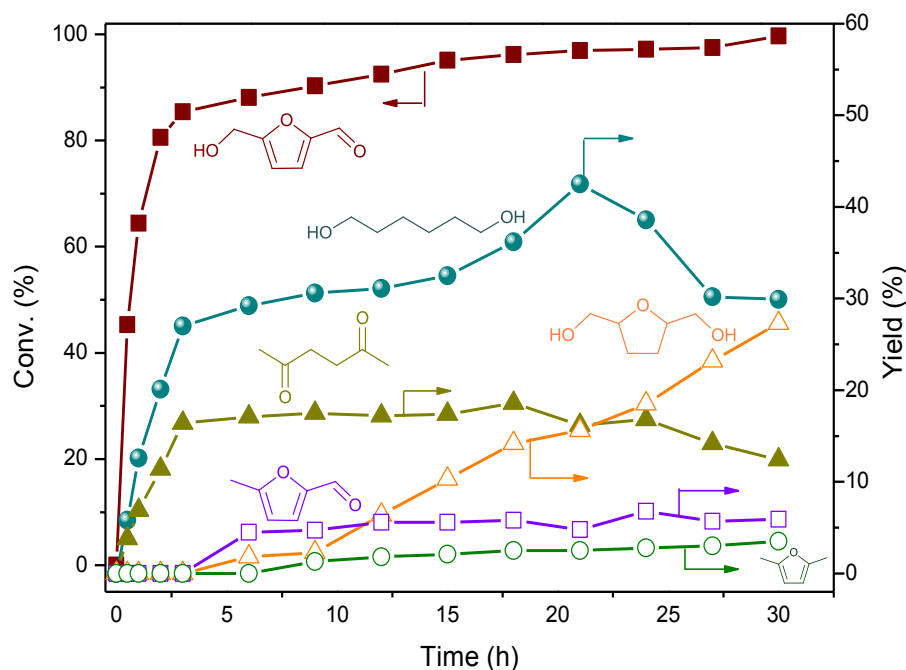


Figure 2: Time course for hydrogenolysis of HMF over Pd/ZrP.

Reaction Conditions: HMF (1 mmol), FA (22 mmol), EtOH (3 mL), 7 wt% Pd/ZrP (50 mg), 413 K.

The rates of consumption of both HMF and HDO were suppressed in the presence of one another, which may explain the maxima for HDO yield (**Figure 3**). A detailed product analysis by GC-MS revealed that HDO is slowly converted into oxepane at longer reaction times. **Figure 3** (a,b) demonstrates the slower conversion of each substrate in presence of another one. The comparative study exhibited HMF's greater affinity for the catalyst surface which in turn caused the higher conversion.

High HDO yields from 15 to 21 h (30 to 42.5%) with low concentration of HMF (<2%) in **Figure 2** are due to the conversion of adsorbed HMF into products with the progress of time (as total product yield increases with time). In **Figure 2**, a conversion of 45% was observed even at 0.5 h, however, in the next half an hour, I can notice only

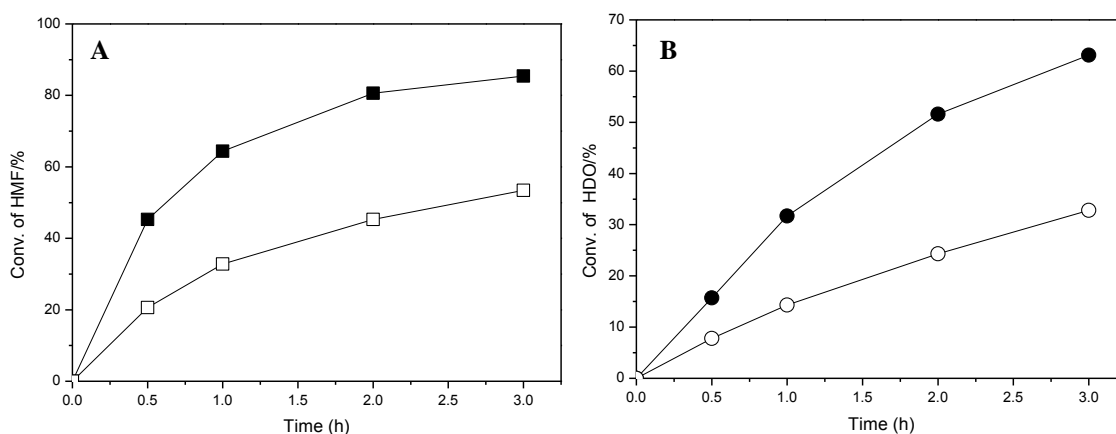


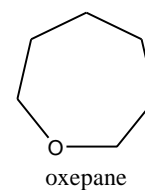
Figure 3: Time course for conversion of (a) HMF and (b) HDO.

Reaction conditions: Substrate (total 1.0 mmol), 7wt% Pd/ZrP (50 mg), EtOH (3 mL), FA (22 mmol), 413 K.

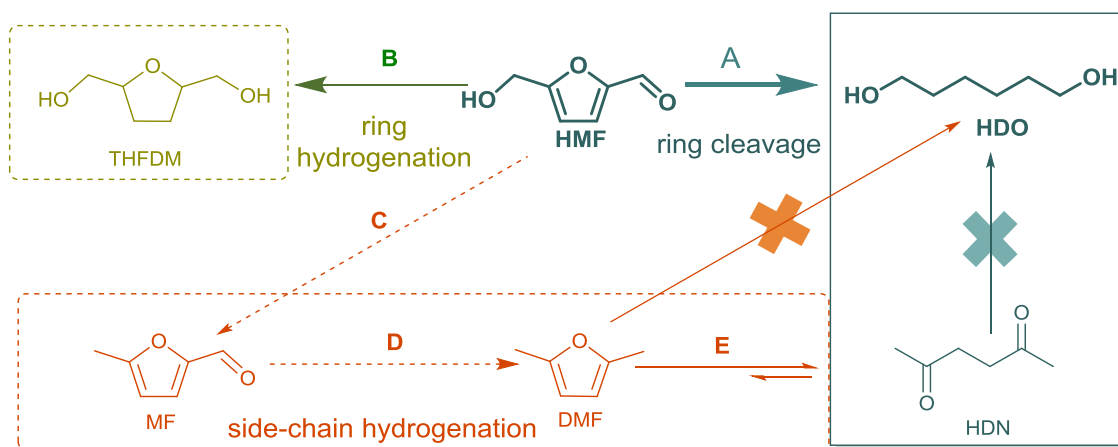
(a) closed square (HMF (1.0 mmol) only), open square (HMF (0.5 mmol) in the presence of HDO (0.5 mmol))

(b) closed circle (HDO (1.0 mmol) only), open circle (HDO (0.5 mmol) in the presence of HMF (0.5 mmol))

19% conversion of HMF, with decreasing to 16% in the next 1 hour. Formation of products leads to slow consumption of HMF, which may be explained by the decrease in initial rate of HMF consumption when HDO was present from the beginning in the above **Figure 3 (a)**. HMF conversion decreased to 21% from 45% by HDO. Similar results were obtained for HDO conversion with the conversion drooping to 8% from 16% after half an hour (**Figure 3 (b)**). The above results indicated that the consumption of both HMF and HDO are suppressed in the presence of one another. Thus, after 21 h when HMF conversion exceeds >95%, the rate of consumption of HDO increases which exhibited a HDO maxima at 21 h. The reaction of HDO as substrate under the same reaction condition slowly produced oxepane by intramolecular dehydration (analyzed by GC-MS).



The reaction pathway for hydrogenolysis of HMF over the synthesized Pd/ZrP is proposed as **Scheme 1**, based on the time course (**Figure 2**), which clearly demonstrated the simultaneous conversion of HMF to HDO, THFDM and HDN. Moreover, even under longer reaction time, no significant change in product distribution was observed, indicating that the ring hydrogenolysis to HDO (**Scheme 1**, step A) or HDN (**Scheme 1**, steps C, D & E) or ring hydrogenation to THFDM (**Scheme 1**, step B) progressed as competitive reaction. MF and DMF were formed in small amounts from HMF as hydrogenation product (**Scheme 1**, steps D and E). Such proposed reaction scheme was in agreement to the observed trend of THFDM, MF, DMF and HDN as substrate under the similar reaction conditions as reported in **Table 2**; no HDO formation is noticed from the hydrogenolysis of MF, DMF and THFDM.



Scheme 1: Various possible reaction pathways from HMF.

In order to certify the formation route of HDO from the hydrogenolysis of HMF ring or THFDM ring, the hydrogenolysis of THFDM on Pd/ZrP was carried under the same reaction conditions, however no HDO or HDN is detected (**Table 2**, entry 5). It indicates that the reaction route from THFDM to HDO is negligible. These results are in correlation with previous studies that the hydrogenolysis of tetrahydrofuran ring is not

possible under those conditions; in which furan ring hydrogenolysis occurs.^{56,57} The results of MF and DMF as a substrate (**Table 2**, entries 2 and 3) suggested that MF is hydrogenated to DMF and successively to HDN. Under the present conditions, the rate of ring cleavage of DMF to HDN is faster than the side chain hydrogenation of HMF to MF and then to DMF. This is the reason why MF and DMF appears late in the reaction progress.

Table 2 : Reactions from different substrates^a

Entry	Starting reagent	Conv./%	Yield/ %				
			HDO	HDN	THFDM	MF	DMF
1	HMF	96.9	42.5	16.2	15.6	4.8	2.5
2	MF	71.1	0.0	23.1	0.0	-	26.6
3	DMF	83.2	0.0	79.6	0.0	0.0	-
4	HDN	21.3	0.0	-	0.0	0.0	11.9
5	THFDM	74.5	0.0	0.0	-	0.0	0.0

^a**Reaction Conditions:** Substrate (1 mmol), EtOH (3 mL), FA (22 mmol), 7 wt% Pd/ZrP (50 mg), 413 K, 21 h.

According to stoichiometry, 8 atoms of hydrogen are required for the conversion of HMF to HDO. To meet the requirement, experiments with different FA amount were performed and compiled in **Table 3**. In fact, 22 mmol of FA produced HDO in highest yield over 7 wt% Pd/ZrP, where 8.2 mmol of FA were consumed. The highest efficiency of FA was observed when using 11 mmol of FA with high metal content *i.e.* 10 wt% Pd/ZrP to achieve the highest yield of HDO (43.6%). High metal content catalyst can break the FA more efficiently than the low metal content catalyst. However, the same yield of HDO could also be obtained using low metal content (7 wt%) catalyst and high FA amount. Therefore, I discouraged the use of high metal content catalyst. In the absence of FA, HDN was formed in major amounts while HDO was also detected in small quantity due to acidity of ZrP surface. When I added the FA, the HDO formation was enhanced

with the decrease of HDN. High acid amount favours a ring hydrogenation to THFDM, which could not be further cleaved into HDO as tetrahydrofuran rings are quite stable. This is the reason that the reaction conditions; favours step B, leads to diminish the progress for step A. On the other hand, it is known that HDN formation is favoured in acidic environment,⁵¹ but high FA content declines the yield of HDN because of the competitive THFDM formation.

Table 3: Effect of formic acid amount^a

Entry	FA / mmol	Conv./%	Yield/ %					Consumed FA/mmol
		HMF	HDO	HDN	THFDM	MF	DMF	
1	0	78.5	5.3	30.5	0	0	0	0
2	11	81.5	24.6	16.5	8.9	0	0	5.7
3 ^b	11	96.7	43.6	15.8	15.7	0	0	7.1
4	16	85.4	28.5	19.1	14.6	0	0	6.8
5	22	96.9	42.5	16.2	15.6	4.8	2.5	8.2
6	32	97.4	30.7	20.8	20.3	5.6	11.1	8.4
7	44	>99	15.2	25.2	26.5	10.6	11.8	8.6
8	65	>99	0	30.6	35.6	14.2	12.1	9.2

^a**Reaction Conditions:** HMF (1 mmol), EtOH (3 mL), 7 wt% Pd/ZrP (50 mg), ^b10 wt% Pd/ZrP, 413 K, 21 h.

Furthermore the hydrogenolysis of HMF to HDO was screened over various Pd amount loading on ZrP as summarized in **Table 4**. It was seen that yield of HDO increased with increase in Pd loading till 7 wt% of Pd/ZrP. Further increase in Pd loading significantly reduces the HDO yield and leads to the high amount of formation of by-products.

Table 4: Screening of metal loading of Pd on ZrP^a

Entry	Pd Loading/ wt%	Conv./%		Yield/ %			
		HMF	HDO	HDN	THFDM	MF	DMF
1	0.1	84.7	27.5	0	0	0	0
2	0.3	86.5	32.3	0	6.7	3.4	0
3	0.5	92.5	37.8	15.2	12.1	4.6	2.4
4	0.7	96.9	42.5	16.2	15.6	4.8	2.5
5	0.8	97.7	35.3	14.5	20.8	5.2	4.4
6	1	98.5	28.3	18.5	24	2.7	4.6

^a**Reaction Conditions:** HMF (1 mmol), EtOH (3 mL), Catalyst (50 mg), FA (22 mmol), 413 K, 21 h, 500 rpm.

3.3.2 XRD of the fresh and used catalyst

It can be seen from **Figure 4** that, ZrP formed is amorphous. XRD pattern of Pd/ZrP calcined at 500 °C showed peak for PdO, Pd is in PdO phase after calcinations. Pd/ZrP after reaction and dried at room temperature showed a characteristic peak for Pd(0), this confirmed that PdO is reduced to Pd during the reaction. Pd/ZrP_after recal *i.e.* Pd/ZrP after reaction and calcinations at 500 °C showed that the Pd again converted to PdO after calcination. That ensures that active site could be regenerated.

3.3.3 Proposed Reaction Mechanism

The present hydrogenolysis of HMF to HDO is proposed to consist of 6 major steps, marked as steps 1-6 in **Figure 5**. In step 1, HMF is adsorbed on the catalyst surface by the electrostatic interactions with both metal as well as acidic ZrP support. The step 2 was proposed based on previous literature,^{49,50} wherein ZrP was held responsible for the furan ring opening with the loss of ring oxygen. In this case, the scissoring of furan ring would have most probably formed hex-1,3-5-triene-1,6-diol (steps 2 & 3). This expected intermediate (hex-1,3-5-triene-1,6-diol) is commercially unavailable but was assumed to appear at a retention time of 6.96 min in GC chromatogram. The same peak was observed with a high intensity for reactions performed without FA. The dissociation of FA (step 4)

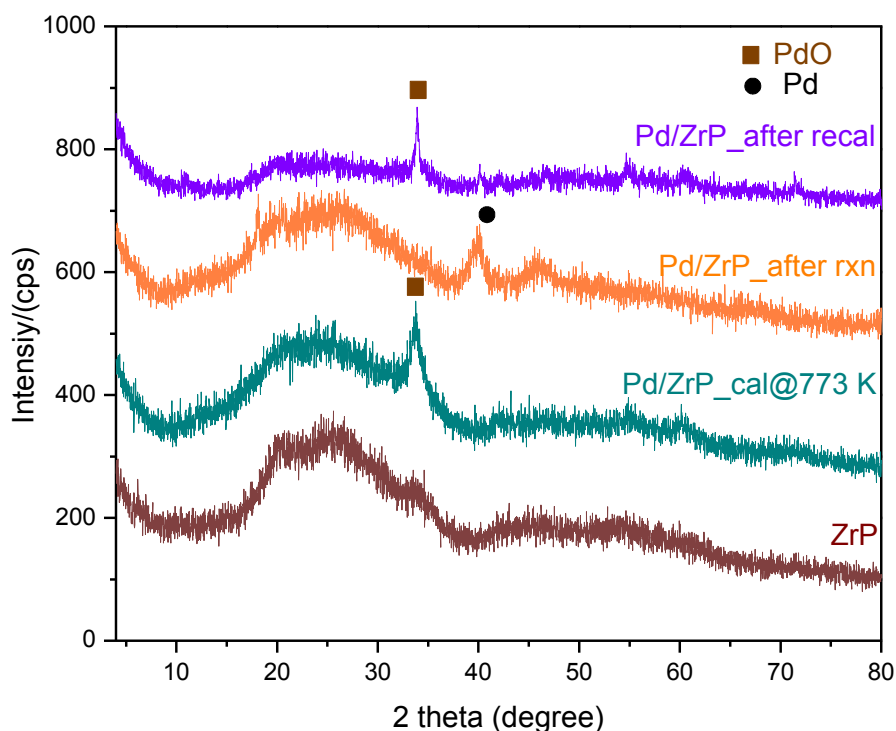


Figure 4: XRD patterns of Pd/ZrP.

may occur at the initial stages of the reaction, however, in order to maintain a cascade of reaction it is shown as step 4. The product generated in step 3 can undergo keto-enol tautomerism (**Figure 5**, step 5). The enol form is expected to dominate in polar protic solvent (ethanol). The ratio of the peak intensity at 6.96 min to that of internal standard (naphthalene) was found to decrease with increasing metal loading on the catalyst. The highest ratio was observed in the absence of FA, which was possibly due to the absence of hydrogen source for hydrogenation of double bonds. The reason for the appearance of the peak for low metal loading could be explained by the inefficient dissociation of FA with low metal content on the catalyst surface. The final step was the hydrogenation of the double bonds to form HDO using Pd/ZrP with FA as the hydrogen source (**Figure 5**, step 6).

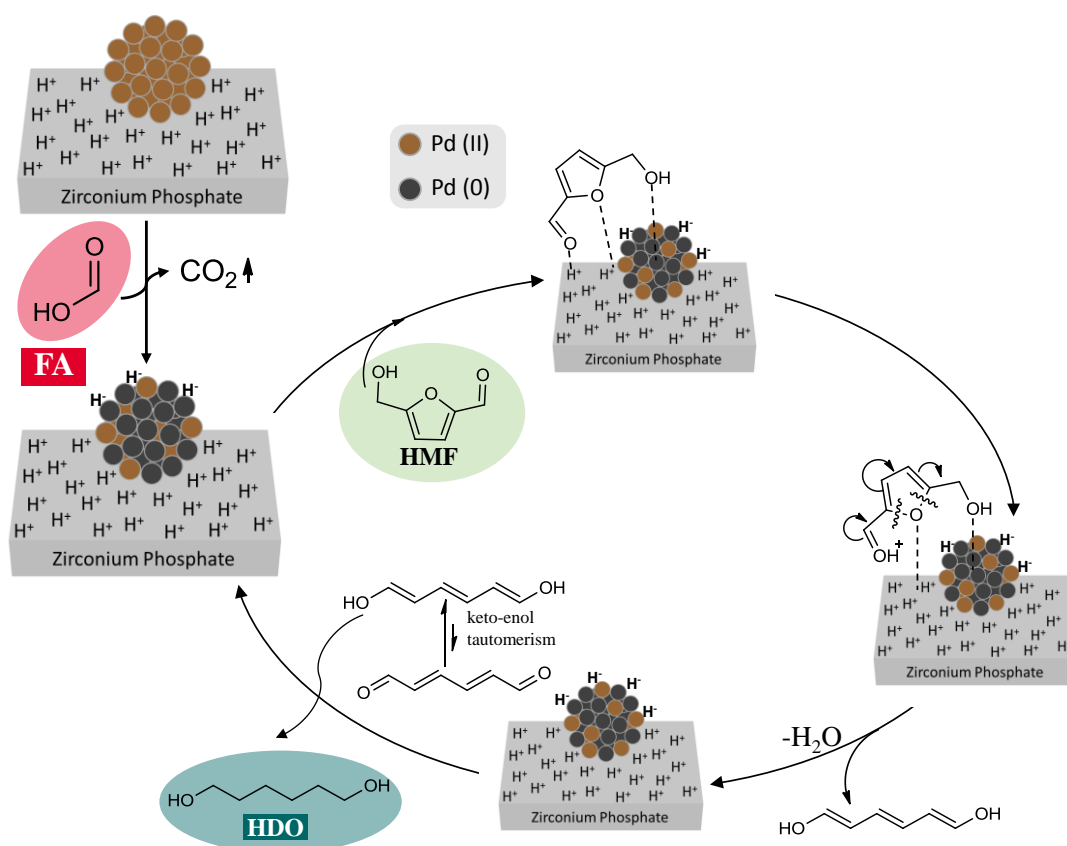


Figure 5: Proposed mechanistic steps demonstrating the role of Pd/ZrP and FA in hydrogenolysis of HMF to HDO in the presence of FA.

3.3.4 Recyclability

The recyclability is an important property of heterogeneous catalyst, so the reusability of the catalyst Pd/ZrP was investigated. The catalyst was simply recovered by centrifugation, through washing with ethanol, drying in vacuum for overnight followed by calcination at 773 K for 6 h. The catalyst could be recycled without any significant loss of activity even after 5 cycles (**Figure 6**). Furthermore, the product was isolated using silica gel column chromatography, eluted with hexane-ethyl acetate solvent system (8:2-2:8) to yield HDO in 39.6% yield (0.467 g from 10 mmol of HMF, in a set of 5 batch reactions of 2 mmol each) as a white to pale yellow solid. ¹H- and ¹³C-NMR confirmed the HDO structure (**Figures 7 and 8**).

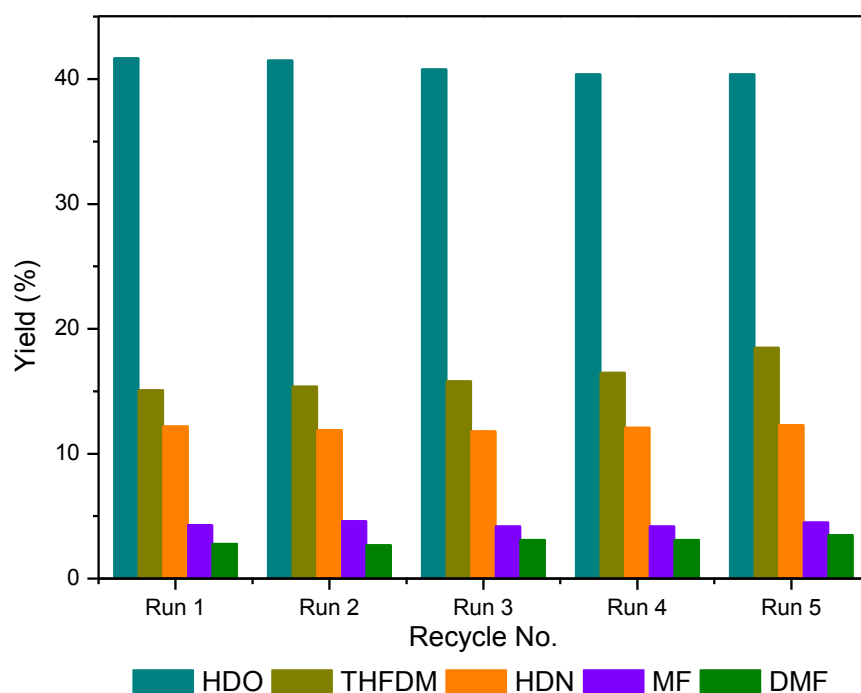


Figure 6: Recyclability of 7 wt% Pd/ZrP for hydrogenolysis of HMF to HDO.

Reaction Conditions: HMF (1 mmol), FA (22 mmol), EtOH (3 mL), 7 wt% Pd/ZrP (50 mg), 413 K, 21 h.

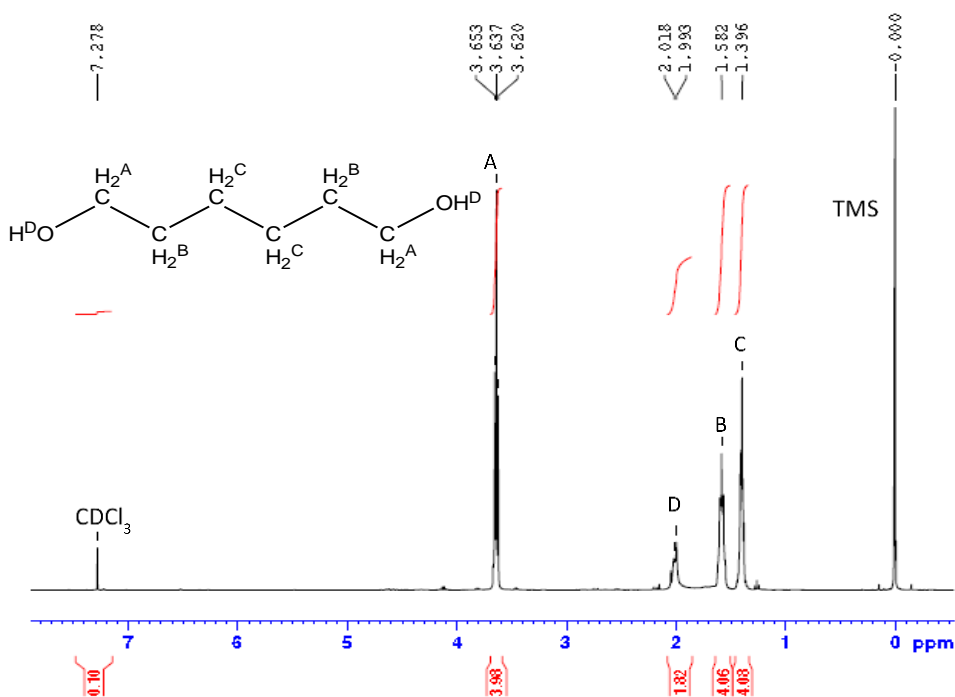


Figure 7: ¹H-NMR of isolated HDO.

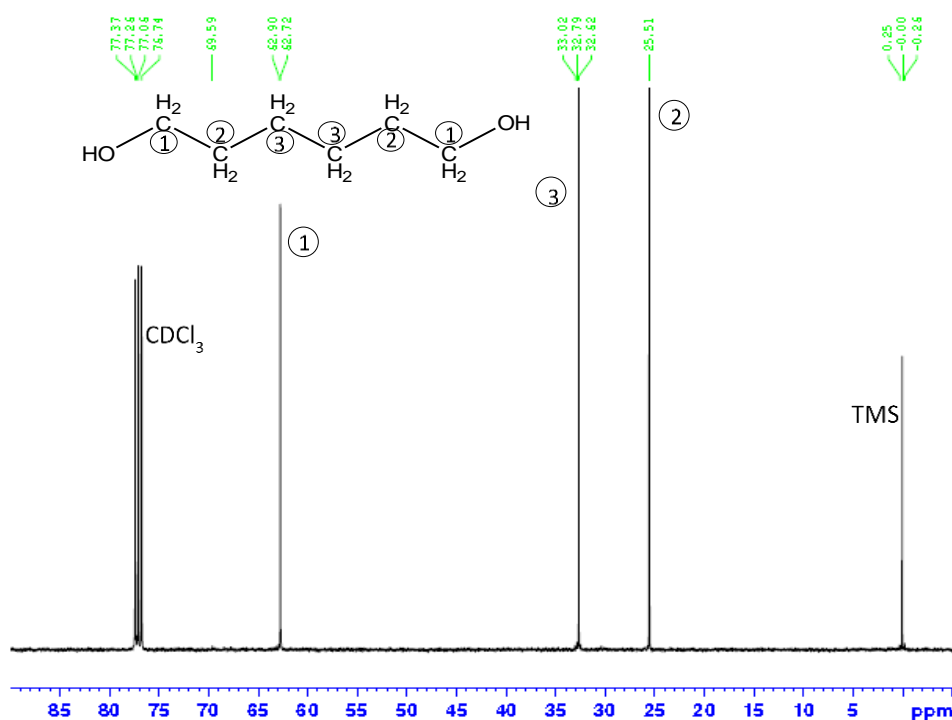


Figure 8: ^{13}C -NMR of isolated HDO.

3.4 Conclusion

In summary, I have developed a new, safe, economical and environmentally benign pathway for the formation of HDO from HMF, a renewable source which can be obtained from hexoses. Using the one-step direct reaction, I converted HMF to yield 43% HDO over reusable Pd/ZrP catalyst and HCOOH as hydrogen source at 413 K for 21 h under an atmospheric pressure. To the best of our knowledge, such a high yield of HDO from HMF is reported for the first time without using high pressure H_2 gas. Experimental data shows that both the catalyst and HCOOH are indispensable for the formation of HDO. It is suggested that the surface acidity for ring cleavage, transition metal for FA dissociation and thereby utilization of in-situ generated hydrogen for hydrogenation are the important aspects for HDO formation from HMF.

3.5 References

1. G. W. Huber, S. Iborra and A. Corma, *Chem. Rev.*, **2006**, *106*, 4044-4098.
2. J. N. Chheda, G. W. Huber and J. A. Dumesic, *Angew. Chem. Int. Ed.*, **2007**, *46*, 7164-7183.
3. G. Berndes and J. Hanson, *Energy Policy*, **2007**, *35*, 5965-5979.
4. K-I. Shimizu, R. Uozumi and A. Satsuma, *Catal. Commun.*, **2009**, *10*, 1849-1853.
5. Takagaki, M. Ohara, S. Nishimura and K. Ebitani, *Chem Commun.*, **2009**, *41*, 6276-6278.
6. J. Tuteja, S. Nishimura and K. Ebitani, *Bull. Chem. Soc. Jpn.*, **2012**, *85*, 275-281.
7. V. V. Ordonsky, J. Van der Schaaf, J. C. Schouten and T. A. Nijhuis, *J. Catal.*, **2012**, *287*, 68-75.
8. M. Bicker, J. Hirth and H. Vogel, *Green Chem.*, **2003**, *5*, 280-284.
9. T. Stahlberg, W. Fu, J. M. Woodley and A. Riisager, *ChemSusChem*, **2011**, *4*, 451-458.
10. I-J. Kuo, N. Suzuki, Y. Yamaguchi and K. C-W. Wu, *RSC Adv.*, **2013**, *3*, 2028-2034.
11. N. K. Gupta, S. Nishimura, A. Takagaki and K. Ebitani, *Green Chem.*, **2011**, *13*, 824-827.
12. A. Villa, M. Schiavoni, S. Campisi, G. M. Veith and L. Prati, *ChemSusChem*, **2013**, *6*, 609-612.
13. B. Girisuta, L. P. B. M. Janssen and H. J. Heeres, *Green Chem.*, **2006**, *8*, 701-709.
14. P. A. Son, S. Nishimura and K. Ebitani, *React. Kinet. Mech. Catal.*, **2012**, *106*, 185-192.

15. R. Weingarten, W. C. Corner Jr. and G. W. Huber, *Energy Environ. Sci.*, **2012**, 5, 7559-7574.
16. V. Choudhary, S. H. Mushrif, C. Ho, A. Anderko, V. Nikolakis, N. S. Marinkovic, A. I. Frenkel, S. I. Sandler and D. G. Vlachos, *J. Am. Chem. Soc.*, **2013**, 9135, 3997-4006.
17. A. S. Amarasekara, D. Green and E. McMillan, *Catal. Commun.*, **2008**, 9, 286-288.
18. A. Takagaki, M. Takahashi, S. Nishimura and K. Ebitani, *ACS Catal.*, **2011**, 1, 1562-1565.
19. H. Choudhary, S. Nishimura and K. Ebitani, *Appl. Catal. A: Gen.*, **2013**, 458, 55-62.
20. T. Thananattathanachon and T. B. Rauchfuss, *Angew. Chem. Int. Ed.*, **2010**, 49, 6616-6618.
21. M. Chidambaram and A. T. Bell, *Green Chem.*, **2010**, 12, 1253-1262.
22. F. C. A. Figuirodo, E. Jorda and W. A. Carvalho, *Appl. Catal. A: Gen.*, **2008**, 351, 259-266.
23. R. H. Fischer and R. Pinkos, F. Stein, US 6,426,438 B1, 2002.
24. R. Jagannathan, S. T. Chaudhari, C. V. Rode and R. V. Chaudhari, *Ind. Eng. Chem. Res.*, **1998**, 37, 2099-2106.
25. T. Buntara, S. Noel, P. H. Phua, I. M. Cabrera, J. G. de Vries and H. J. Heeres, *Angew. Chem. Int. Ed.*, **2011**, 50, 7083-7087.
26. T. Buntara, S. Noel, P. H. Phua, I. M. Cabrera, J. G. de Vries and H. J. Heeres, *Top Catal.*, **2012**, 55, 612-619.

27. T. Buntara, S. Noel, P. H. Phua, I. M. Cabrera, J. G. de Vries and H. J. Heeres, WIPO Patent Application WO/2011/149339.
28. K. Chen, S. Koso, T. Kubota, Y. Nakagawa and K. Tomishige, *ChemCatChem*, **2010**, *5*, 547-555.
29. M. Chia, Y. J. P-Torres, D. Hibbitts, Q. Tan, H. N. Pham, A. K. Datye, M. Neurock, R. J. Davis and J. A. Dumesic, *J. Am. Chem. Soc.*, **2011**, *133*, 12675-12689.
30. T. Nishiguchi, H. Imai, Y. Hirose and K. Fukuzumi, *J. Catal.*, **1976**, *41*, 249-257.
31. R. Xing, W-Qi and G. W. Huber, *Energy. Enviorn. Sci.*, **2011**, *4*, 2193-2205.
32. J. J. Bozell, *Science*, **2010**, *329*, 522-523.
33. A. Corma, S. Iborra and A. Velty, *Chem. Rev.*, **2007**, *107*, 2411-2502.
34. A. Boddien, D. Mellmann, F. Gartner, R. Jackstell, H. Junge, P. J. Dyson, G. Laurenczy, R. Ludwig and M. Beller, *Science*, **2011**, *333*, 1733-1736.
35. Q-Y. Bi, X-L. Du, Y-M. Liu, Y. Cao, H-Y. He and K-N. Fan, *J. Am. Chem. Soc.*, **2012**, *134*, 8926-8933.
36. G. Wienhöfer, I. Sorribes, A. Boddien, F. Westerhaus, K. Junge, H. Junge, R. Llusar and M. Beller, *J. Am. Chem. Soc.*, **2011**, *133*, 12875-12879.
37. K. Tedsree, T. Li, S. Jones, C. W. A. Chan, K. M. K. Yu, P. A. J. Bagot, E. A. Marquis, G. D. W. Smith and S. C. E. Tsang, *Nat. Nanotechnol.*, **2011**, *6*, 302-307.
38. R. B. Borade, B. Zhang and A. Clearfield, *Catal. Lett.*, **1997**, *45*, 233-235.
39. M. C. C. Costa, R. A. W. Johnstone and S. Whittaker, *J. Mol. Catal. A: Chem.*, **1998**, *129*, 79-89.

40. C. Marcu, I. Sandulescu and J. M. Miller, *J. Mol. Catal. A: Chem.*, **2003**, *203*, 241-250.
41. A. Clearfield and T.S. Takur, *J. Catal.*, **1980**, *65*, 185-194.
42. K. Segawa, Y. Kurusu, Y. Nakajima and M. Kinoshita, *J. Catal.*, **1985**, *94*, 491-498.
43. A. La Ginestra, P. Partono, M.L. Berardelli, P. Galli, C. Ferragina and M. A. Massucci, *J. Catal.*, **1987**, *103*, 346-356.
44. G. Ramis, P.F. Rossi, G. Busca, V. Lorenzelli, A. La Ginestra and P. Partono, *Langmuir*, **1989**, *5*, 917-923.
45. R. Joshi and U. Chudasama, *Ind. Eng. Chem. Res.*, **2010**, *49*, 2543-2547.
46. N. Li, G. A. Tompsett and G. W. Huber, *ChemSusChem*, **2010**, *3*, 1154-1157.
47. N. Li, G. A. Tompsett, T. Zhang, J. Shi, C. E. Wyman and G. W. Huber, *Green Chem.*, **2011**, *13*, 91-101.
48. R. Waidmann, A. W. Pierpont, E. R. Batista, J. C. Gordan, R. L. Martin, L. A. Silks, R. M. West and R. Wu, *Catal. Sci. Technol.*, **2013**, *3*, 106-115.
49. M. V. Herrers, S. Werkmeister, K. Junge, A. Borner and M. Beller, *Catal. Sci. Technol.*, **2014**, *4*, 629-632.
50. R. Weingarten, G. A. Tompsett, W. C. Conner Jr. and G. W. Huber, *J. Catal.*, **2011**, *279*, 174-182.
51. K. Nakajima, T. Fukui, H. Kato, M. Kitano, J. N. Kondo, S. Hayashi and M. Hara, *Chem. Mater.*, **2010**, *22*, 3332-3339.
52. R. J. Madon and J. P. O'connell, *AIChE J.*, **2004**, *24*, 904-911.
53. G. Del Angel and J. I. Benitez, *React. Kinet. Catal. Lett.*, **1993**, *51*, 547-553.

54. J. M. Bassett, G. Dalmai-Imelik, M. Primet and R. Mutin, *J. Catal.*, **1975**, 37, 22-36.
55. The use of excess water instead of EtOH is not favorable for the present HDO production.
56. W. E. Kaufmann and R. Adams, *J. Am. Chem. Soc.*, **1923**, 45, 3029-3044.
57. H. A. Smith and J. F. Fajek, *J. Am. Chem. Soc.*, **1949**, 71, 415-419.

Chapter 4

*Selective Oxidation of Long Chain Aliphatic
Diols to mono-Hydroxycarboxylic acid over
Reusable Hydrotalcite Supported Capped AuPd
Bimetallic Nanoparticle Catalysts using H₂O₂ as
Oxidant*

Selective Oxidation of Long Chain Aliphatic Diols to mono-Hydroxycarboxylic acid over Reusable Hydrotalcite Supported Capped AuPd Bimetallic Nanoparticle Catalysts using H₂O₂ as Oxidant

Abstract

Selective oxidation of 1,6-hexanediol (HDO) into 6-hydroxycaproic acid (HCA) was achieved over hydrotalcite-supported capped AuPd bimetallic nanoparticles as heterogeneous catalyst using aqueous H₂O₂. The selectivity of the HCA from HDO oxidation was noticed to be considerably dependent on choice of capping agent as well as on Au/Pd mole ratio; and Au₄₀Pd₆₀-DDAO/HT possessed the highest catalytic activity with 81% HCA yield and 93% selectivity.

The supported bimetallic capped (PVP, PVA and DDAO) nanoparticles structure was characterized using various instrumental techniques. The chemical and electronic properties were studied using X-ray photoelectron spectroscopy and Pd-K-edge and Au-L_{III}-edge extended X-ray absorption fine structure (EXAFS) spectroscopy and Pd-L_{III} and Au-L_{III} edge X-ray absorption near edge structure (XANES) spectroscopy. Alloy-structure-dependent electronic behavior (*e.g.* Au 5d electronic density) and surface properties (*e.g.* Au-Pd bonds) were revealed for these NPs based heterogeneous catalysts. The results were consistently accounted by considering the size, surface electronic and alloying effects of the NPs for catalytic activity. Furthermore, the same reaction conditions were utilized to obtain the selective mono-hydroxycarboxylic acid from selective oxidation of other aliphatic diols such as 1,7-heptanediol, 1,8-octanediol and 1,2-hexanediol.

4.1 Introduction

For a sustainable future of the chemical industry, a continuous supply of feedstock from renewable sources (like biomass) rather than the depleting non-renewable sources of petroleum is required.^{1,2} Among the diverse routes of biomass utilization, selective oxidation presents a significant importance from an industrial as well as academic point of view for production of valuable chemicals and intermediates.³⁻⁶ One chemical of such immense value is 6-hydroxycaproic acid (HCA), that has potential applications in dermo-pharmaceuticals, cosmetics and in polycaprolactone (PCL) production for polymer industries.⁷⁻⁹ But, HCA is expensive and scarcely isolable thus the PCL is rarely synthesized from HCA and utilization of caprolactone *via* ring opening polymerization to produce PCL is the major route.⁷⁻⁹

The classical route to HCA synthesis includes metal-catalyzed a) reduction of adipic acid (AA) at 523 K with 300 bar H₂,¹⁰ b) formed as a by-product in oxidation of cyclohexane and cyclohexanone (derivatives of fossil resources).¹¹⁻¹³ Undoubtedly, the synthesis of HCA from renewable sources over a heterogeneous catalyst is interesting and challenging. The present work focused on HCA synthesis by the selective oxidation of 1,6-hexanediol (HDO), which is directly obtained from 5-hydroxymethyl furfural (HMF, biomass resource) using heterogeneous catalysts.¹⁴⁻¹⁶

Here my main focus is on the selective oxidation of long chain aliphatic diol (HDO) to ω -hydroxycarboxylic acid (HCA) (**Figure 1**), because of its potential application in bio-renewable PCL production. A wide array of publications can be seen for selective oxidation of C4-C5 diol, but hardly any report could be found for longer than C5 aliphatic chain. Additionally, a very recent study by Ide *et al.*, said that selective oxidation of primary alcohol group gradually become difficult as the carbon chain or alkyl

group increases between two hydroxyl groups when using Pt/C catalyst with acetic acid as additive at 343 K under 10 bar O₂.¹⁷ Other researchers have also discussed complication involved for the selective oxidation of long chain aliphatic diol.^{18,19}

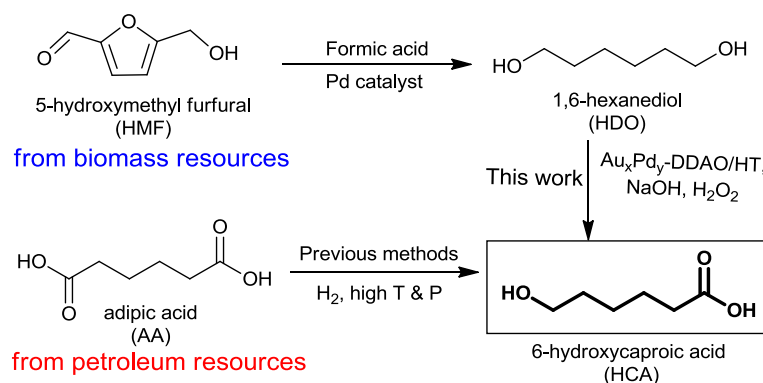


Figure 1: Comparison of conventional and present studies.

From last 2-3 decades, many efforts have been made to produce active and selective heterogeneous catalysts, out of which metal nanoparticle (NP)-based heterogeneous catalysts are extensively investigated.^{20,21} In general, the kind of capping agents has been considered to affect the chemical and physical properties of metal NPs.²²⁻²⁵ Recently, bimetallic NPs with capping agents have gained significant attentions owing to their novel catalytic properties, which are different from their monometallic counterparts.²⁶⁻²⁸ Among them, the catalysis of capped bimetallic Au-Pd has been widely explored for oxidations of alcohol,²⁶⁻²⁸ methane²⁹ and CO³⁰. A short time ago Nishimura *et al.*²⁴ and Duangta *et al.*,²⁸ from our research group highlighted the importance of PVP and starch as ligand, and its influence on the catalytic properties of bimetallic NPs for selective oxidation reactions. In 2010, Kishida *et al.*³¹ and very recently, our research group³² utilized *N,N*-dimethyldodecylamine *N*-oxide (DDAO, **Figure 2**) as a capping agent for the synthesis of Ag nanowires and CoPd NPs, respectively. The metal NPs are known to be weakly stabilized through multiple coordination of the N and O sites (amine

oxide) of DDAO so that the reactants can access the NP surface. Herein, I extended the scope of DDAO for preparation of AuPd bimetallic NPs supported on hydrotalcite (HT)³³⁻³⁵ for selective oxidation of HDO to HCA under mild conditions, which has not been reported previously.

4.2 Experimental Section

4.2.1 Materials

Hydrogen tetrachloroaurate (III) ($\text{HAuCl}_4 \cdot 4\text{H}_2\text{O}$), palladium chloride (PdCl_2), ethylene glycol (EG), adipic acid (AA), 1,6-hexanediol (HDO), 30% hydrogen peroxide (H_2O_2), 1-hexanol, hexanoic acid, potassium iodide (KI), soluble starch chloroform, polyvinyl alcohol-3500 (partially hydrolyzed) and ICP grade Au and Pd standards were obtained from Wako Pure Chemical Industries, Ltd.. Kanto Chemical Co., Inc. supplied sodium hydroxide (NaOH), potassium chloride (KCl), and sulfuric acid (H_2SO_4), sodium thiosulfate ($\text{Na}_2\text{S}_2\text{O}_3$), ammonium molybdate. *N,N*-dimethyldodecylamine *N*-oxide (DDAO), 1,2-hexanediol, 2-hydroxyhexanoic acid, 1,7-heptanediol, pimelic acid, 1,8-octanediol, 8-hydroxy octanoic acid, suberic acid and QuadraPure® TU was purchased from Sigma-Aldrich, Co. LLC.. Acros Organics provided 6-hydroxycaproic acid and poly *N*-vinyl pyrrolidone (PVP) K29-32, molecular weight 58,000. Melatonin and hydrotalcite (HT, $\text{Mg}/\text{Al} = 5.4$) was obtained from TCI Chemicals Pvt Ltd.. and Tomita Pharmaceuticals Co. Ltd. respectively.

4.2.2 Catalyst Preparation

Au_xPd_y -Capped/HT catalysts have been synthesized as reported in literature²⁴ with some modifications. In a typical synthesis, an aqueous solution (50 mL) of $\text{HAuCl}_4 \cdot 4\text{H}_2\text{O}$ (x mmol) and PdCl_2 (y mmol) including KCl were mixed with DDAO or PVP or PVA as

capping agent and stirred for 5 min at room temperature. Thereafter, EG (50 ml) was added into the aqueous mixture and again stirred for 5 min at room temperature, then the obtained mixture was refluxed for 2 h at 413 K, followed by addition of HT (1.0 g) to the formed colloidal dispersion to stabilize the formed $\text{Au}_x\text{Pd}_y\text{-X}$ NPs onto the surface of HT. The resultant mixture was stirred again for 1 h at 413 K. The obtained precipitates were cooled, filtered, washed and dried in *vacuo* overnight. The Au and Pd content were varied in the range of 0 to 100, and the total amount of both metals in the mixed solution ($x + y$) was kept as 0.1 mmol; *i.e.* the prepared $\text{Au}_x\text{Pd}_y\text{-X/HT}$ catalysts contain 0.1 mmol metal per gram in stoichiometry.

4.2.3 Catalytic Testing

All experiments to test the catalytic activity were performed in a schlenk tube attached to a condenser. The catalytic activity was evaluated for HDO oxidation in basic aqueous media with H_2O_2 as oxidant to obtain HCA. In a typical reaction procedure, 1,6-hexanediol (60 mg, 0.5 mmol) and catalyst (25 mg) were weighed and added in to the schlenk tube, and was dissolved in 3.5 mL deionized water. 0.75 mL of 30% H_2O_2 and 0.5 M NaOH was added to the above mixture and the schlenk tube was mounted on a preheated oil bath at 353 K. The mixture was allowed to react for various time intervals with continuous magnetic stirring. After the reaction, a part of the resultant solution was diluted 20 times with aqueous H_2SO_4 (10 mM), and the catalyst was filtered off using a Milex[®]-LG 0.20 μm filter. The obtained filtrate was analyzed by high performance liquid chromatography (HPLC, WATERS 600) using an Aminex HPX-87H column (Bio-Rad Laboratories, Inc.) attached to a refractive index detector. An aqueous 10 mM H_2SO_4

(mobile phase) was run through the column (maintained at 323 K) at a flow rate of 0.5 mLmin⁻¹. The conversion and yield(s) were determined with a calibration curve method.

Recycling tests were performed to check stability of the catalysts during the reaction. In each run, after the reaction, the catalyst was separated by centrifugation, the supernatant liquid was stored, and then analysis of products and leaching test of catalysts were performed. The catalyst was washed thoroughly with deionized water, dried in vacuum for overnight, and then the dried catalyst was used for further reactions.

4.2.4 Isolation of product

The catalyst was separated from the reaction mixture via centrifugation followed by filtration using a Milex®-LG 0.20 µm filter. The obtained mixture was acidified till pH=1-2 by adding aq. H₂SO₄ drop wise. The compound was extracted with CHCl₃ (four times). The combined organic layers were condensed under reduced pressure to obtain a colorless compound (81.7% yield). The product was dissolved in CDCl₃ and subjected to NMR spectroscopy for identification of product.

4.2.5 Hot filtration test

1,6-Hexanediol (60 mg, 0.5 mmol) and catalyst (25 mg) were weighed and added into the Schlenk tube, and was dissolved in 3.5 mL deionized water. 0.75 mL of 30% H₂O₂ and 0.5 M NaOH was added to the above mixture and the Schlenk tube was mounted on a preheated oil bath at 353 K. After 2 h of reaction progress, the catalyst was separated at the reaction temperature by centrifugation followed by filtration using a Milex®-LG 0.20 µm and the reaction was continued with the filtrate at 353 K for additional 4 h.

4.2.6 Radical Scavenger test

The melatonin (0.3 mmol, 70 mg) as hydroxyl radical scavenger was added to the reaction flask along with the reagents for the oxidation of HDO and proceeded for the reaction.

4.2.7 Catalyst Poisoning Test

The QuadraPure® TU was added to the reaction flask along with the reagents for the oxidation of HDO and proceeded for the reaction. 33.4 mg of QuadraPure® TU was used with 25 mg of Au₄₀Pd₆₀-X/HT catalyst (6.38 mg Pd, 7.84 mg Au).

4.2.7 Characterization

Nuclear Magnetic Resonance (NMR) spectroscopy was executed on Brücker advance 400 MHz instrument using CDCl₃ as a solvent. Crystal structure was analyzed by powder X-ray diffraction (PXRD) with a SmartLab (Rigaku Co.) using a Cu K α radiation (λ = 0.154 nm) at 40 kV and 30 mA in the range of 2θ = 4-80°. The diffraction patterns were analyzed with the database in the joint committee of powder diffraction standards (JCPDS). For inductively coupled plasma atomic emission spectroscopy (ICP-AES) analysis, an ICPS-7000 ver. 2 (Shimadzu Co.) was employed to quantify the real Au and Pd amount loaded over HT and to evaluate the metal leaching, if any, during the reaction. Contents of metal (Au and/or Pd) in the catalyst and/or the reaction medium were estimated by a calibration curve method. An H-7100 (Hitachi, Ltd.) operating at 100 kV was utilized to acquire the morphology of catalyst by a transmission electron microscopy (TEM) image. The samples for TEM measurements were dispersed in ethanol, and the supernatant liquid was dropped onto a copper grid before drying in *vacuo* overnight. The electronic state of Au/Pd on HT was analyzed by X-ray photoelectron spectroscopy (XPS). The experiments

were conducted on an AXIS-ULTRA DLD spectrometer system (Shimadzu Co. and Kratos Analytical Ltd.) using an Al target at 15 kV and 10 mA in an energy range of 0-1200 eV. The binding energies were calibrated with the C 1s level (284.5 eV) as an internal standard reference. The samples for XAS study were pressed into a pellet and measured in transmission mode. Data analysis was performed with the use of the software package REX2000. After the $\chi(k)$ function was extracted from the EXAFS data, Fourier transformation was performed on the k^3 -weighted data in the ranges $k = 3.1$ - 10.1 \AA^{-1} for the Au L_{III}-edge spectra.

4.3. Results and Discussion

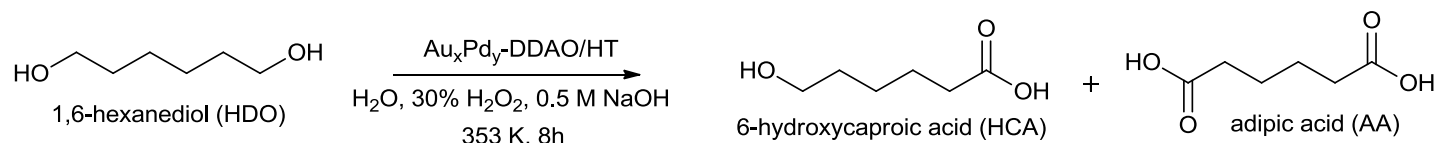
4.3.1 Catalytic Activity

Firstly, a series of AuPd bimetallic NPs were prepared with DDAO using modified polyol reduction method²⁴. The resultant NPs were supported on HT (Mg/Al=5.4) and denoted as Au_xPd_y-DDAO/HT, where x and y represents mole ratio of Au and Pd, respectively. HT-supported both monometallic and bimetallic NP catalysts were tested for the oxidation of HDO to HCA at 353 K under alkaline medium with 30% aq. H₂O₂ as a greener oxidant^{36,37}. **Table 1** summarizes the results for HDO oxidation together with the average particle size and actual metal loading measured by TEM and ICP-AES respectively. The average particle size was noticed to be around 4-6 nm except for monometallic Au₁₀₀-DDAO/HT (28.4 nm, **Figure 2**), which showed an extremely low activity (entry 1). Also monometallic Pd catalyst (Pd₁₀₀-DDAO/HT) with particle size of 4.8 nm had low HCA yield (entry 6). Interestingly, the co-presence of both Au and Pd (Au_xPd_y-DDAO/HT) bimetallic catalysts dramatically enhanced the HCA yield and selectivity (entries 2-5). Among the various Au_xPd_y-DDAO/HT catalysts, Au₄₀Pd₆₀-

DDAO/HT possessed the highest catalytic activity with 81% HCA yield (93% selectivity). AA was the only by-product observed using these catalysts. (The HPLC analysis of the reaction mixture denied the presence of any other water-soluble products after the reaction. Also, both ^1H - and ^{13}C -NMR spectroscopy of the reaction mixture extracted by the organic solvent (chloroform) only identified the three compounds of HDO, HCA and AA.) A remarkable difference in the catalytic behavior for oxidation of HDO to HCA was observed with the change in Au/Pd molar ratio (Table 1) without any significant effect on particle size distribution of Au_xPd_y -DDAO/HT catalysts. These results indicate the important role of synergistic interaction between Au and Pd for the excellent catalytic performance on the $\text{Au}_{40}\text{Pd}_{60}$ -DDAO/HT.

To study the reaction pathway, the reaction over the $\text{Au}_{40}\text{Pd}_{60}$ -DDAO/HT catalyst was performed in the presence of melatonin as water soluble radical scavenger of hydroxyl radicals (OH^\bullet).^{38,39} We noticed that the presence of melatonin (0.3 mmol) prohibited the selective oxidation of HDO (5% yield of HCA yield with traces of AA), suggesting a radical pathway under the present reaction conditions. Formation of radicals over metal NPs in presence of hydrogen peroxide has been reported previously,^{40,41} which seems to play a key factor during the HDO oxidation.

The catalytic activity of $\text{Au}_{40}\text{Pd}_{60}$ -DDAO/HT was compared with analogous Au-Pd nanoparticles on other supports to identify their role (**Table 2**). Though, all catalysts promoted the formation of HCA to some extent, $\text{Au}_{40}\text{Pd}_{60}$ -DDAO/HT stands out with the highest catalytic activity perhaps the basic sites of HT helps in enhancing the catalytic performance as compared to neutral and/or not so strong basic supports.

**Table 1:** Screening of metal ratio of DDAO-stabilized Au_xPd_y for HDO oxidation into HCA^a

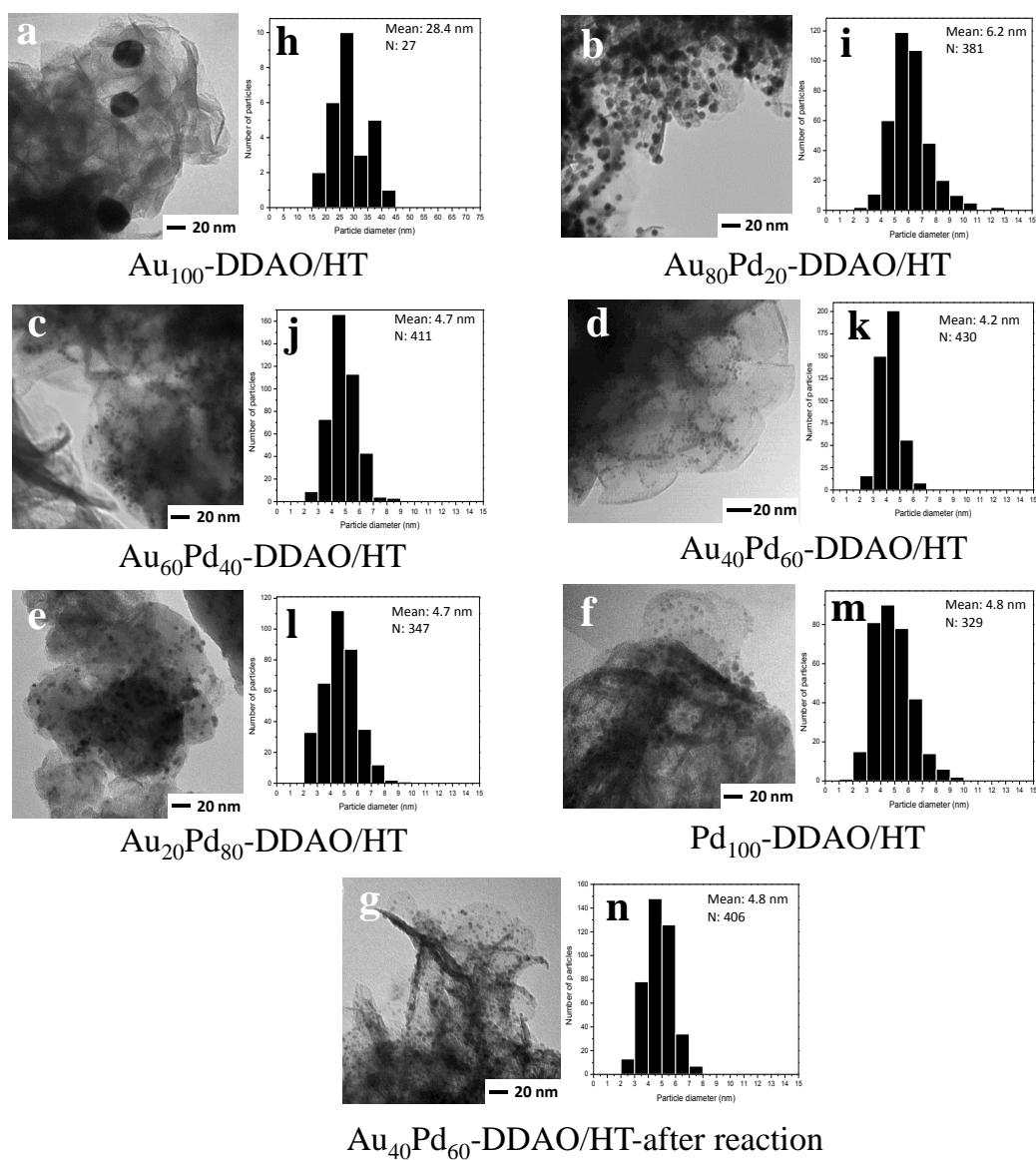
Entry	Catalyst	Conv./% ^b	Yield (sel.)/% ^b			Actual metal loading $\times 10^{-3}/\text{mmol g}^{-1\text{c}}$		TON ^d	Average size /nm ^e
		HDO	HCA	AA		Au	Pd		
1	$\text{Au}_{100}\text{-DDAO/HT}$	18	12 (67)	0 (0)		93.2	-	27	28.4
2	$\text{Au}_{80}\text{Pd}_{20}\text{-DDAO/HT}$	86	45 (52)	10 (12)		72.2	16.2	100	6.2
3	$\text{Au}_{60}\text{Pd}_{40}\text{-DDAO/HT}$	90	72 (80)	6 (7)		50.6	34	170	4.7
4	$\text{Au}_{40}\text{Pd}_{60}\text{-DDAO/HT}$	87, 87 ^f	81, 81 ^f (93, 92 ^f)	4, 4 ^f (5, 5 ^f)		33.7	55.6	184	4.2
5	$\text{Au}_{20}\text{Pd}_{80}\text{-DDAO/HT}$	36	8 (22)	0 (0)		17.4	71.7	19	4.5
6	$\text{Pd}_{100}\text{-DDAO/HT}$	10	7 (70)	0 (0)		-	89.4	16	4.8
7	$\text{Au}_{40}\text{Pd}_{60}\text{-DDAO/HT}^g$	38	24 (63)	1 (3)		-	-	-	4.2
8	$\text{Au}_{40}\text{Pd}_{60}\text{-DDAO/HT}^h$	12	9 (75)	0 (0)		-	-	-	4.2
9	blank	7	5 (-)	0 (0)		-	-	-	-

^a**Reaction Conditions:** HDO (0.5 mmol), catalyst (25 mg, $\text{Au}+\text{Pd}$ = 0.0025 mmol), 30% aq. H_2O_2 (0.75 mL, 6 mmol), 0.5 M NaOH (0.75 mL), H_2O (3.5 mL), 353 K, 8 h. ^bAnalyzed by HPLC. ^cEstimated with ICP-AES analysis. ^dCalculated based on total metal amount. ^eDetermined by TEM. ^fWith QuadraPure® TU (33.4 mg). ^gWithout 30% aq. H_2O_2 . ^hWithout 0.5M NaOH.

Table 2 : HDO oxidation with Au₄₀Pd₆₀-DDAO/supports ^a

Entry	Catalyst	Conv/ %	Yield (Sel.)/%	
		HDO	HCA	AA
1	Au ₄₀ Pd ₆₀ -DDAO/HT	87	81 (93)	4 (5)
2	Au ₄₀ Pd ₆₀ -DDAO/CeO ₂	75	52 (69)	2 (3)
3	Au ₄₀ Pd ₆₀ -DDAO/C	76	50 (66)	6 (8)
4	Au ₄₀ Pd ₆₀ -DDAO/TiO ₂ (anastase)	70	50 (71)	3 (4)
5	Au ₄₀ Pd ₆₀ -DDAO/TiO ₂ (rutile)	61	39 (64)	2 (3)

^a**Reaction Conditions:** HDO (0.5 mmol), Catalyst (25 mg), 30% H₂O₂ (0.75 mL, 6 mmol), 0.5 M NaOH (0.75 mL), H₂O (3.5 mL), 353 K, 8 h.

**Figure 2:** TEM images (a-g) and particle size distribution (h-n) of Au_xPd_y-DDAO/HT catalysts.

The presence of NaOH and H₂O₂ is crucial to bring the above high catalytic activity, as the absence of any of them, leads to low HCA yields (**Table 1**, entries 7-9). The catalytic activity of the Au₄₀Pd₆₀-DDAO/HT was noticed to be strongly influenced by amounts of added base and oxidant (**Table 3**), 6 mmol of 30% aq. H₂O₂ and 0.75 mL of 0.5 M NaOH was optimized to afford the highest HCA yield of 81% with 87% HDO conversion (entry 13, **Table 3**). Further increase in H₂O₂ and NaOH lead to decrease in selectivity of HCA and formed AA in large quantity.

Table 3: Oxidation of HDO over the Au₄₀Pd₆₀-DDAO/HT catalyst with various amounts of H₂O₂ and 0.5 M NaOH^a

Entry	30% H ₂ O ₂	0.5 M NaOH	Conv./%	Yield (sel.)/%	
	/mL (mmol)	/mL	HDO	HCA	AA
1 ^b	0.0 (0)	0.0	1	0 (0)	0 (0)
2 ^b	0.0 (0)	0.5	5	4 (-)	0 (0)
3 ^b	0.5 (4)	0.0	6	4 (-)	0 (0)
4 ^b	0.5 (4)	0.5	7	5 (-)	0 (0)
5	0.0 (0)	0.0	36	19 (53)	2 (10)
6	0.0 (0)	0.5	36	23 (64)	0 (0)
7	0.5 (4)	0.0	11	9 (-)	0 (0)
10	0.5 (4)	0.5	66	60 (91)	2 (3)
11	1.0 (8)	0.5	69	62 (90)	2 (3)
12	0.5 (4)	1.0	72	63 (88)	2 (3)
13	0.75 (6)	0.75	87	81 (93)	4 (4)
14	1.0 (8)	1.0	89	81 (91)	5 (5.6)
15	1.0 (8)	1.5	90	71 (79)	13 (14)
16	1.5 (12)	1.0	90	71 (79)	11 (12)

^a**Reaction Conditions:** HDO (0.5 mmol), Au₄₀Pd₆₀-DDAO/HT (25 mg), Total media (5.0 mL), 353 K, 8 h, ^bwithout Au₄₀Pd₆₀-DDAO/HT.

In addition, the large scale reactions with 5 and 10 fold increase in starting material was also studied (**Table 4**). 125 mg of same catalyst (Au₄₀Pd₆₀-DDAO/HT) with

2.5 mmol of the HDO as starting material yielded 78% of HCA with 84% selectivity. Moreover a bit larger amount of catalyst could also promote the HDO oxidation at 5 mmol-scale with the similar efficiency to reach a high TON of 265 (entry 3, **Table 4**), suggesting scaling-up of the reaction is possible.

Table 4: Large scale oxidation of HDO over the Au₄₀Pd₆₀-DDAO/HT catalyst^a

Entry	Cat/ mg	30% H ₂ O ₂ / mL (mmol)	0.5M NaOH/ mL	Conv./%	Yield (Sel.)/%		TON
				HDO	HCA	AA	
1	125	3.75 (30)	3.75	93	78 (84)	5 (5)	175
2	100	3.75 (30)	3.75	89	75 (84)	3 (3)	209
3 ^b	150	7 (55)	7	78	71 (91)	2 (3)	265

^a**Reaction Conditions:** HDO (2.5 mmol, ^b5mmol), H₂O, 353 K, 8 h, ^b12 h.

4.3.2 ¹H- and ¹³C- NMR of the Product

For the authentication of the product, the product was isolated as mentioned above in experimental section. The isolated HCA was obtained as oily liquid in 81.7% yield, while the yield calculated from HPLC was 83.6 %. The isolated HCA was subjected to NMR spectroscopy and was compared with the literature data of HCA (**Figure 3 and 4**).

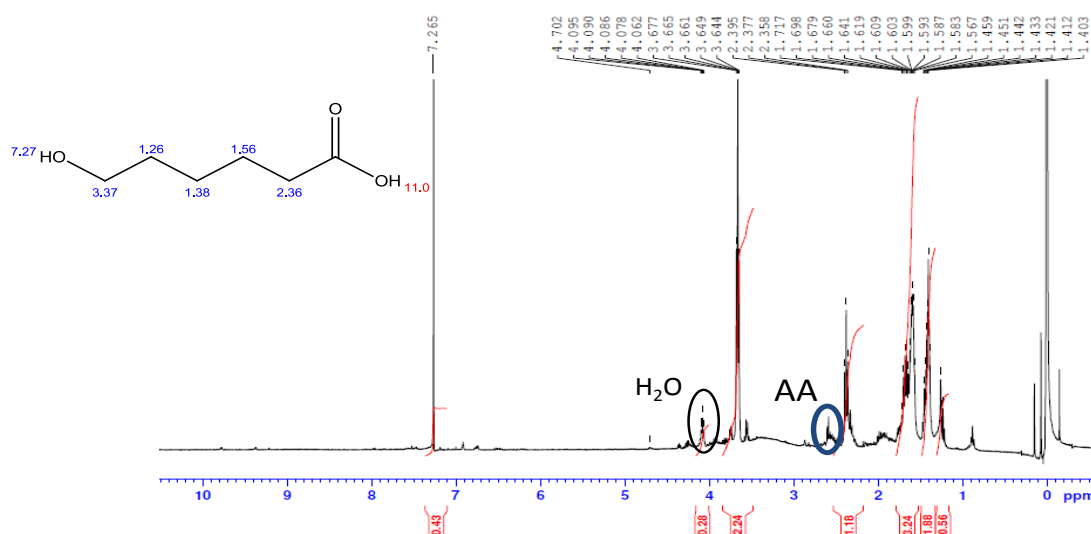


Figure 3: ¹H-NMR of isolated product

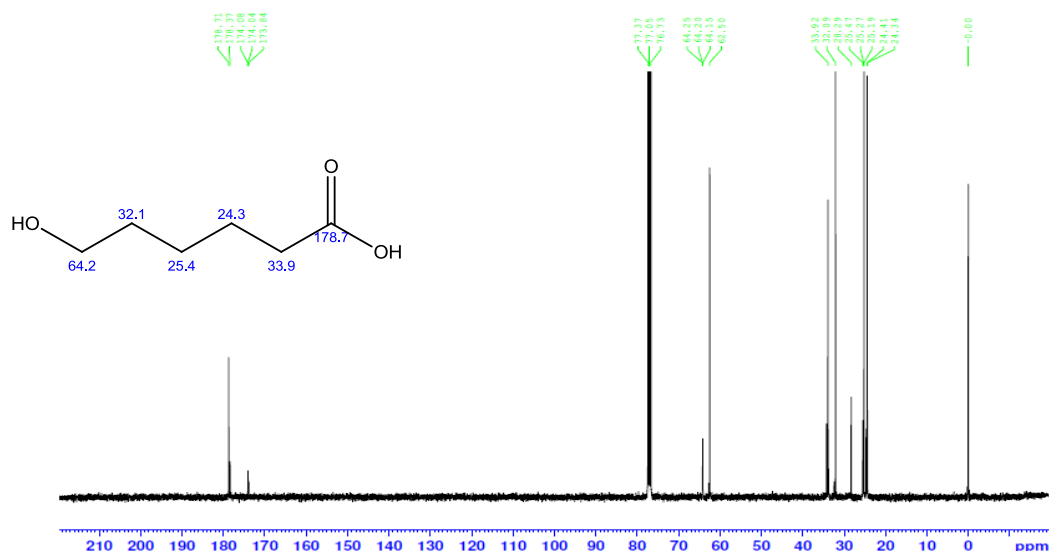


Figure 4: ^{13}C -NMR of the isolated product

Reaction Conditions: HDO (0.5 mmol), $\text{Au}_{40}\text{Pd}_{60}$ -DDAO/HT (25 mg), 0.5 M NaOH (0.75 mmol), 30% H_2O_2 (0.75 mL), H_2O (3.5 mL), 353 K, 24 h, 500 rpm. Under this condition, the isolated yield and the HPLC yield for HCA was calculated to be 81.7% and 83.6%, respectively.

Literature NMR Data of 6-hydroxycaproic acid:

^1H -NMR (300 MHz, CDCl_3) δ 7.6 (s, 1 H), 3.6 (t, 2 H), 2.3 (t, 2 H), 1.6-1.4 (m, 4 H), 1.4-1.2 (m, 4 H). ^{13}C -NMR (75 MHz, CDCl_3) δ 178.9, 62.3, 34.0, 31.9, 25.1, 24.4. (Ref: A. Binaco *et al.*, *Chem. Commun.*, **2010**, 1494).

4.3.3 Recyclability

One of the important criteria to be taken care for heterogeneous catalytic system is the possibility of metal leaching in the reaction mixture and catalyst reusability. In present study, the catalyst was found to be highly reusable at least up to 5 times without any further treatment (**Figure 5**). It was observed that the reaction does not proceed when the catalyst was filtered off after 2 h of the reaction (**Figure 6**). ICP-AES experiments of the filtrate demonstrated that neither Au nor Pd leached into the solution. Additionally the presence of QuadraPure® TU, known as homogeneous metal species scavenger,^{42,43}

didn't influence the catalytic activity (entry 4f, **Table 1**). These experiments authenticate the heterogeneous nature of the Au₄₀Pd₆₀-DDAO/HT catalyst under our reaction conditions.

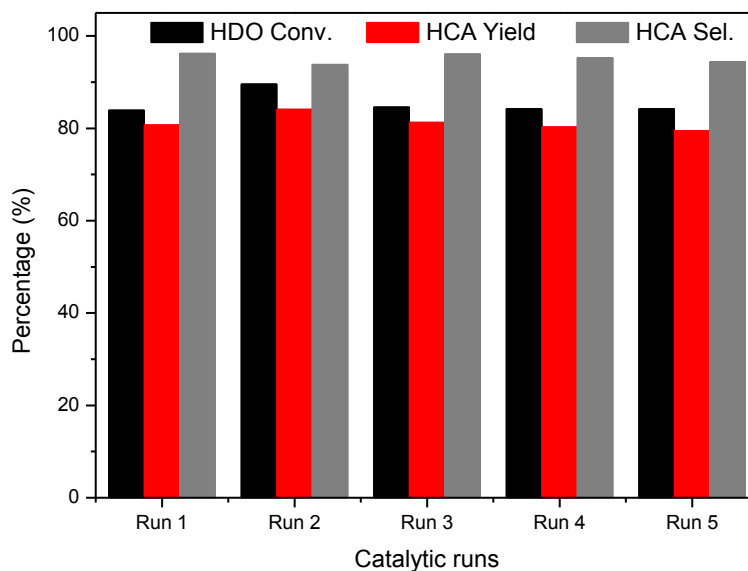


Figure 5: Recyclability of catalyst for selective oxidation of HDO to HCA.

Reaction Conditions: HDO (0.5 mmol), Au₄₀Pd₆₀-DDAO/HT (25 mg), 0.5 M NaOH (0.75 mmol), 30% H₂O₂ (0.75 mL), H₂O (3.5 mL), 353 K, 8 h, 500 rpm.

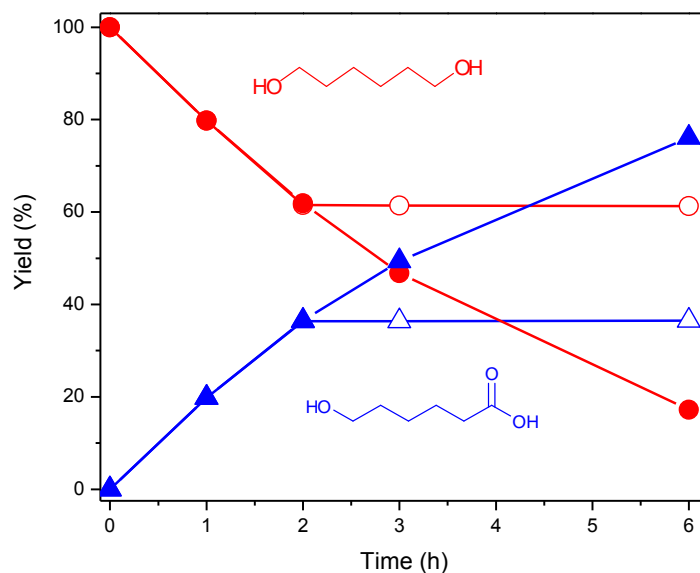


Figure 6: Heterogeneity test.

Reaction Conditions: HDO (0.5 mmol), Au₄₀Pd₆₀-DDAO/HT (25 mg), 0.5 M NaOH (0.75 mmol), 30% H₂O₂ (0.75 mL), H₂O (3.5 mL), 353 K, 6 h, 500 rpm. HDO (red circle), HCA (blue triangle); closed : HDO and HCA yield. open : when catalyst was filtered off after 2 h.

A comparison of the XRD patterns (**Figure 7**) and TEM images (**Figure 2**) of the fresh and spent $\text{Au}_{40}\text{Pd}_{60}$ -DDAO/HT catalysts revealed that there is no significant change in the catalyst morphology. It was seen that AuPd NPs were homogeneously dispersed on the HT surface even after the reaction, with a slight increase in mean particle size of NPs from 4.2 to 4.8 nm. Au L_{III}-edge and Pd K-edge XANES and EXAFS results also suggested robust local structure around Au and Pd after the reaction (**Figure 8**), indicating the capped bimetallic AuPd NPs are quite stable under these reaction conditions.

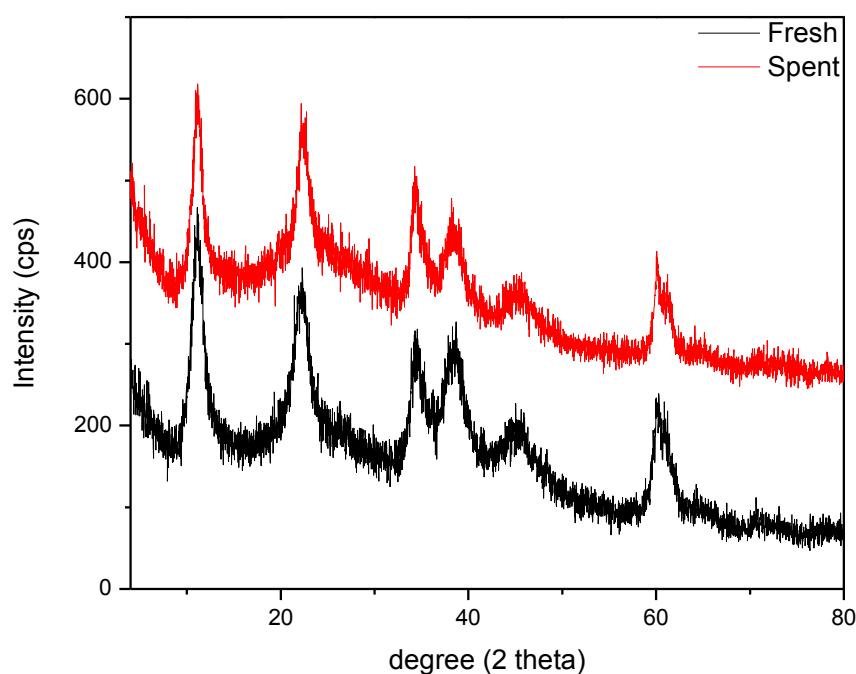


Figure 7: XRD patterns of $\text{Au}_{40}\text{Pd}_{60}$ -DDAO/HT fresh and spent catalysts.

(All diffraction peaks are due to layered structure of hydrotalcite support.)

4.3.4 UV-Vis spectroscopy

For understanding of the superiority of the $\text{Au}_{40}\text{Pd}_{60}$ -DDAO/HT catalyst, the series of AuPd bimetallic catalysts were characterized by means of various spectroscopic methods.

Figure 9 shows the representative UV–Vis spectra of monometallic and Au-Pd bimetallic catalysts. The monometallic Au catalyst exhibited a characteristic surface plasmon

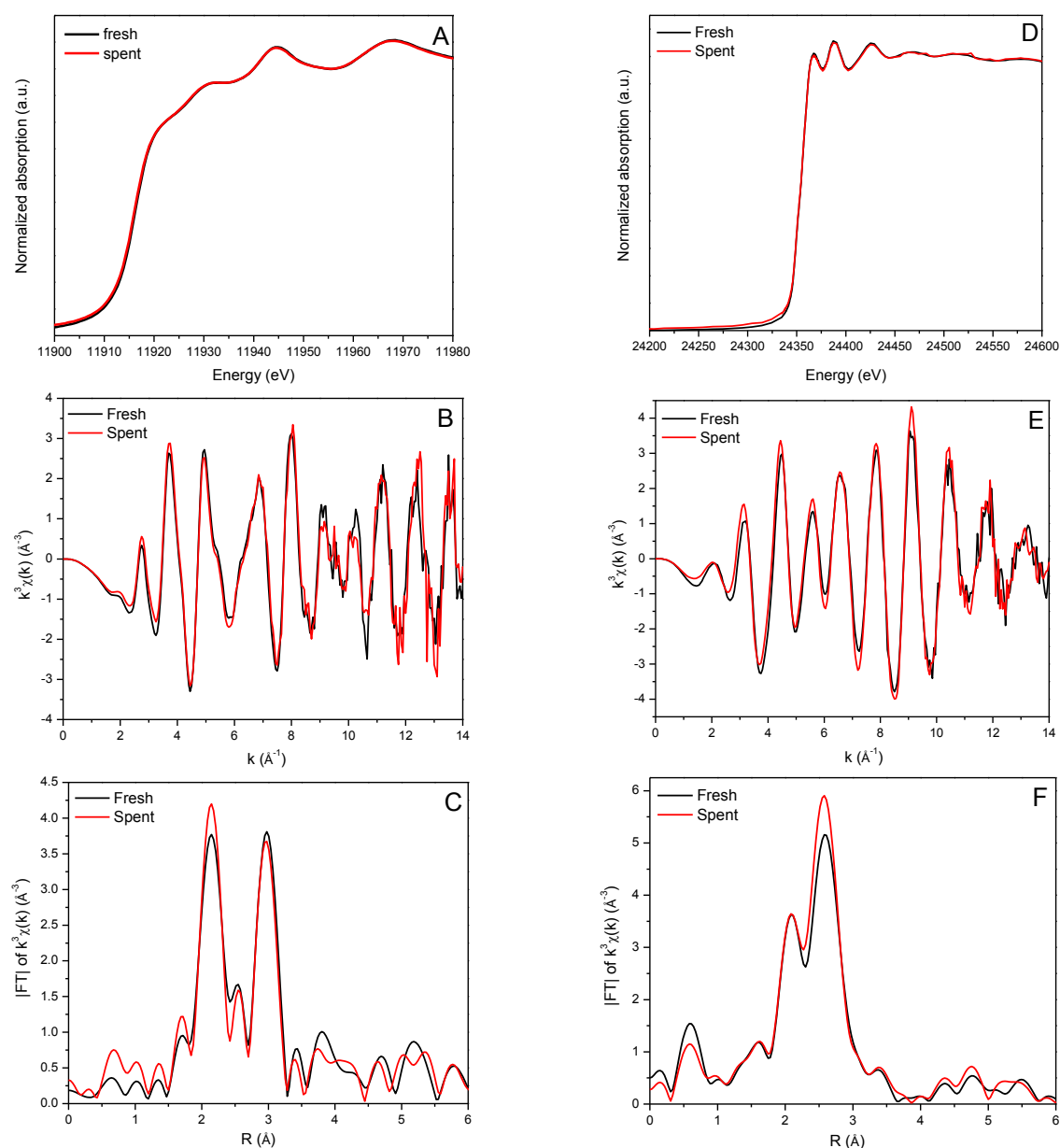


Figure 8: Au L_{III}-edge (A) XANES and EXAFS (B) k^3 -weighted and (C) FT spectra and Pd K-edge (D) XANES and EXAFS (E) k^3 -weighted and (F) FT spectra for fresh and spent Au₄₀Pd₆₀-DDAO/HT catalysts

resonance (SPR) absorption peak at 524 nm due to Au NPs.^{45,46} Admixing of Pd to Au resulted in strong diminishment of the SPR absorption peak, and a very weak hump was observed in Au₈₀Pd₂₀-DDAO/HT and Au₆₀Pd₄₀-DDAO/HT. No distinct SPR absorption peak over the entire spectral range can be detected in the Au₄₀Pd₆₀-DDAO/HT, Au₂₀Pd₈₀-

DDAO/HT and Pd₁₀₀-DDAO/HT. The weakening plasmon band in the bimetallic samples is attributed to the existence of interactions between Au and Pd species rather than formation of separated Au and Pd particles NPs and Au mother surface.²⁴

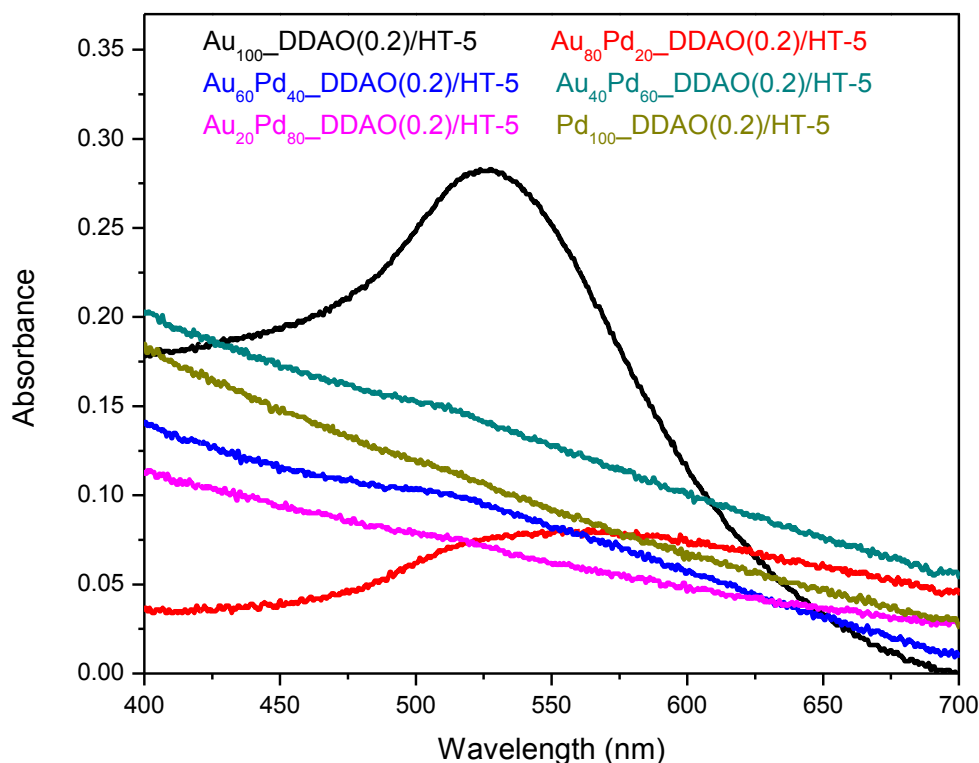


Figure 9: UV-Vis spectra of Au_xPd_y-DDAO/HT catalysts.

4.3.5 X-ray Photoelectron spectroscopy

Thereafter, the surface interaction between Pd and Au atoms was studied by the XPS. **Figure 10** shows XPS of core-level binding energies (BEs) for Au4f of the Au_xPd_y-DDAO NPs. The BEs of Au4f_{5/2} (87.7 eV) and Au4f_{7/2} (84.0 eV) in the Au₁₀₀-DDAO NPs are assigned to Au4f orbitals in metallic Au.⁴⁶ A clear negative shift in BE for Au4f was observed for AuPd samples. The maximum shift of -0.5 eV relative to the BE of pure Au NPs was observed for the Au₄₀Pd₆₀-DDAO NPs. This negative BE shift is an indication of increase in the electron density on Au to form negatively-charged Au species, suggesting a modification in the electronic structure in the presence of Pd.

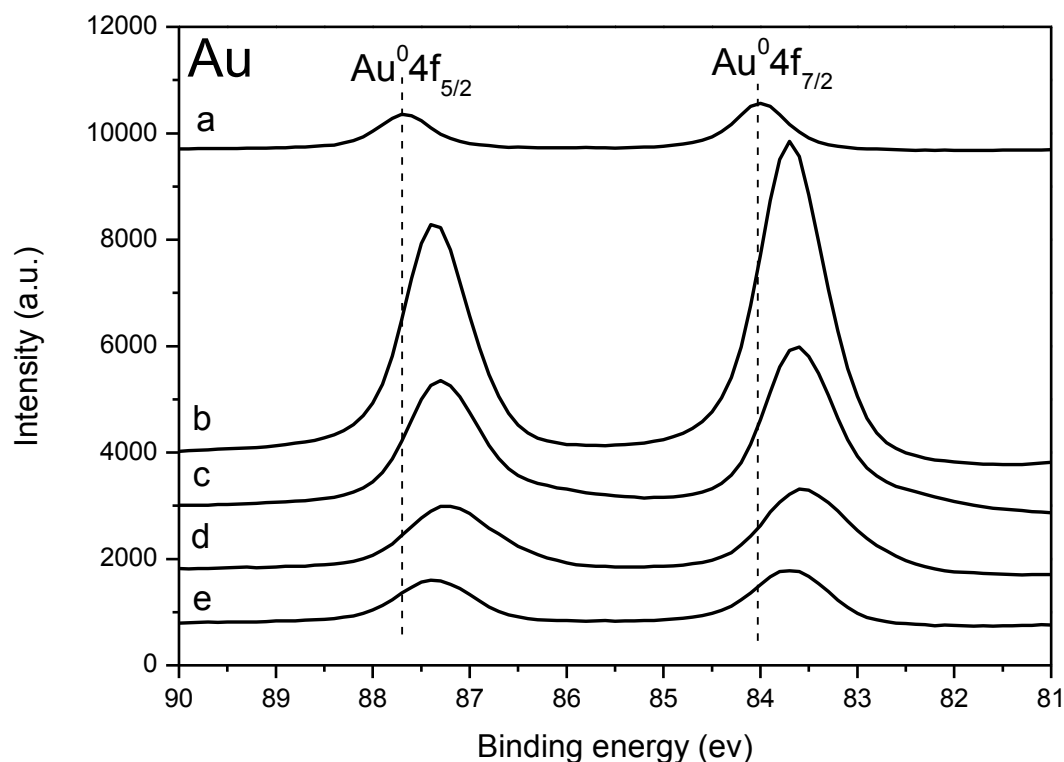


Figure 10: Au 4f XPS spectra of Au_xPd_y -DDAO NPs. (a) Au_{100} -DDAO NPs, (b) $\text{Au}_{80}\text{Pd}_{20}$ -DDAO NPs, (c) $\text{Au}_{60}\text{Pd}_{40}$ -DDAO NPs, (d) $\text{Au}_{40}\text{Pd}_{60}$ -DDAO NPs and (e) $\text{Au}_{20}\text{Pd}_{80}$ -DDAO NPs.

In Pd3d XPS (**Figure 11**) for Pd_{100} -DDAO NPs the $\text{Pd}3d_{3/2}$ was observed at higher BE values (340.8 eV) in comparison to that of metallic $\text{Pd}3d_{3/2}$ (340.1 eV), which indicates the Pd have partially cationic state. The BE of $\text{Pd}3d_{3/2}$ shifted to slightly lower BEs (~ -0.2 - ~ -0.4 eV) with the increase in Au content due to gain in electrons in d-orbitals of Pd atoms. According to the previous literatures, the lower BEs of both Au4f and Pd3d in bimetallic NPs with respect to their monometallic NPs can be stated as a charge flowing into Au and Pd, and hence suggesting electronic interactions between Au and Pd in AuPd-DDAO catalysts.^{30,47,48} A large shift for Au $4f_{7/2}$ (-0.5 eV) and for Pd3d_{3/2} (-0.3 eV) in the $\text{Au}_{40}\text{Pd}_{60}$ -DDAO NPs suggested the strongest interaction between Au and Pd at this mole ratio.

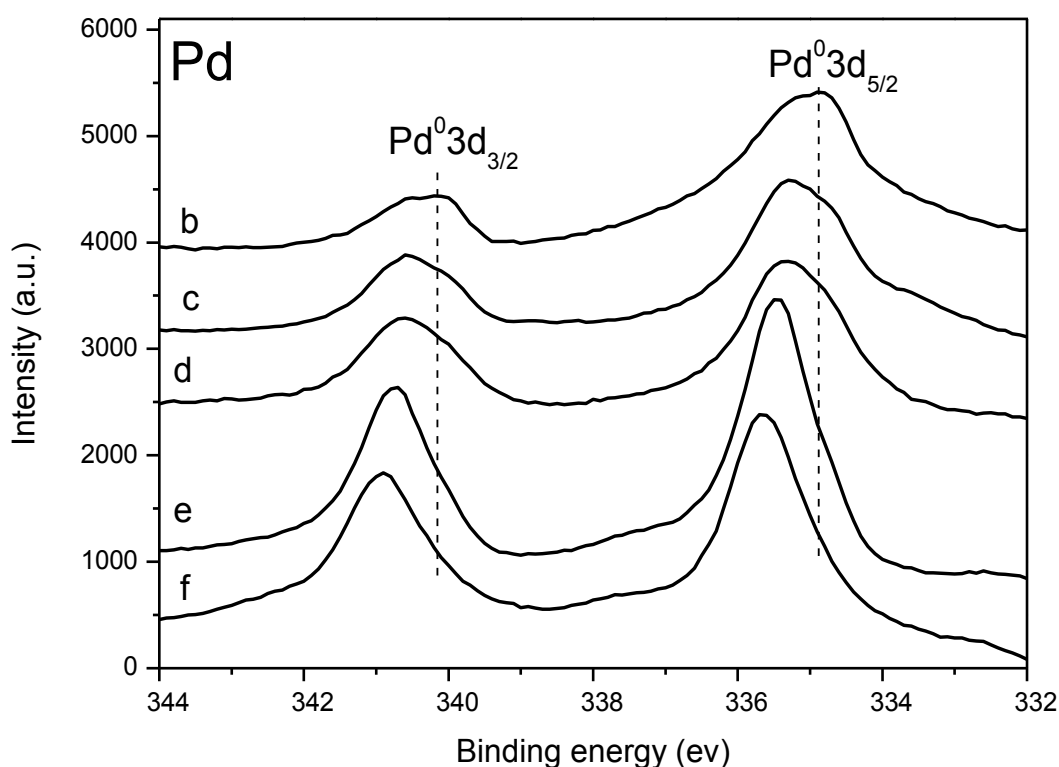


Figure 11: Pd 3d XPS spectra of Au_xPd_y -DDAO NPs. (b) $\text{Au}_{80}\text{Pd}_{20}$ -DDAO NPs, (c) $\text{Au}_{60}\text{Pd}_{40}$ -DDAO NPs, (d) $\text{Au}_{40}\text{Pd}_{60}$ -DDAO NPs, (e) $\text{Au}_{20}\text{Pd}_{80}$ -DDAO NPs and (f) Pd_{100} -DDAO NPs.

4.3.6 X-ray Absorption spectroscopy

Further investigation on the nature of supported Au-Pd bimetallic nanoparticles was conducted with XAS study of Au L_{III} -edge, and Pd K- and L_{III} -edges. The Au L_{III} -edge XANES spectra of Au_xPd_y -DDAO/HT catalysts together with Au foil are shown in **Figure 12**. The white line (WL) intensity, the first feature after edge jump, decreases for AuPd bimetallic catalysts with increase in Pd content, and almost disappears for the $\text{Au}_{20}\text{Pd}_{80}$ -DDAO/HT. This decrease in the intensity implies that d-electron density has been increased in Au for AuPd bimetallic as compared to Au foil or the Au_{100} -DDAO/HT.^{24,49,50} It has been previously shown by many researchers that the increase in d-electron density of Au is due to Au-Pd d-d interactions or Au-Pd bond formation.^{51,52} In addition to that, the intensity of second band just after the white line feature (11935

eV) is more prominent for higher Pd content, which would ascertain interactions between Au and Pd atoms.^{47,51}

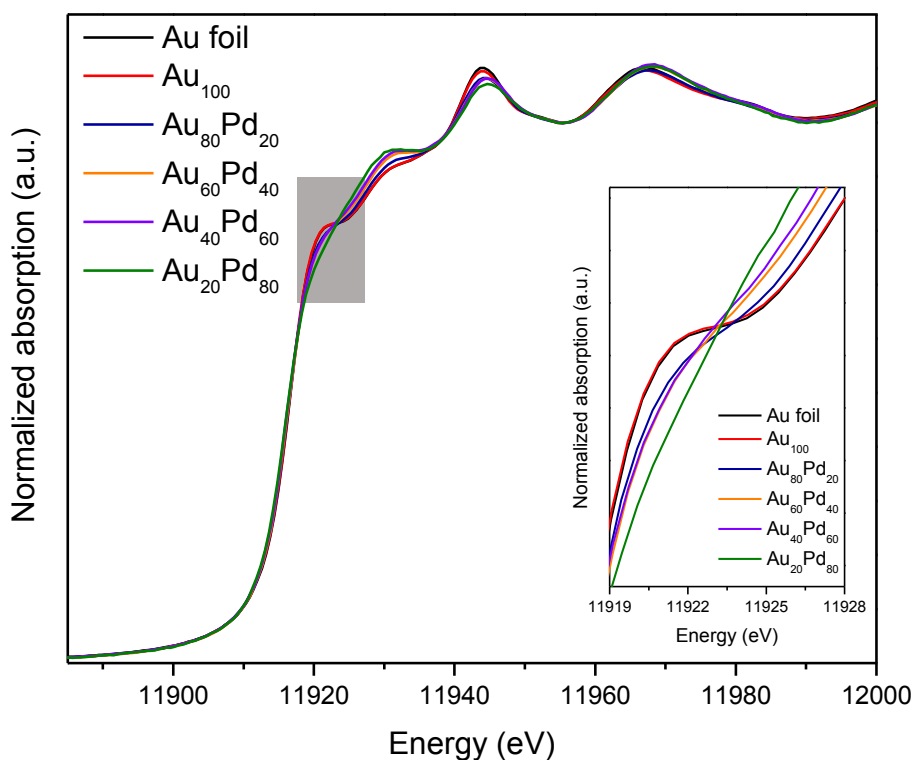


Figure 12: Au L_{III}-edge XANES of Au_xPd_y-DDAO/HT. The inset magnifies the white line region.

Figure 13A shows k^3 -weighted Au L_{III}-edge EXAFS oscillation pattern for Au foil and catalysts. The EXAFS oscillation patterns also support the presence of AuPd heterometallic bond formation with diminishing of doublet characteristics at 5.2 \AA^{-1} . The FT of Au L_{III}-edge EXAFS spectra were also plotted in **Figure 13B**. The AuPd bimetallic catalysts showed intense doublet peaks at 2.1 and 2.9 \AA as compared to Au foil and Au₁₀₀-DDAO/HT. The appearance and intensification of the doublet with increase in Pd content is an indication of Au-Pd bonds⁴⁷⁻⁴⁹ in AuPd bimetallic NPs-based heterogeneous catalysts.

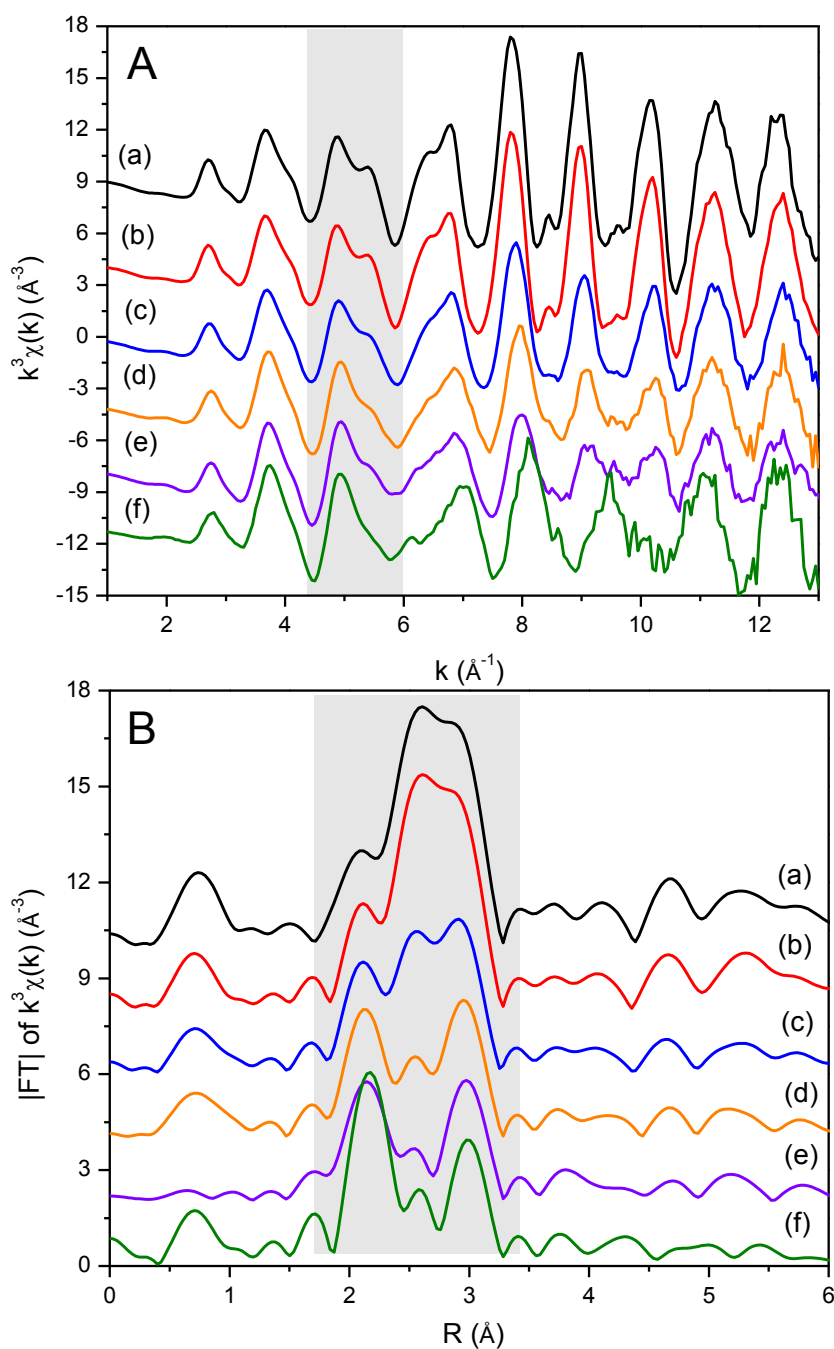


Figure 13: (A) Au L_{III}-edge EXAFS k^3 -weighted and (B) FT spectra for Au_xPd_y-DDAO/HT catalysts, (a) Au foil (b) Au₁₀₀-DDAO/HT (c) Au₈₀Pd₂₀-DDAO/HT (d) Au₆₀Pd₄₀-DDAO/HT (e) Au₄₀Pd₆₀-DDAO/HT (f) Au₂₀Pd₈₀-DDAO/HT.

The Pd XAS features in K- and L_{III}-edges of the Au₄₀Pd₆₀-DDAO/HT (**Figure 14**) also supported the strong correlation between Pd and Au. The two features at 24389 and 24428 eV in Pd K-edge XANES spectra were observed at lower energy for AuPd

bimetallic catalysts than for Pd foil (**Figure 14A**). The Pd K-edge XANES of the Au₄₀Pd₆₀-DDAO/HT was very close to that of Pd foil, while the height of Au₄₀Pd₆₀-DDAO/HT in Pd L_{III}-edge was little higher than Pd metal (**Figure 14B**). These suggested the depletion of electron in Pd 4d state in Au₄₀Pd₆₀-DDAO/HT was caused by the presence of Pd-Au bonds.

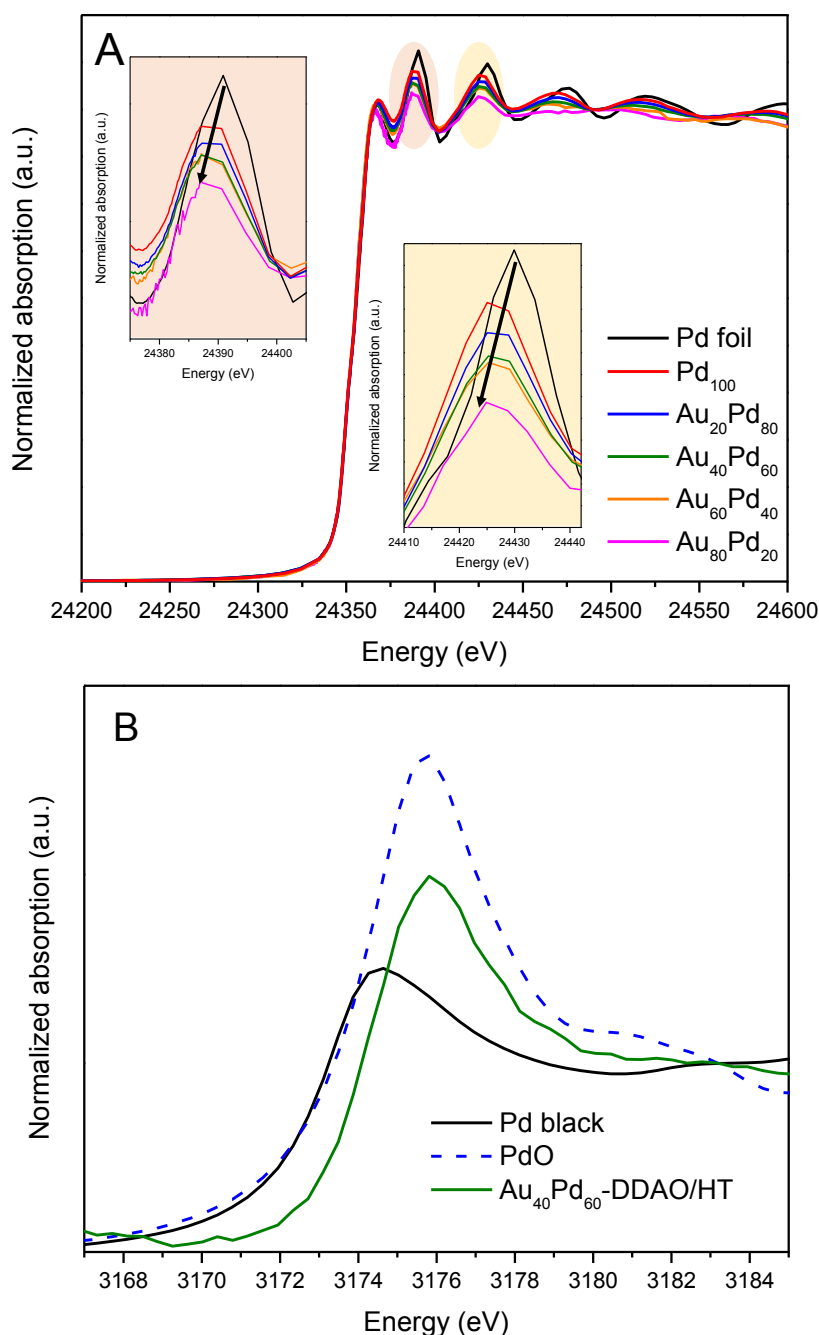


Figure 14: (A) Pd K-edge and (B) Pd L_{III}-edge XANES of the Au_xPd_y-DDAO/HT.

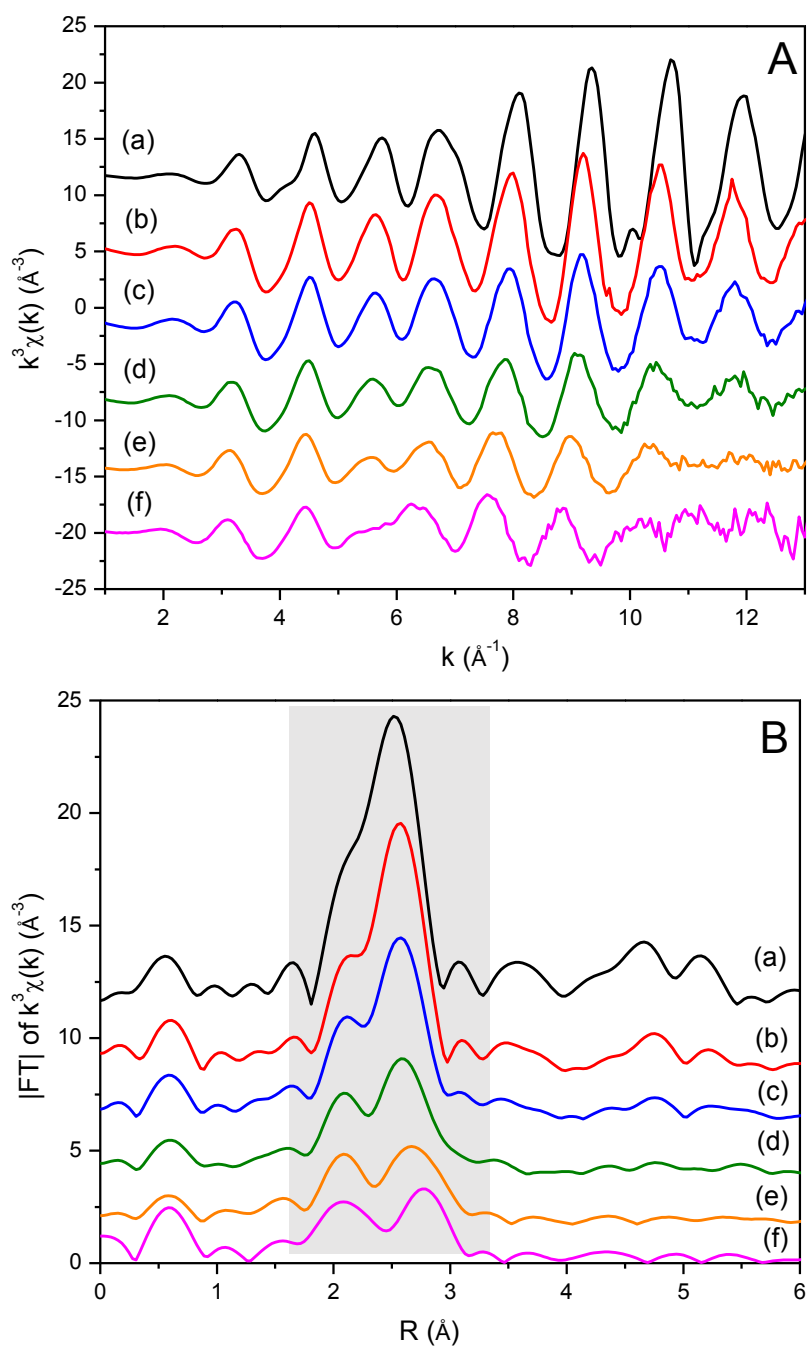


Figure 15: (A) Pd K-edge EXAFS k^3 -weighted and (B) FT spectra for $\text{Au}_x\text{Pd}_y\text{-DDAO/HT}$ catalysts, (a) Pd foil (b) $\text{Pd}_{100}\text{-DDAO/HT}$ (c) $\text{Au}_{20}\text{Pd}_{80}\text{-DDAO/HT}$ (d) $\text{Au}_{40}\text{Pd}_{60}\text{-DDAO/HT}$ (e) $\text{Au}_{60}\text{Pd}_{40}\text{-DDAO/HT}$ (f) $\text{Au}_{80}\text{Pd}_{20}\text{-DDAO/HT}$.

From the above observations, it can be inferred that electronic properties of Au and Pd are significantly changed in the bimetallic catalysts as a consequence of Au-Pd

interactions (bond formation). These particular interactions might be responsible for the high catalytic activity of the Au₄₀Pd₆₀-DDAO/HT for the selective oxidation of HDO to HCA.

4.4 Role of Capping Agent

It is well-known that the metal composition, size and shape of NPs have notable influence on their catalytic properties. In addition the surface capping agents (organics or polymers) which are generally used in the synthesis of NPs to keep the particles suspended,⁵³ also influences the catalytic activity to a significant extent. The development of colloidal synthesis has the ability of precisely tailor the structural characteristics (size, shape and distribution) usually by varying the type or amount of a capping agent.⁵⁴⁻⁵⁶ On the other hand, the choice of capping agent would significantly affect the electronic properties of bimetallic NPs along with the alterations in size- and/or shape-dependent properties of the NPs. Multiple of research groups have explained the size-dependent properties of metal NPs but only some of them have discussed the influence from capping agents.⁵⁷⁻⁶¹ Overall, the role of the capping agent in catalytic activity and selectivity is not yet well-understood in spite of its importance to model nanoparticle systems for studying heterogeneous catalysis.

This above mentioned studies suggested that the synergistic interactions between Au and Pd or Au-Pd nanoalloy center plays crucial role in the significant catalytic performance Au₄₀Pd₆₀-DDAO/HT for selective oxidation of HDO towards HCA. But, this study with AuPd-DDAO bimetallic nanoparticles raises some additional interesting questions. Does the capping agent used affect the selectivity of HCA formation? How the change in the capping agent does influences the reaction? To shed light to these questions,

the catalytic activities of Au₄₀Pd₆₀-PVP/HT and Au₄₀Pd₆₀-PVA/HT bimetallic NPs are examined and compared to those of the Au₄₀Pd₆₀-DDAO/HT studied previously. The chemical structure of the capping agents used in this study are presented in **Figure 16**.

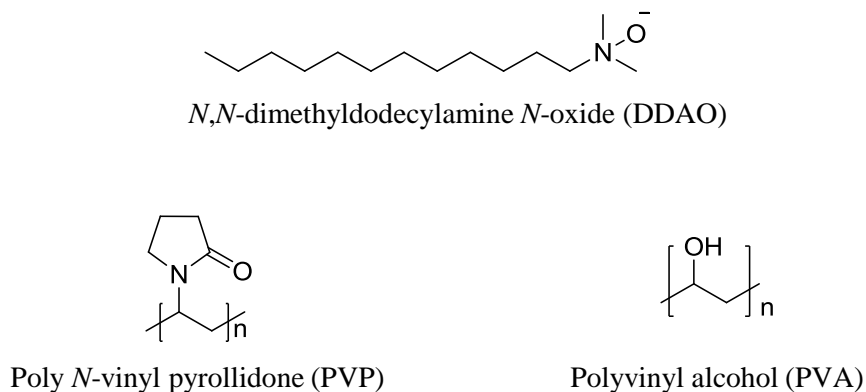


Figure 16: Chemical structure of capping agents used in this study

4.4.1 Catalytic Activity

To probe the structural effects on the reactivity of these capped bimetallic catalysts, selective oxidation of HDO to HCA was conducted with Au₄₀Pd₆₀-X/HT as heterogeneous catalyst under the previously optimized reaction conditions (**Table 5**). All three catalysts were observed to be highly active for HDO, but selectivity of HCA was seen to be influenced with the choice of capping agent used. **Table 5** also describes the average particle size of bimetallic NPs observed by TEM and the real amount of metal loading on HT by ICP-AES measurements.

From **Table 5**, it was observed that the PVP and PVA capped catalyst leads to the high conversions of HDO (>90%), however, the selectivity for HCA was observed to be low (60~70%) (entries 1-2). In spite of low metal loading in case of PVA capped catalyst, it showed efficient catalytic activity and leads to the 90% HDO conversion. While the superior activity was observed with DDAO capped catalyst which afforded the highest

selectivity of 93% for HCA with 87% HDO conversion (entry 3). The choice of capping agent in addition of HCA selectivity also effected the average particle size.

Table 5: Selective oxidation of HDO to HCA over Au₄₀Pd₆₀-**X**/HT ^a

Entry	Catalyst	Conv/ % ^c	Yield (sel.)/% ^c		metal loading		Metal
		HDO	HCA	AA	Au	Pd	P. Size ^e
1	Au ₄₀ Pd ₆₀ -PVP/HT	94	58 (62)	29 (31)	37	57	2.8
2	Au ₄₀ Pd ₆₀ -PVA/HT	90	61 (68)	19 (21)	12	21	3.5
3	Au ₄₀ Pd ₆₀ -DDAO/HT	87	81 (93)	4 (5)	34	56	4.2

^a**Reaction Conditions:** HDO (0.5 mmol), catalyst (25 mg), 30% H₂O₂ (0.75 mL), 0.5 M NaOH (0.75 mL), H₂O (3.5 mL), 353 K, 8 h. ^banalysed by HPLC, ^canalysed by ICP-AES ($\times 10^{-3}$ mmol g⁻¹) ^edetermined from TEM.

4.4.2 Catalyst Characterization

4.4.2.1 Transmission Electron Microscopy

TEM images and particle size distribution of the AuPd bimetallic NPs capped with PVP, PVA and DDAO are shown in **Figure 17**. Average diameter obtained for capped NPs was 2.8 nm for PVP, 3.5 nm for PVA and 4.2 nm for DDAO. The results suggested that the NPs are well dispersed on heterogeneous surface and choice of capping agent influences the average particle size and particle size distribution.

The correlation between the catalytic activity and the particle size distribution can be explained as, the smallest size NPs leads to the lowest selectivity of HCA formation and large particles with DDAO capped produces HCA with high selectivity.

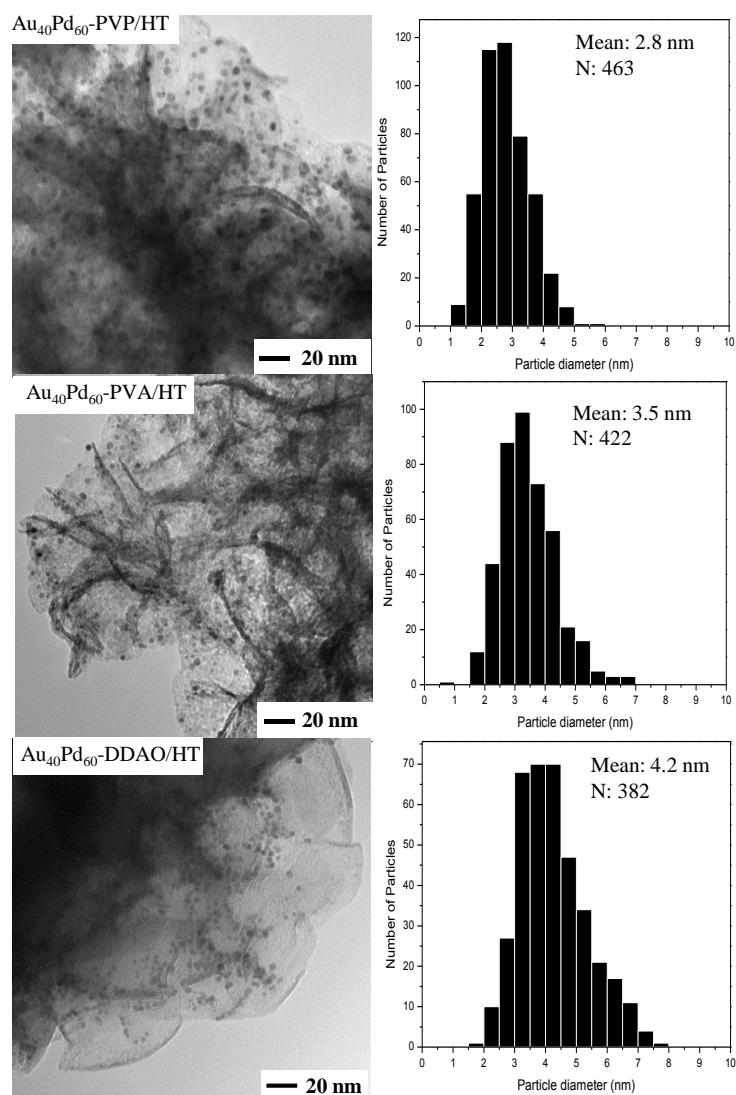


Figure 17: TEM images and Particle size distribution of AuPd-X/HT.

4.4.2.2 X-ray Diffraction Pattern

To characterize the capped AuPd bimetallic NPs the X-ray diffraction pattern were recorded and plotted in **Figure 18**. The diffraction signals were clearly visible in case of DDAO capped catalyst while the same features were not so sharp in case of PVP and PVA. The weakening of diffraction peak could be either due to the formation of nano-crystalline AuPd bimetallic NPs or presence of variety of Au-Pd species. As, not much

information could be collected from XRD, the further characterizations were carried out to get the clear picture for superior catalytic activity of DDAO capped catalysts.

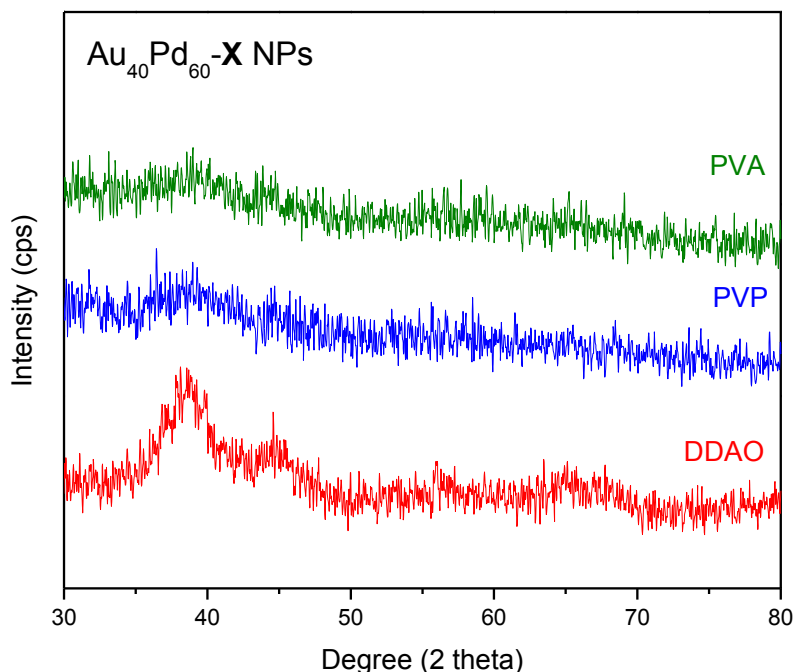


Figure 18: XRD patterns of AuPd-X NPs.

4.4.2.3 X-ray Absorption Spectroscopy

To get the information on the electronic effect and nanostructure caused by different capping agents and its correlation with the catalytic activity, the X-ray absorption spectroscopy were measured for Au-L_{III} and Pd-L_{III} and K-edge for Au₄₀Pd₆₀-X/HT catalysts.

4.4.2.3.1 XANES study of Au and Pd L_{III}-edge

The Au L_{III}-edge probes the transition of 2p electrons to the 5d orbitals; the XANES spectra of the Au L_{III}-edge of Au₄₀Pd₆₀-X/HT is shown in **Figure 19**. For all three bimetallic AuPd catalysts, a significant decrease in the white line intensity which corresponds to the first feature after the edge jump at 11925 eV occurs. The decrease in

white line intensity is observed for the increase in the d-electron density of Au. Which might possibly be due to electron transfer from Pd into 5d Au orbitals *via* Au-Pd alloying.⁵² The inset image of **Figure 19** clearly shows a more electronegative Au species in case of PVP and PVA capped catalysts as compared to DDAO capped catalysts, indicating more prominent Au-Pd alloying in case of PVP and PVA. Another important feature at the Au-L_{III} edge was the lower intensity of the second band (11935 eV) with DDAO capped catalysts opposed to that of PVP and PVA capped. This feature again signified the lower level of mixing of the Au and Pd metals in DDAO capped catalyst.

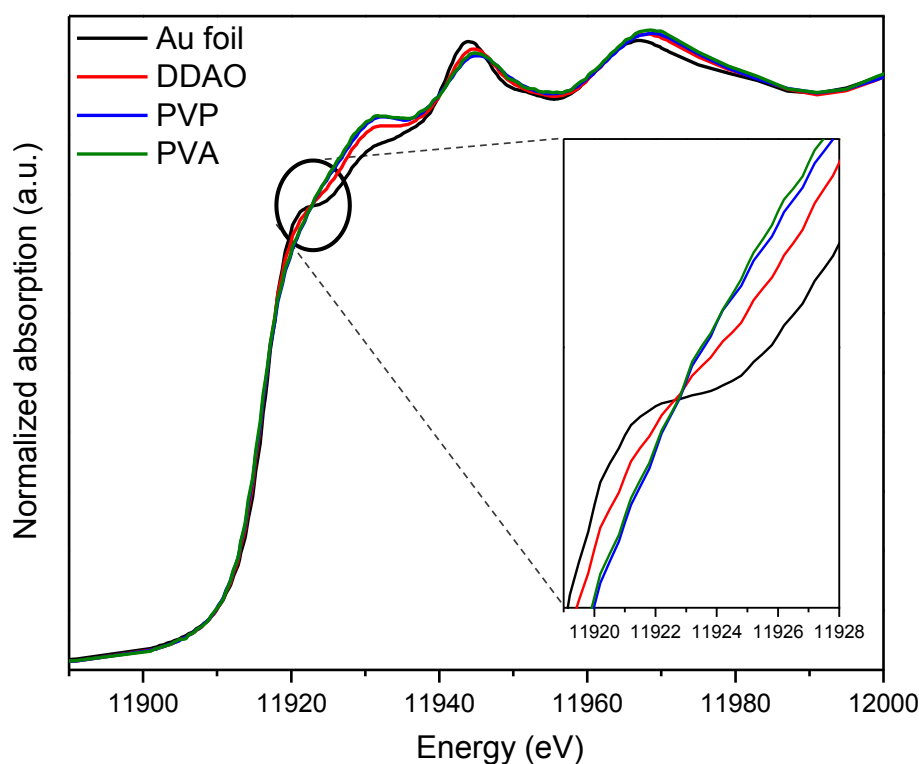


Figure 19: Au L_{III}-edge XANES of AuPd-X/HT catalysts.

The Pd L_{III} XANES spectra is shown in **Figure 20** for the catalysts studied. A significant decrease in white line intensity was seen from PVA > PVP > DDAO capped catalysts. The less intense white line for DDAO capped catalyst, indicated the presence of more d-electrons in Pd.⁶⁰ Similarly, Au L_{III}-edge data above suggested lowest electrons

in Au d-orbitals of DDAO capped catalysts among the three. Combining the results from both Au and Pd L_{III}-edge XANES suggested the lesser electronic interactions between Au and Pd metals (or low extent of Au-Pd alloying) when bimetallic NPs were synthesized with DDAO in contrast of PVP and PVA as capping agent.

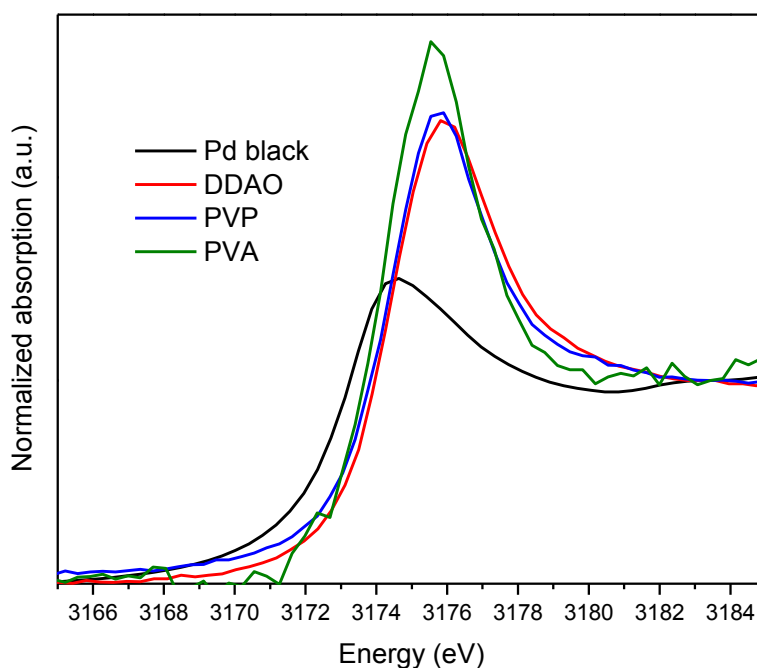


Figure 20: Pd L_{III}-edge XANES of AuPd-X/HT catalysts.

4.3.2.3.2 FT and EXAFS studies of Au L_{III}-edge and Pd K-edge

Figure 21 shows the k^3 -weighted (A) and Fourier transformed EXAFS (B) of the catalysts and Au foil for Au L_{III}-edge. It was noticed that the EXAFS oscillation pattern was very much similar to that of Au foil for Au₄₀Pd₆₀-DDAO/HT, while it differs for Au₄₀Pd₆₀-PVP/HT and Au₄₀Pd₆₀-PVA/HT (in the range of 5-7 Å). This observation could be due to increase in neighboring Pd atoms in surrounding of Au atoms, resulting in the formation of high number of Au-Pd bonds.⁶⁰

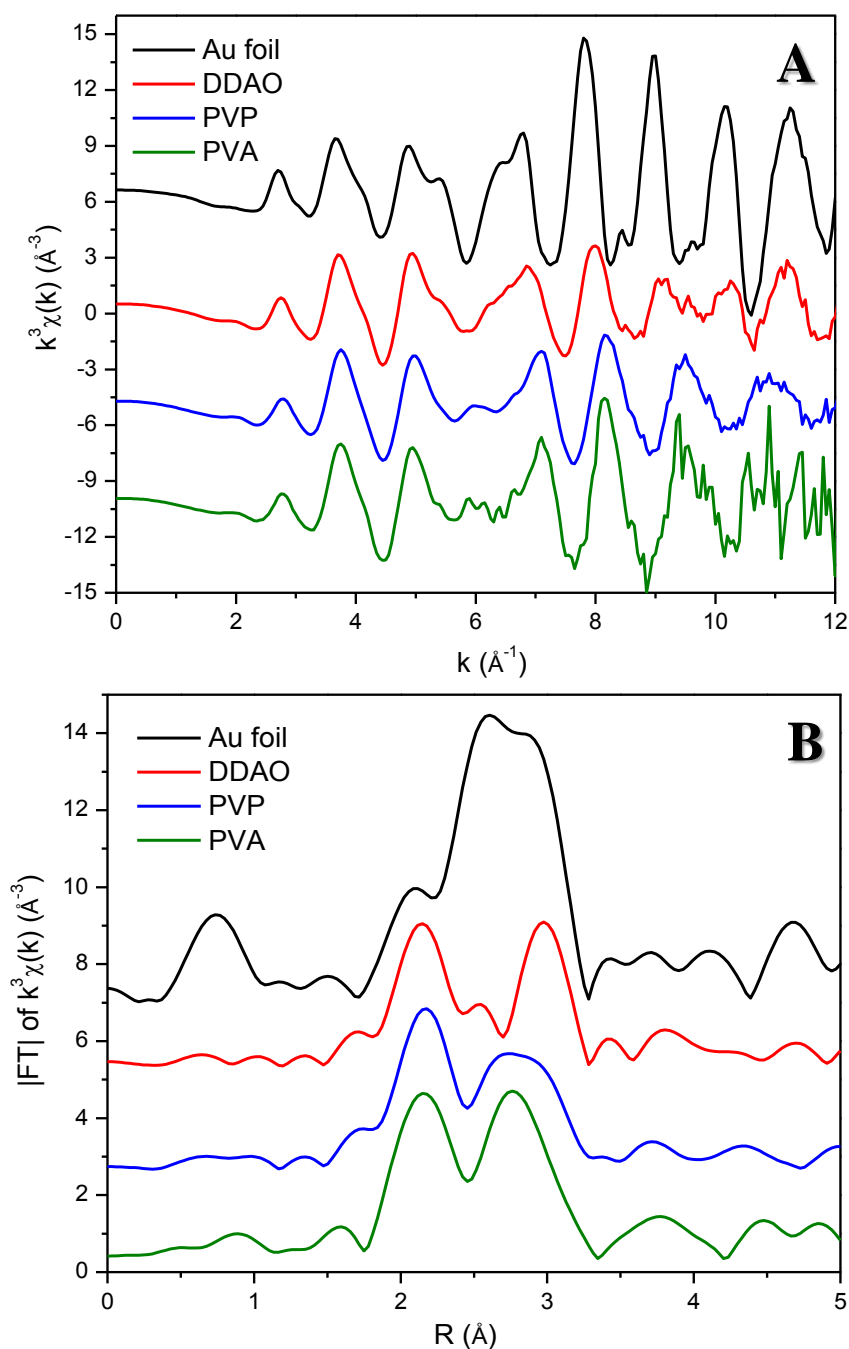


Figure 21: Au L_{III}-edge EXAFS (A) k^3 -weighted and (B) FT spectra for Au₄₀Pd₆₀-X/HT catalysts.

The formation of Au–Pd bonds was also reflected in the Au L_{III} Fourier transformed EXAFS spectra (**Figure 21B**). In contrast to the Au foil reference, all catalysts had intense doublet peaks in the region of 1.7–3.3 Å. The splitting of the peak arises from the interference between the EXAFS oscillations of the Au–Au and Au–Pd

bonds.⁶¹ The shape of FT-EXAFS spectra of DDAO, PVP and PVA capped bimetallic catalysts was found to be much different from each other. The DDAO capped catalyst exhibit less intense doublets than the PVP and PVA capped catalysts, which supports the formation of less Au-Pd bonds in DDAO capped catalysts.

Thus, from less intense splitting and similar EXAFS oscillations pattern of DDAO capped catalyst hints that the extent of alloying between Au and Pd is very low. On contrary the extent of alloying is high when bimetallic NPs were capped with PVP or PVA.

Pd K-edge k -space EXAFS had very similar patterns for all the AuPd bimetallic catalysts and the reference Pd foil (**Figure 22A**). The FT of Pd K-edge EXAFS spectra also described in **Figure 22B**. Similarly to FT of Au L_{III}-edge, in Pd K-edge splitting in the region of 2-3 Å was observed for bimetallic catalysts in comparison to Pd foil, which again confirms the formation of Au-Pd random alloy in bimetallic capped catalysts. The intensification of doublet in case of PVP and PVA capped adds on to therevious conclusion that the extent of alloying between two metals in low in DDAO and high in case of PVP and PVA capped catalysts.

XAS studies on Au L_{III}-edge, Pd K-edge and Pd L_{III}-edge indicated the presence of Au-Pd bond formation or alloying between Au and Pd in all DDAO, PVP and PVA capped bimetallic catalysts. But, the electronegativity of Au and extent of alloying was found to be different with different capping agents used. The high electronegative Au species and more prominent alloying was noticed for PVP and PVA capped catalysts. here as, moderately negative Au species and weak alloying or mixing of Au and Pd metals was noticed with Au₄₀Pd₆₀-DDAO/HT.

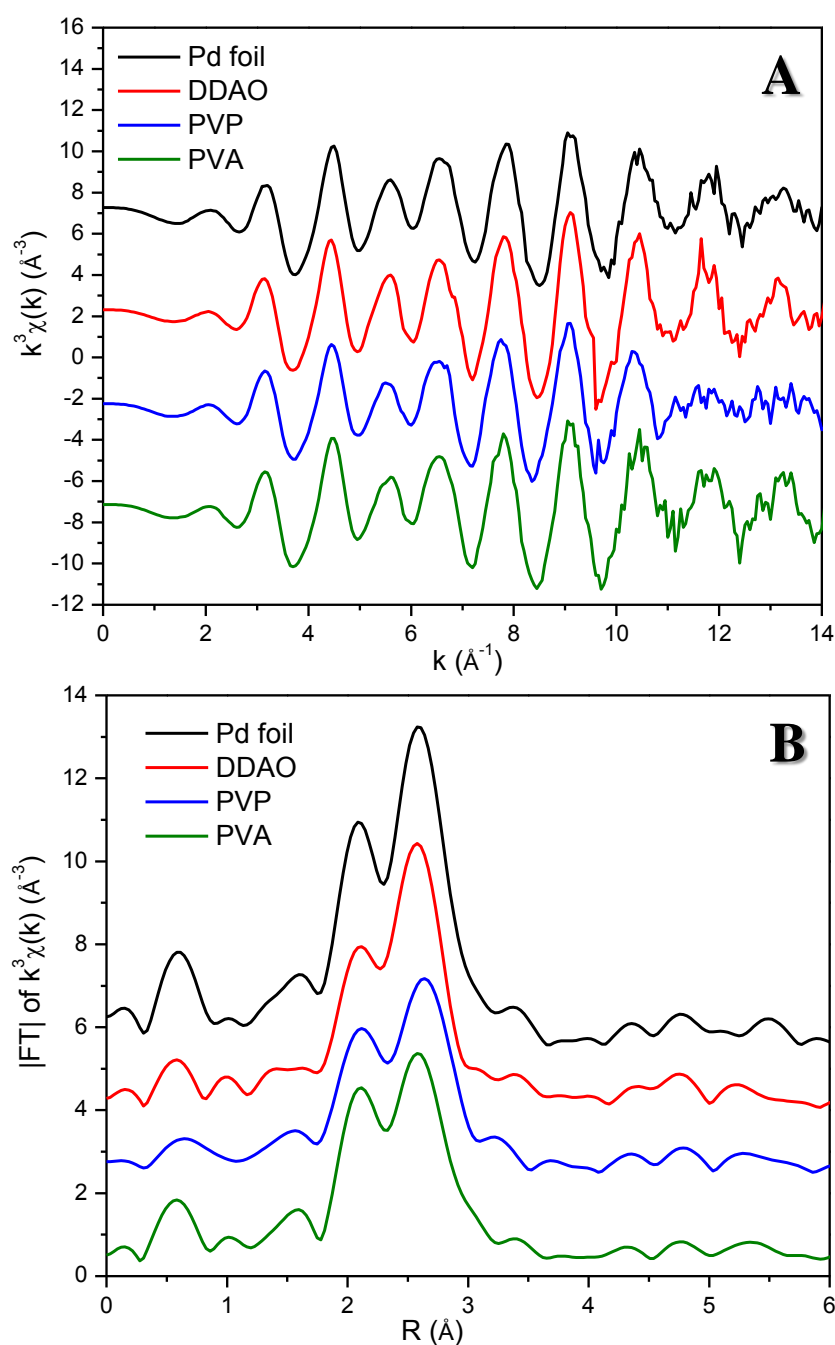


Figure 22: Pd K-edge EXAFS (A) k^3 -weighted and (B) FT spectra for Au₄₀Pd₆₀-X/HT catalysts.

From the catalytic activity and the catalyst characterization of differently capped bimetallic catalysts, it can be concluded that moderately negatively charged Au species and a few Au-Pd heterometallic bond (low extent of Au-Pd alloying) leads to high selectivity of HCA. On the other side highly negatively charged Au species with high

number of Au-Pd bond (high extent of Au-Pd alloying) resulted in to low selectivity of HCA by forming of AA as side-product (over oxidation).

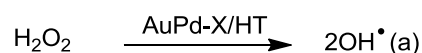
4.5 Proposed Reaction Mechanism

The reaction mechanism has been proposed based on the experimental facts and the literature review. The important experimental results are listed again over here. As, mentioned earlier the use of melatonin as water soluble radical melatonin as water-soluble radical quencher of hydroxyl radicals (OH^\bullet) indicated that the reaction mechanism might follow a radical pathway: *i.e.* H_2O_2 is split into hydroxyl radicals that acts as an oxidizing agent in the reaction. Thus, Step-1 of **Figure 23** is proposed as the decomposition of H_2O_2 over bimetallic AuPd surface and these resulted OH^\bullet deposited on the metal surface. There are precedents in literature for formation of such radicals over metal NPs in the presence of hydrogen peroxide.^{42,43}

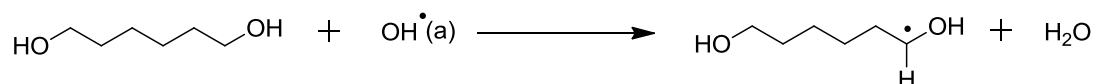
Step-2 is the abstraction of proton by adsorbed OH^\bullet to generate a carbon centered radical, the formation of carbon centered in the reaction mixture was suggested by the following observation. The reaction with melatonin as radical scavenger in absence of H_2O_2 also decrease the reaction rate by 50%, and melatonin is also capable of scavenging carbon centered radical (not as efficiently as OH^\bullet),⁶² thus it can be inferred that the carbon centered radical has been formed in our reaction conditions.

After the generation of carbon centered radical, the next step is the addition of adsorbed OH^\bullet to the carbon centered radical to form hydrate in the step-3. Both the abstraction of proton and addition by OH^\bullet has been reported as chemical reaction by OH^\bullet in aqueous solutions.⁶³ Finally the step-4 is the base mediated transformation of hydrate to give 6-hydroxycaproate as the final product.

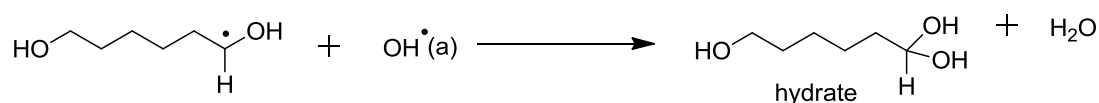
Step-1: Decomposition of H_2O_2 on metal surface



Step-2: Abstraction of proton by adsorbed OH^\bullet



Step-3: Addition of adsorbed OH^\bullet



Step-4: Base-catalyzed transformation of hydrate to carboxylate

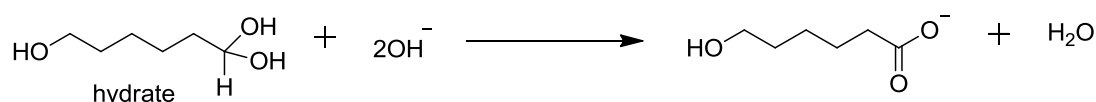


Figure 23: Proposed Reaction Mechanism

The selective oxidation with DDAO capped catalysts as compared to PVP and PVA capped catalysts can be now explained following this mechanism. From the above discussion, it was understood that moderately negatively charged Au species has been generated in case of DDAO capped catalysts with lower extent of alloying between Au and Pd, while the opposite was observed for PVP and PVA capped catalysts. It is known from the literature that, higher the electron density in 5d orbitals of Au (high electronegativity of Au), weaker the Au-O bond.^{64,65} Thus, the OH radicals are comparatively less stabilized in case of PVP and PVA than that of DDAO capped catalysts. The high negative charge on Au makes the controlled or selective oxidation difficult and over oxidation leads to the formation of AA in good quantities. While the stronger bond of Au and OH^\bullet in DDAO capped catalysts helps to maintain the high selectivity of mono-oxidation to form HCA as major product.

4.6 Catalytic Activity of other Aliphatic Alcohols

After successful completion of the selective oxidation of C6 aliphatic diol (HDO), the catalytic system was further verified for selective oxidation of longer chain aliphatic diol systems such as C7 and C8 aliphatic diols. The results clearly show that the system is acceptable for the selective synthesis of respective mono-hydroxycarboxylic acid from 1,7-heptanediol and 1,8-octanediol with high selectivity (**Figure 24**, entries 1 and 2). The reaction under same conditions affords oxidation of primary alcohol group selectively when both primary and secondary alcohol group were present for *e.g.* selective oxidation of 1,2-hexanediol to 2-hydroxyhexanoic acid was successfully achieved over Au₄₀Pd₆₀-DDAO/HT in high yield and selectivity (**Figure 24**, entry 3). In addition the present catalytic system also oxidized non-activated alcohol systems (1-hexanol) to its corresponding carboxylic acid (hexanoic acid) (**Figure 24**, entry 4).

4.7 Conclusion

A series of hydrotalcite supported DDAO-capped bimetallic AuPd NPs were prepared, and their catalytic activities were explored for HDO oxidation. A maximum of HCA yield (81%) at 87% HDO conversion was achieved with reusable Au₄₀Pd₆₀-DDAO/HT catalyst in basic aqueous media using H₂O₂. The spectroscopic investigations suggested AuPd interactions to provide negatively charged-Au species, which might be responsible for the excellent catalysis in the selective oxidation of one primary OH group of C6 aliphatic diol, HDO. The further investigation on catalytic activity of supported AuPd bimetallic NPs capped with other capping agents such as PVP and PVA highlights the important role of capping agent in this particular selective oxidation of HDO. The characterization of differently capped catalysts concluded that the DDAO as capping agent could lead to

synthesis of moderately negatively charged Au species in AuPd bimetallic NPs system with a few heterometallic Au-Pd bond formation. These particular sites of Au-Pd bond and specific $\text{Au}^{\delta-}$ species was found to play the key role in the production of mono-hydroxycarboxylic acid from long chain aliphatic diols with high selectivity.

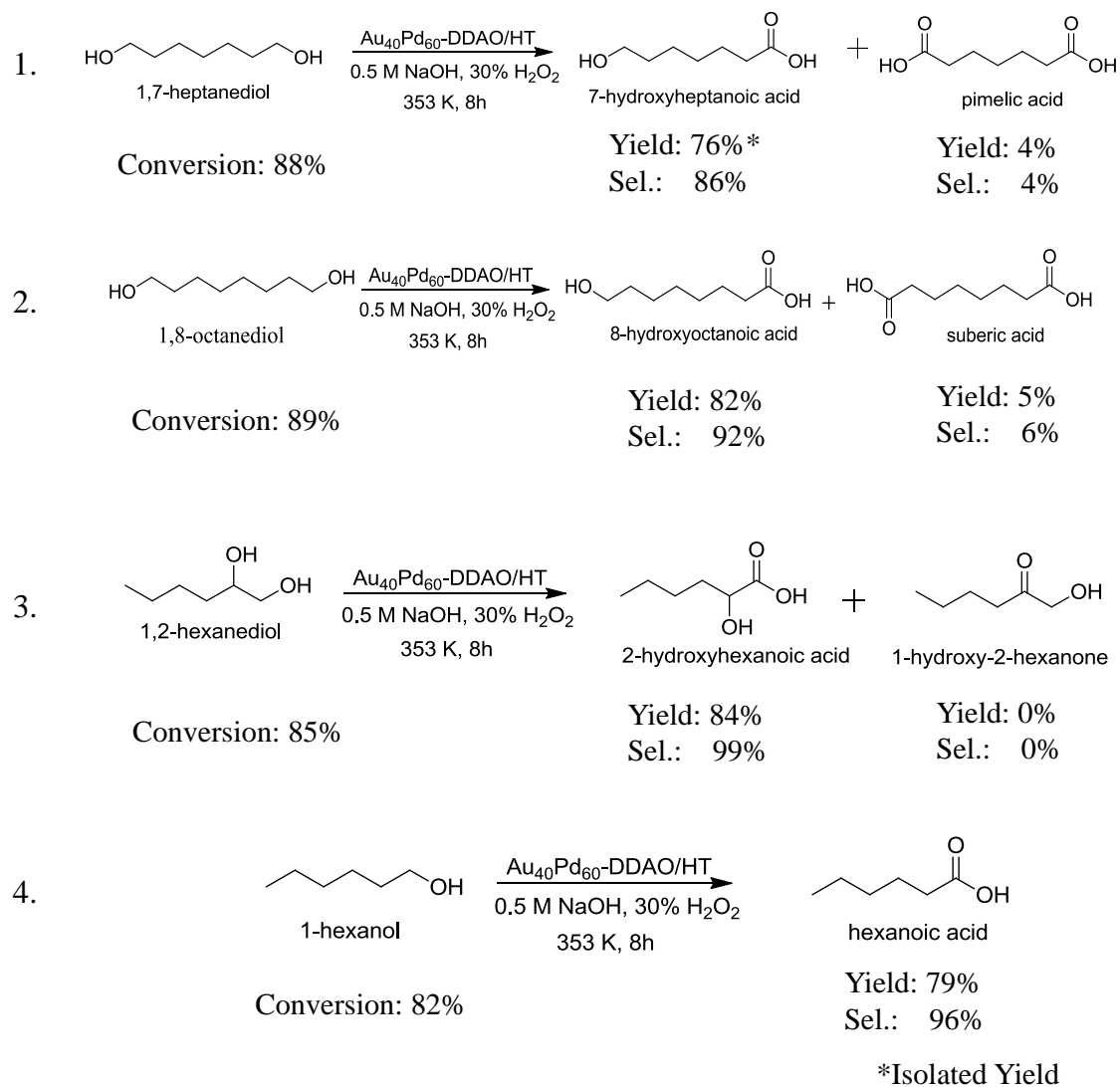


Figure 24: Catalytic activity for other aliphatic alcohols

4.8 References

1. For example: G. W. Huber, J. N. Chheda, C. J. Barrett and J. A. Dumesic, *Science*, **2005**, *308*, 1446-1450.
2. J. C. Serrano-Ruiz, R. Luque and A. Sepúlveda-Escribano, *Chem. Soc. Rev.*, **2011**, *40*, 5266-5281.
3. F. Jin and H. Enomoto, *Energy Environ. Sci.*, **2011**, *4*, 382-397.
4. N. K. Gupta, S. Nishimura, A. Takagaki and K. Ebitani, *Green Chem.*, **2011**, *13*, 824-827.
5. M. Besson, P. Gallezot and C. Pinel, *Chem. Rev.*, **2014**, *114*, 1827-1870.
6. H. Choudhary, S. Nishimura and K. Ebitani, *App. Catal. B: Environ.*, **2015**, *162*, 1-10.
7. M. Labet and W. Thielemans, *Chem. Soc. Rev.*, **2009**, *38*, 3484-3504.
8. R. Orchel, K. Jelonek, J. Kasperczyk and Z. Dzierżewicz, *Acta Pol. Pharm.-Drug Res.*, **2010**, *67*, 710-714.
9. A. Georgia, Lactates-Advances in Research and Application, ed. Q. A. Acton, 2013, Scholarly Edition, pp. 127.
10. R. H. Fischer, R. Pinkos and F. Stein, 2002, US6426438 B1.
11. I. Belkhir, A. Germain, F. Fajula and E. Fache, Studies in Surface Science and Catalysis, ed. S. T. Oyama, A. M. Gaffney, J. E. Lyons and R. K. Grasselli, Third World Congress on Oxidation Catalysis, Elsevier, 1997, pp. 577.
12. N. d'Alessandro, L. Liberatore, L. Tonucci, A. Morvillo and M. Bressan, *New J. Chem.*, **2001**, *25*, 1319-1324.
13. Y. Usui and K. Sato, *Green Chem.*, **2003**, *5*, 373-375.

14. T. Buntara, S. Noel, P. H. Phua, I. M. Cabrera, J. G. de Vries and H. J. Heeres, *Angew. Chem. Int. Ed.*, **2011**, 50, 7083-7087.
15. M. Chia, Y. J. P-Torres, D. Hibbitts, Q. Tan, H. N. Pham, A. K. Datye, M. Neurock, R. J. Davis and J. A. Dumesic, *J. Am. Chem. Soc.*, **2011**, 133, 12675-12689.
16. J. Tuteja, H. Choudhary, S. Nishimura and K. Ebitani, *ChemSusChem*, **2014**, 7, 96-100.
17. M. S. Ide and R. J. Davis, *J. Catal.*, **2013**, 308, 50-59.
18. H. Tohma, T. Maegawa, S. Takizawa and Y. Kita, *Adv. Synth. Catal.*, **2002**, 344, 328-337.
19. S. Kara, D. Spickermann, J. H. Schrittwieser, A. Weckbecker and C. Leggewie, *ACS Catal.*, **2013**, 3, 2436-2439.
20. S. Schauermann, N. Nilius, S. Shaikhutdinov and H.-J. Freund, *Acc. Chem. Res.*, **2013**, 46, 1673-1681.
21. Z. Guo, B. Liu, Q. Zhang, W. Deng, Y. Wang and Y. Yang, *Chem. Soc. Rev.*, **2014**, 43, 3480-3524.
22. D. I. Enache, J. K. Edwards, P. London, B. Solsona-Espriu, A. F. Carley, A. A. Herzing, M. Watanabe, C. J. Kiely, D. W. Knight and G. J. Hutchings, *Science*, **2006**, 311, 362-365.
23. H. Zhang, T. Watanabe, M. Okumura, M. Haruta and N. Toshima, *Nat. Mater.*, **2012**, 11, 49-52.
24. S. Nishimura, Y. Yakita, M. Katayama, K. Higashimine and K. Ebitani, *Catal. Sci. Technol.*, **2013**, 3, 351-359.

25. D. Tongsakul, S. Nishimura and K. Ebitani, *J. Phys. Chem. C*, **2014**, *118*, 11723-11730.
26. N. Toshima and T. Yonezawa, *New J. Chem.*, **1998**, *22*, 1179-1201.
27. H. B. Liu, U. Pal, A. Medina, C. Maldonado and J. A. Ascencio, *Phys. Rev. B*, **2005**, *71*, 075403-6.
28. D. Tongsakul, S. Nishimura and K. Ebitani, *ACS Catal.*, **2013**, *3*, 2199-2207.
29. M. H. Ab Rahim, M. M. Forde, R. L. Jenkins, C. Hammond, N. Dimitratos, J. A. Lopez-Sanchez, A. F. Carley, S. H. Taylor, D. J. Willock, D. Murphy, C. J. Kiely and G. J. Hutchings, *Angew. Chem. Int. Ed.*, **2013**, *52*, 1280-1284.
30. J. Xu, T. White, P. Li, C. H. He, J. G. Yu, W. K. Yuan and Y. F. Han, *J. Am. Chem. Soc.*, **2010**, *132*, 10398-10406.
31. H. Matsune, Y. Kuramitsu, S. Takenaka and M. Kishida, *Chem. Lett.*, **2010**, *39*, 717-719.
32. H. Choudhary, S. Nishimura and K. Ebitani, *ChemCatChem*, Accepted for Publication in 2015, DOI. 10.1002/ctc.201500166.
33. B. F. Sels, D. E. De Vos, M. Buntinx, F. Pierard, A. KirschDe Measmarker and P. A. Jacobs, *Nature*, **1999**, *400*, 855-857.
34. K. Kaneda, K. Mori, T. Mizugaki and K. Ebitani, *Bull. Chem. Soc. Jpn.*, **2006**, *79*, 981-1016.
35. S. Nishimura, A. Takagaki and K. Ebitani, *Green Chem.*, **2013**, *15*, 2026-2042.
36. Catalytic Oxidations with Hydrogen Peroxide as Oxidant, ed. G. Strukul, Kluwer Academic, Dordrecht, The Netherlands, 1992.
37. R. Noyori, M. Aoki and K. Sato, *Chem. Commun.*, **2003**, 1977-1986.
38. J. M. Richardson and C. W. Jones, *Adv. Synth. Catal.*, **2006**, *348*, 1207-1208.

39. H. Choudhary, S. Nishimura and K. Ebitani, *J. Mater. Chem. A*, **2014**, 2, 18687-18696.
40. H. J. Bromme, W. Morke, E. Peschke, H. Ebel and D. Peschke, *J. Pineal Res.*, **2000**, 29, 201-208.
41. M. Yoshida, A. Fukuda, M. Hara, A. Terada, Y. Kitanaka and S. Owada, *Life Sci.*, **2003**, 72, 1773-1780.
42. D. W. McKee, *J. Catal.*, **1969**, 14, 355-364.
43. S. Navalon, R. Martin, M. Alvaro and H. Garcia, *Angew. Chem. Int. Ed.*, **2010**, 49, 8404-8407.
44. S. Link and M. A. El-Sayed, *J. Phys. Chem. B*, **1999**, 103, 4212-4217.
45. H. Yang, D. Tang, X. Lu and Y. Yuan, *J. Phys. Chem. C*, **2009**, 113, 8186-8193.
46. R. E. Watson, J. Hudis and M. L. Periman, *Phys. Rev. B*, **1971**, 4, 4139.
47. A. Murugadoss, K. Okumura and H. Sakurai, *J. Phys. Chem. C*, **2012**, 116, 26776-26783.
48. R. Wang, Z. Wu, C. Chen, Z. Qin, H. Zhu, G. Wang, H. Wang, C. Wu, W. Dong, W. Fana and J. Wang, *Chem. Commun.*, **2013**, 49, 8250-8252.
49. P. Dash, T. Bond, C. Fowler, W. Hou, N. Coombs and R. W. J. Scott, *J. Phys. Chem. C*, **2009**, 113, 12719-12730.
50. S. Nishimura, N. Ikeda and K. Ebitani, *Catal. Today*, **2014**, 232, 89-98.
51. S. Marx and A. Baiker, *J. Phys. Chem. C*, **2009**, 113, 6191-6201.
52. T. Balcha, J. R. Strobl, C. Fowler, P. Dash and R. W. J. Scott, *ACS Catal.*, **2011**, 1, 425-436.
53. S. M. Humphrey, M. E. Grass, S. E. Habas, K. Niesz, G. A. Somorjai, T. D. Tilley, *Nano Lett.*, **2007**, 7, 785-790.

54. G. C. Bond and D. T. Thompson, *Catal. Rev. Sci. Eng.*, **1999**, *41*, 319-388.
55. F. Porta, L. Prati, M. Rossi, S. Coluccia and G. Martra, *Catal. Today*, **2000**, *61*, 165-172
56. D. Zhao, Y. H. Wang and B. Q. Xu, *J. Phys. Chem. C*, **2009**, *113*, 20903-20911.
57. M. Turner, V. B. Golovko, O. P. Vaughan, P. Abdulkin, A. Berenguer-Murcia, M. S. Tikhov, B. F. Johnson and R. M. Lambert, *Nature*, **2008**, *454*, 981-983.
58. N. Shalkevich, W. Escher, T. Bu, B. Michel, L. Si-Ahmed and D. Poulidakos, *Langmuir*, **2010**, *26*, 663-670.
59. W. Chen and S. W. Chen, *Angew. Chem. Int. Ed.*, **2009**, *48*, 4386-4389.
60. F. Liu, D. Wechsler and P. Zhang, *Chem. Phys. Lett.*, **2008**, *461*, 254-259.
61. R. J. Davis and M. Boudart, *J. Phys. Chem.*, **1994**, *98*, 5471-5477.
62. S. Fujisawa, Y. Kadoma, M. Ishihara, K. Shibuya and I. Yokoe, *In-Vivo*, **2006**, *20*, 215-220.
63. L. M. Dorfman and G. E. Adams, Reactivity of Hydroxyl radical in aqueous solutions, **1973**, Chapter 1, pp 1.
64. S. Jalili, A. Z. Isfahani and R. Habibpour, *Int. J. of Indus. Chem.*, **2013**, *4*, 1-12.
65. B. Hammer and J. K. Nørskov, Advances in Catalysis, volume 45, Theoretical Surface Science and Catalysis—Calculations and Concepts, **2000**, pp 85.

Chapter 5

*Base-free Chemoselective Transfer Hydrogenation
of Nitroarenes to Anilines with Formic Acid as
Hydrogen Source by a Reusable Heterogeneous
Pd/ZrP Catalyst*

Base-free Chemoselective Transfer Hydrogenation of Nitroarenes to Anilines with Formic Acid as Hydrogen Source by a Reusable Heterogeneous Pd/ZrP Catalyst

Abstract

A highly efficient, chemoselective, environmentally-benign method is developed for the catalytic transfer hydrogenation (CTH) of nitroarenes using FA as a hydrogen source. Various supported Pd catalysts were examined for this transformation, and Pd supported ZrP (Pd/ZrP) proved to be the best catalyst for CTH of nitrobenzene. Applicability of the Pd/ZrP catalyst is also explored for hydrogenation of various substituted nitroarenes. The Pd/ZrP catalyst showed high specificity for hydrogenation of nitro groups even in the presence of other reducible functional groups such as --C=C , --COOCH_3 , and $\text{--C}\equiv\text{N}$. To investigate the reaction mechanism, a Hammett plot was obtained for CTH of *p*-substituted nitroarenes. The active site is thought to be in situ generated Pd(0) species as seen from XRD and TEM data. The Pd/ZrP catalyst is reusable at least up to 4 times while maintaining the same activity and selectivity. To the best of our knowledge, this is one of the best methodologies for CTH of nitroarenes under base-free conditions with high activity and chemo-selectivity over heterogeneous Pd-based catalysts.

5.1 Introduction

Anilines are important intermediates and key precursors in the synthesis of dyes, pigments, agrochemicals, pharmaceuticals pesticides, herbicides, and fine chemicals.¹⁻³ The conventional synthesis methods for aniline are: transition metal-catalyzed (a) cross-coupling reaction of ammonia with aryl halides,⁴⁻⁸ phenol derivatives⁹ and aromatic boronic acid¹⁰ or (b) hydrogenation of corresponding nitroarenes.^{11,12} The latter approaches of catalytic reduction of nitroarenes are particularly attractive owing to their high atom efficiency and compatibility with large scale processes.

Industrial preparation of aniline performed by Bechamp process involving Fe/HCl as a reducing agent¹³ has now been replaced by more environmentally-benign catalytic protocols. Hydrogenation of nitroarenes using high pressure H₂ gas in conjunction with a range of heterogeneous catalysts has been the area of interest of a number of publications.¹⁴⁻¹⁹ Commercially available Ni or Pt based heterogeneous catalysts are commonly used for this transformation, however, the drawbacks of these catalysts are their poor selectivity and inapplicability for substituted nitroarenes.

Great attempts for serving high selectivity in the reduction of nitro group even under the presence of other reducible functional groups have been reported by using addition of stoichiometric reducing agents such as sodium hydrosulfite,²⁰ iron, tin or zinc in ammonium hydroxides,^{21,22} silanes,^{23,24} decaboranes,^{25,26} and formates.²⁷⁻²⁹ However, these processes are not environmentally sustainable, and the high selectivity is generally achieved on the expense of activity. Therefore, there is a strong incentive to develop chemoselective methods for reduction of substituted nitroarenes without using toxic additives and hydrogen gas.

Catalytic transfer hydrogenation (CTH), in which hydrogen donors are used instead of pressurized-hydrogen gas, is more advantageous way from the view point of a cost and handling; it eradicates the use of any special equipment for high pressured gas. Moreover, it is said that CTH enhances the selectivity in the reduction process via competitive adsorption of the liquid hydrogen donor on catalyst surface.³⁰ Therefore, CTH methods induced the considerable technical improvement over the rather messy traditional reduction with homogeneous transitional metals and acid reported in previous literatures.³¹ A wide variety of homogeneous and heterogeneous catalytic systems are developed for CTH of nitroarenes in combination with iso-propanol–potassium hydroxide or formic acid-organic base as hydrogen source.^{32–36} Other organic compounds known as the hydrogen donor in CTH are sodium formate, methanol, hydrazine, indoline, tetrahydroquinolines, 3-pyrroline, piperidine, pyrrolidine, glucose, and glycerol.^{37–43}

Formic acid (FA), a non-toxic liquid at room temperature, has been suggested as the promising hydrogen donor. It can be traditionally obtained from biomass processing and produces CO₂ as sole product; i.e. it is a safe, cheap and high potential hydrogen donor.^{44–46} Though high efficiencies of FA as hydrogen source have been obtained in combination with a high amount of organic bases, these homogeneous bases result in increase of complexity and cost in practice. Very recently, Beller and coworkers⁴⁷ reported base-free CTH reactions of nitroarenes with FA using homogeneous iron complex as catalyst affording high activity and selectivity under mild conditions. Despite accomplishment of many studies, search for an efficient, chemoselective, base-free, heterogeneously-catalyzed, cost-effective and environmentally-benign procedure for CTH of nitroarenes is of continuing interest.

The extensive research on hydrogenation reactions suggested that the presence of Brønsted acid plays an crucial role for such reactions.^{48,49} I recently demonstrated zirconium phosphate (ZrP) acted as an efficient solid acid support which possessed a high ratio of Brønsted/Lewis acid sites⁵⁰ for Pd catalyzed hydrogenolysis of 5-hydroxymethyl furfural to 1,6-hexanediol using FA as a hydrogen source.⁵¹ This result fascinated us to pursue potential applications of Pd/ZrP as the catalyst in CTH reactions of organic substrates such as nitroarenes.

In this study, a convenient and highly chemoselective approach is developed for base-free CTH reactions of nitroarenes under environmentally-benign conditions using FA and Pd/ZrP as a hydrogen source and a reusable heterogeneous catalyst, respectively. The catalytic system was further applied for the CTH of various substituted nitroarenes to the corresponding anilines, and a plausible mechanistic pathway is proposed based on the experimental results.

5.2 Experimental

5.2.1 Materials

All reagents and solvents were obtained from commercial suppliers and used without further purification. Zirconium chloride oxide octahydrate ($\text{ZrOCl}_2 \cdot 8\text{H}_2\text{O}$), sodium dihydrogen phosphate ($\text{NaH}_2\text{PO}_4 \cdot 2\text{H}_2\text{O}$), nitric acid, hexane, toluene, *N,N*-dimethylformamide (DMF), chloroform, dichloromethane (DCM), iso-propanol (*i*-PrOH), methanol, butanol, ethylacetate, ethanol, and naphthalene were purchased from Kanto Chemicals Co. Inc. Methyl-3-nitrobenzoate, methyl-4-aminobenzoate and 4-chloronitrobenzene were provided by Aldrich. Formic acid, niobic acid, sulphated zirconia, palladium nitrate, nitrobenzene, aniline, 3-nitrotoluene, 3-aminotoluene, 4-

chloroaniline, 2-nitroanisole, 2-anisidine, methyl-3-aminobenzoate, 4-nitrobenzonitrile, 4-aminobenzonitrile, and tetrahydrofuran were supplied by Wako Chemicals. 4-Nitrostyrene, 4-aminostyrene, 2-nitrobiphenyl, 2-aminobiphenyl, 1-nitronaphthalene, and 1-aminonaphthalene were provided by Tokyo Chemical Industry (TCI) Co. Ltd. HY zeolite (Si/Al = 2.8, JRC-Z-HY-5.5), ZSM-5 (Si/Al = 45, JRC-Z5-90H(1)), and SiO₂-Al₂O₃ (Si/Al = 2.1, JRC-SAH-1) were obtained from the Catalysis Society of Japan.

5.2.2 Catalyst Preparation

Synthesis of ZrP: Zirconium phosphate (ZrP) with a molar ratio of P/Zr = 2 has been prepared as mentioned in our previous report.²¹ An aqueous solution of 0.1 M ZrOCl₂·8H₂O (100 mL) and 0.2 M sodium dihydrogen phosphate (100 mL) was mixed at pH 1-2 drop wisely with continuous stirring at 343 K. The obtained gelatinous precipitates were digested for 1 h at 343 K, filtered, washed with water, and dried under vacuum at room temperature. The obtained material was converted to the acid form by treating with 1 M HNO₃ for 30 min with occasional shaking. The sample was then separated from the acidic solution by decantation, and washed with distilled water for removal of adhering acid. This acid treatment was repeated at least five times. After final washing, the material was dried at room temperature, and then characterized with XRD, N₂ adsorption (BET surface area 140 m² g⁻¹) and applied for further studies.

Synthesis of Pd/ZrP: Pd/ZrP was prepared by an adsorption method as mentioned in our previous report²¹ with some modification. Pd(NO₃)₂ (46.1 mg) was resolved into an aqueous solution (20 mL), and then ZrP (1 g) was mixed under stirring for 2 h at room temperature. The solid was filtered, washed with water and dried at room temperature for

overnight under vacuum. Then, 2.1 wt% Pd/ZrP catalyst as a brown colored powder was obtained.

5.2.3 Characterizations

Characterization of the catalyst was conducted using several techniques. X-ray diffraction pattern (XRD) was recorded with a Rigaku Smart Lab diffractometer using Cu $K\alpha$ radiation within $2\theta = 2-80$ range. Transmission Electron Microscopy (TEM) study was carried out in a Hitachi H-7100 instrument operating at an accelerating voltage at 100 kV. TEM samples were prepared by dispersing the catalyst powder in ethanol under ultrasonic radiation for 1-2 min, and then the resulted solution was dropped on a copper grid followed by slow evaporation of solvent under vacuum at room temperature. Inductive Coupled Plasma-Atomic Emission Spectroscopy (ICP-AES) for determination of the actual amount of metal loading and metal leaching test of reaction mixture was measured on Shimadzu ICPS-7000 Ver. 2. Nuclear Magnetic Resonance (NMR) spectroscopy was executed on Brücker advance 400 MHz instrument using $CDCl_3$ as a solvent.

5.2.4 Catalytic Reactions

Reaction of various nitroarenes was performed in a Schlenk glass tube attached to a reflux condenser. In a typical CTH reaction, requisite amounts of substrate and catalyst were weighed and mixed in ethanol solvent in the presence of FA. The reactor was heated on an oil bath at 313 K for t h. After the completion of reaction for desired time, the reactant was cooled to room temperature, and naphthalene was added as an internal standard. The filtrate was analyzed by a Shimadzu gas chromatography (GC-17A) with an Agilent DB-1 column and a flame ionization detector. Conversion, yield and selectivity were calculated using the calibration curve method following these equations:

$$\% \text{ Conversion} = 100 - \left(\frac{\text{mmol of reactant detected}}{\text{mmol of reactant taken}} \times 100 \right)$$

$$\% \text{ Yield} = \frac{\text{mmol of product formed}}{\text{mmol of reactant taken}} \times 100$$

$$\% \text{ Selectivity} = \frac{\% \text{ yield}}{\% \text{ conversion}} \times 100$$

5.3 Results and Discussion

5.3.1 Catalytic Activity

Our own experience⁵¹ and literature survey⁵²⁻⁵⁵ of Brønsted acid mediated CTH reaction served as the starting point of our studies. Pd was selected because it is known as an active metal for several hydrogenation reactions.⁵⁶⁻⁶⁰ Initial experiments were conducted to explore the role of support for Pd using FA for CTH of nitrobenzene to aniline at 313 K. Numerous supports including ZrP with high number of Brønsted acid sites,⁵⁰ zeolites, niobic acid, sulphated-zirconia, and γ -alumina having moderate Brønsted acid sites were chosen. As shown in **Table 1**, all catalysts promoted the formation of aniline to a considerable extent under the general condition (1 mmol, 313 K, 2 h). Especially, Pd/ZrP and Pd/ZSM-5 stand out with the high activities towards aniline as the sole product (entries 1 and 6), which could be attributed to high amount of Brønsted acid sites of these catalysts. It has been understood that with the increase in Si/Al ratio, the Brønsted acid sites increases due to extra framework aluminium, thus the activity is associated with the tetrahedrally coordinated aluminium species in close proximity to Brønsted acid sites in ZSM-5.⁶¹⁻⁶³ Pd supported on HY and SiO₂-Al₂O₃ having low Si/Al ratio were also found to be fairly active (entries 8 and 11). Though the number of Brønsted acid sites owing to

Table 1: Nitrobenzene reduction using various Palladium catalysts and FA^a

Entry	Catalyst	Particle size /nm ^b	NB	AN	Sel. /%
			Conv. /%	Yield /%	
1	Pd/ZrP	3.5	>99	>99	>99
2 ^c			>99	>99	>99
3 ^d			99	99	100
4 ^e			99	99(97 ^g)	100
5 ^f			<1	0	0
6	Pd/ ZSM-5	2.8	100	98	98
7 ^c			61	59	97
8	Pd/HY zeolite	3.8	98	92	94
9	Pd/Nb ₂ O ₅	H.D.	90	84	93
10	Pd/ γ -Al ₂ O ₃	H.D.	87	79	91
11	Pd/SiO ₂ -Al ₂ O ₃	3.5	87	75	86
12	Pd/SO ₄ ²⁻ /ZrO ₂	-	8	4	-
13	ZrP		5	4	-
14	Blank		<1	0	0
15 ^f	Blank		<1	0	0

^a**Reaction Conditions:** Nitrobenzene (NB, 1 mmol, ^c5 mmol, ^e20 mmol), Ethanol (5 mL, ^c20 mL, ^e50 mL), FA (3 mmol, ^c15 mmol, ^e60 mmol), Temp. (313 K, ^d353 K), Time (2 h, ^c3 h, ^d15 min, ^e12 h), 2.1wt% Pd catalyst (20 mg, ^c^e50 mg). ^bDetermined by TEM observation. ^fWithout FA. ^gIsolated yield. H.D.: Hardly distinguished.

Si-O-Al units would increase with decrease of Si/Al ratio, Pd/HY zeolite (Si/Al = 2.8) showed little higher activity than Pd/SiO₂-Al₂O₃ (Si/Al = 2.1). It is known that not only the amount of Brønsted acid sites but also the hydrophobicity derived from Si/Al ratio and topology strongly contributed on the catalysis over Si-O-Al type of materials. These factors also supposedly influenced on their catalytic activities for the reaction. Notable yields (79–84%) of aniline were attained with Pd supported on Nb₂O₅ and γ -Al₂O₃ having moderate Brønsted acid sites (entries 9 and 10). Surprisingly, Pd supported on SO₄²⁻/ZrO₂ was found to be least active for this CTH. It has been reported that there is high probability of leaching of Brønsted acid sites of SO₄²⁻/ZrO₂ in polar protic solvents.^{64,65} The Pd

loading onto $\text{SO}_4^{2-}/\text{ZrO}_2$ was carried out in water in our case. This catalyst synthetic methodology is believed to result in loss of Brønsted acid sites of $\text{SO}_4^{2-}/\text{ZrO}_2$ in accordance with previous literatures.

Additionally, the sulfate ions may also act as poison for the active Pd. It is well known that BaSO_4 poisons Pd's activity in the Rosenmund reduction. Thus leaching of Brønsted acid sites and poisoning of Pd by sulfate ions could be one of the reasons for low activity of $\text{Pd}/\text{SO}_4^{2-}/\text{ZrO}_2$. Though many supports including ZrP can afford small size particles between 2.8 and 3.8 nm as shown in **Figure 1**, it was observed that there is no correlation between Pd mean particle size and the activity of catalyst. This fact suggested that the high number of Brønsted acid sites of support is one of the key factors for novel activity in CTH reaction of NB using FA. The high activities of the Pd/ZrP and Pd/ZSM-5 lead us to further examine the 5 mmol-scale CTH of nitrobenzene. Remarkably, Pd/ZrP catalyst showed higher activity than Pd/ZSM-5 (entries 2 and 7).

The metal-free ZrP showed very less activity with only 4% conversion of nitrobenzene (entry 13), resultantly, clarifies the necessity of metal for the CTH process with FA. Furthermore, the CTH reaction was also examined in the absence of Pd/ZrP catalyst and/or FA (entries 5, 14 and 15). In all three cases, the reaction scarcely occurred. It follows that, the observed high catalytic activity could be accounted for the presence of both Pd/ZrP and FA. Moreover, the present transfer hydrogenation methodology is so effective that it can completely reduce nitrobenzene in just 15 minutes at 353 K without any loss in selectivity (entry 3).

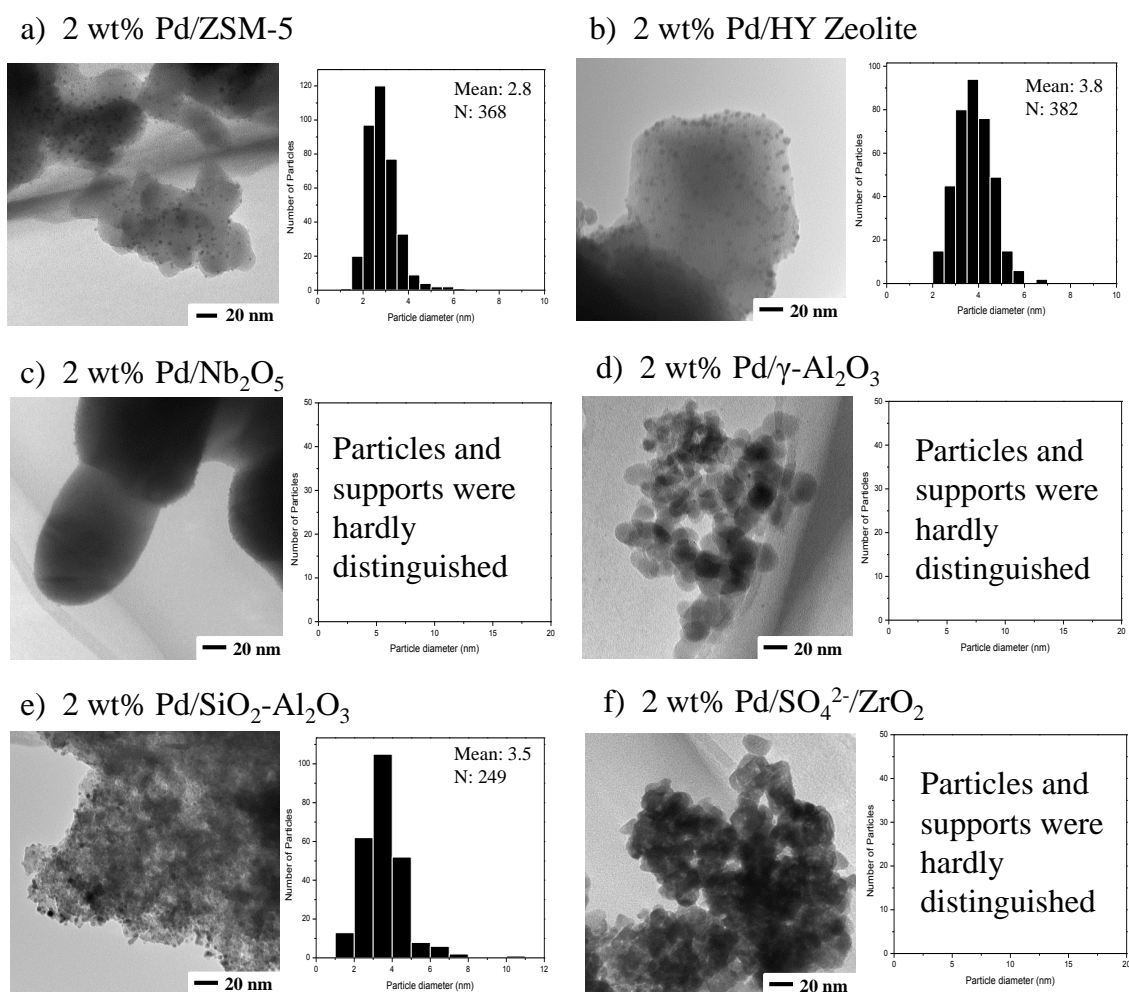
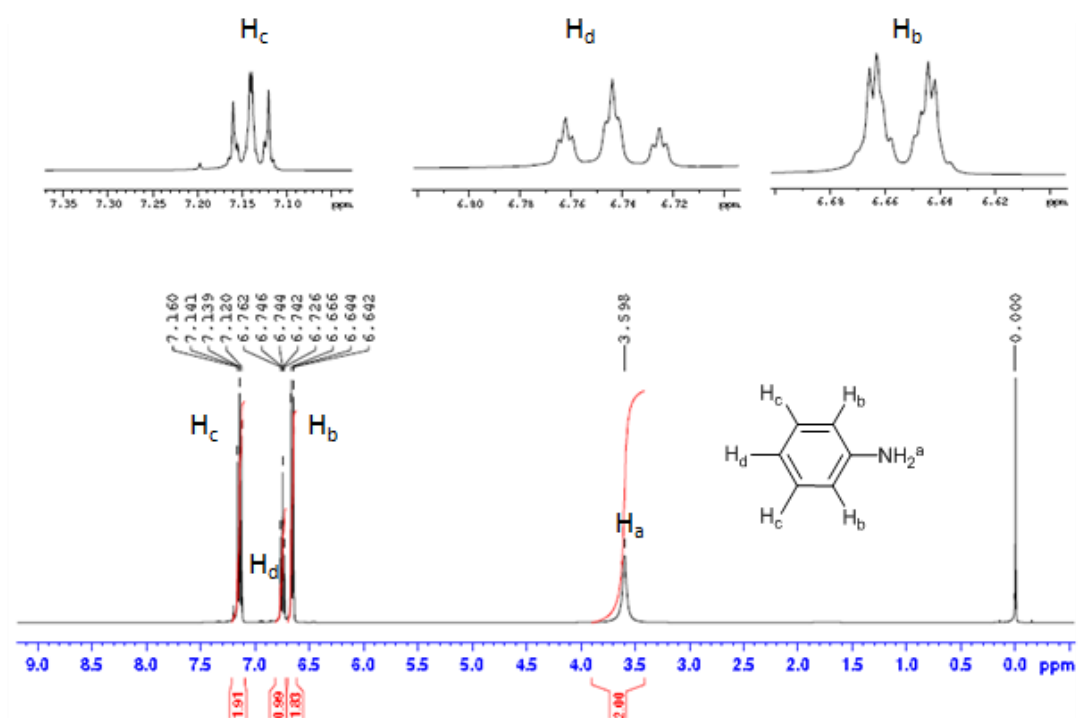
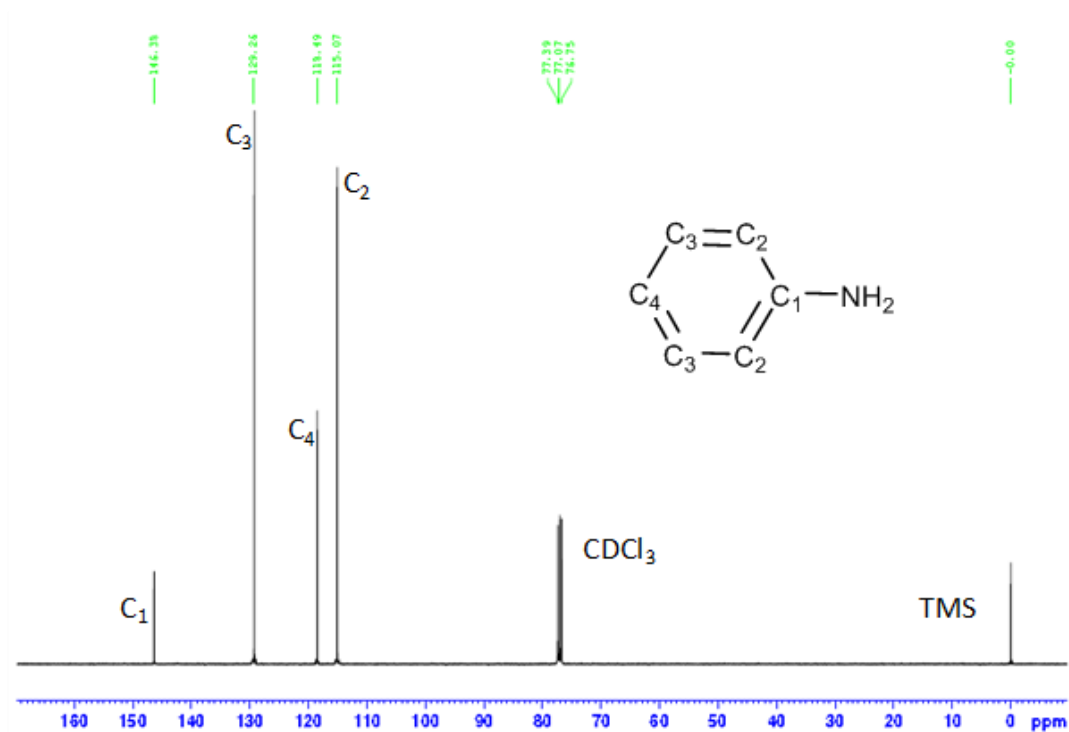


Figure 1: TEM images and particle size distribution of the supported Pd catalysts.

A 20 mmol-scale transfer hydrogenation was also performed to check the viability of the process. Remarkable activity (yield >99%) was observed at 313 K with a TON of 1977 (entry 4). After completion of the reaction, the catalyst was simply removed by a filtration method. The filtrate was condensed under reduced pressure to obtain aniline as crude product. Aniline was obtained in 97% as isolated yield (entry 4g). ¹H- and ¹³C-NMR were conducted with the crude product only (**Figure 2 and 3**) and compared with NMR of authentic aniline. NMR analysis confirms that the NMR of crude product exactly matches with authentic aniline and no extra peak was observed. ¹H-NMR (CDCl₃, TMS, 400 MHz): δ 3.5 (s, 2H, amino), 6.6–7.1 (m, 5H, phenyl ring) ppm.

**Figure 2:** ^1H -NMR of the isolated aniline.**Figure 3:** ^{13}C -NMR of the isolated aniline.

Type of solvent was found to be crucial in transfer hydrogenation of nitrobenzene under our reaction conditions. Various aprotic and protic solvents were attempted to use for the CTH reaction of nitrobenzene over Pd/ZrP with FA as shown in **Table 2**. Alcoholic solvents showed good activity for the CTH, among which ethanol led to the near full conversion of nitrobenzene with almost 100% yield of aniline (entry 1). *iso*-Propanol which would act both as a solvent and hydrogen donor⁶⁶ showed good activity with 76% conversion but with low selectivity (entry 2). Butanol and methanol also gave mild or low activity (entries 3 and 4). It is known that alcohols can serve as a hydrogen source in transfer hydrogenation,^{67,68} however, the reaction without FA in ethanol solvent did not give any product in our case (**Table 1**, entry 5). Accordingly, the contribution from alcohol solvents as the hydrogen source in this reaction system is negligible. None of the aprotic solvent catalyzed the CTH of nitrobenzene to a significant extent (entries 5-10) under present reaction conditions.

Table 2: Screening of different solvents in the CTH reaction of nitrobenzene towards aniline over Pd/ZrP.^a

Entry	Solvent	NB	AN	
		Conv. /%	Yield /%	Sel. /%
1	Ethanol	>99	>99	>99
2	<i>iso</i> -Propanol	76	60	79
3	<i>n</i> -Butanol	54	47	87
4	Methanol	40	27	67
5	Toluene	40	5	-
6	Tetrahydrofuran	10	5	-
7	<i>N,N</i> -Dimethylformamide	7	5	-
8	Ethylacetate	7	3	-
9	Chloroform	6	2	-
10	Dichloromethane	4	2	-

^a**Reaction Conditions:** NB (1 mmol), 2.1wt% Pd/ZrP (20 mg), Solvent (5 mL), FA (3 mmol), 313 K, 2 h, 500 rpm. NB: Nitrobenzene; AN: Aniline.

5.3.2 Time course of the reaction

To investigate the route of the reaction, the yield and selectivity of aniline were monitored as a function of reaction time, as shown in **Figure 4**. Nitrobenzene conversion and aniline formation exactly follows each other and selectivity was near 100% throughout the reaction process under present reaction conditions. Remarkably, no intermediate was detected; this suggests that either there is no formation of intermediates or they react immediately on catalytic surface before desorbing.

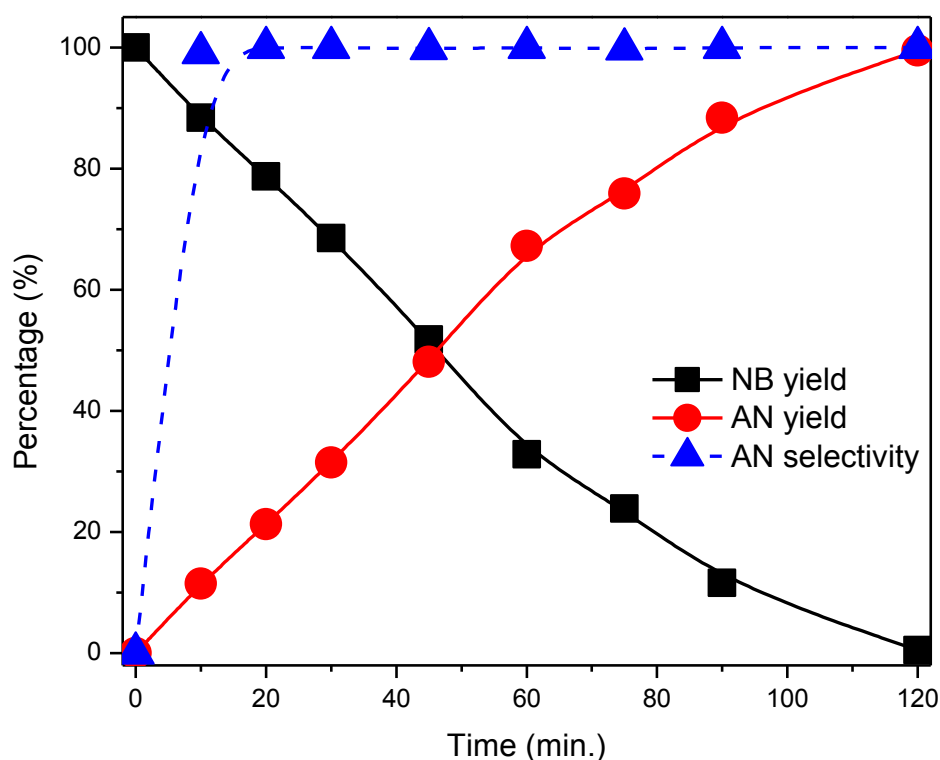


Figure 4: Time course for transfer hydrogenation of nitrobenzene.

Reaction Conditions: Nitrobenzene (1 mmol), 2.1wt% Pd/ZrP (20 mg), Ethanol (5 mL), FA (3 mmol), 313 K.

5.3.3 Reusability

Recyclability of the catalyst is an important criteria in heterogeneous catalytic system. On that account, the reusability of catalyst for CTH of nitrobenzene was investigated. In each

run, after the reaction, the catalyst was separated by centrifugation, washed thoroughly with ethanol, dried in vacuum for overnight, and then the dried catalyst was used for further reaction. The results in **Figure 5** indicated that the Pd/ZrP catalyst can be reused at least 4 times without losing the activity and selectivity. The aliquots of the reaction mixture after first and fourth run were analyzed by ICP-AES, no Pd was detected in the solutions.

The hot filtration test was also conducted in order to re-affirm the ideal heterogeneity of Pd/ZrP. For this, the catalyst was removed after 1 h and reaction was continued with the filtrate. The results showed that the reaction didn't proceed. These confirmed that there was no significant leaching of metal from the catalyst surface and the reaction is truly heterogeneous.

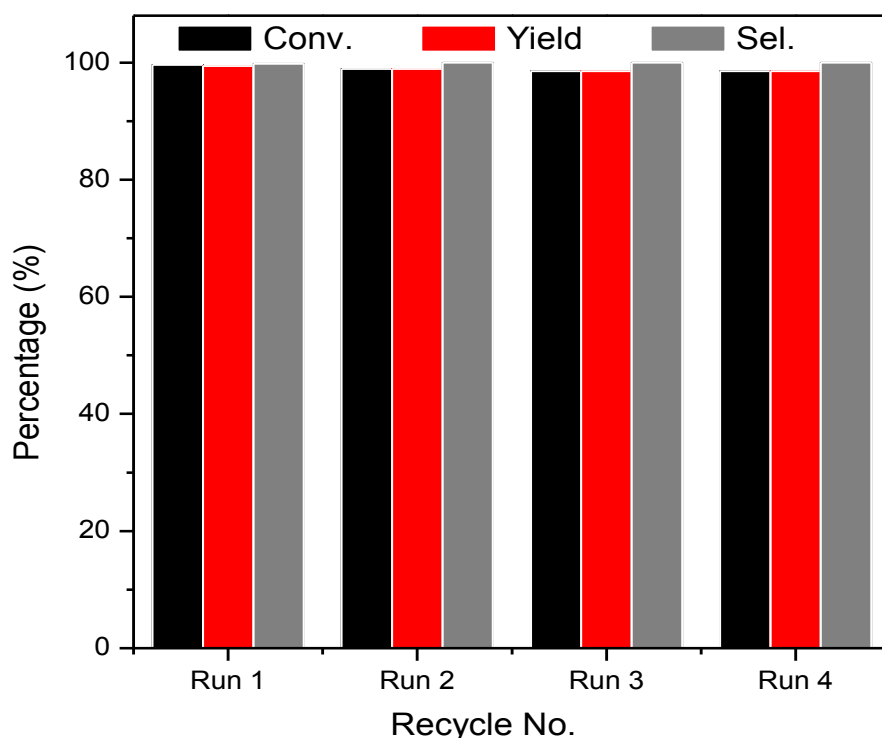


Figure 5: Reusability of Pd/ZrP for transfer hydrogenation of nitrobenzene.

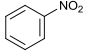
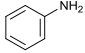
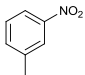
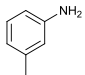
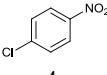
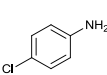
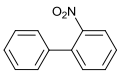
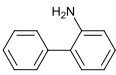
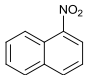
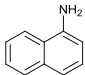
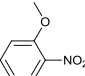
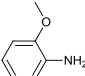
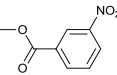
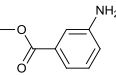
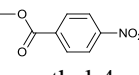
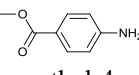
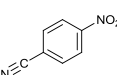
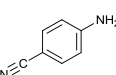
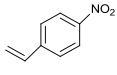
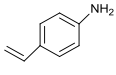
Reaction Conditions: Nitrobenzene (1 mmol), 2.1wt% Pd/ZrP (20 mg), Ethanol (5 mL), FA (3 mmol), 313 K, 2 h.

5.3.4 CTH of substituted nitroarenes

After optimizing the conditions for CTH reaction of nitrobenzene over Pd/ZrP, I further examined the scope of this catalytic system for CTH reactions of various substituted nitroarenes. The results shown in **Table 3** are under optimum reaction conditions for each substrate. It was seen that longer reaction time is required for CTH reaction of substituted nitroarenes to achieve >90% yield of the corresponding anilines. Entries 2 and 3 are for 3-nitrotoluene and 4-chloronitrobenzene, respectively. Notably, this catalyst system can efficiently transfer hydrogen to produce substituted anilines at 313 K. Halo-nitroarenes have tends to undergo hydrogenolysis (of C–X bond), but in our case no hydrogenolysis was proceeded and 4-chloroaniline was formed in 93% yield with >99% selectivity. Nitro groups attached to a naphthalene and biphenyl ring were also successfully reduced with excellent yield and selectivity of the corresponding anilines (entries 4 and 5). Reductions of nitro groups in the presence of other functional groups such as $-\text{OCH}_3$, $-\text{COOCH}_3$ (entries 6–8) proceeded with high tolerance for these functional groups to afford the corresponding anilines with >90% yield and selectivity.

The nitro group was selectively hydrogenated in the presence of easily reducible nitrile group with 91% yield (97% selectivity) of 4-aminobenzonitrile (entry 9). The most challenging task was the chemo-selective reduction of nitro group in the presence of $\text{C}=\text{C}$ as the reactivity order for hydrogenation of olefins are next to nitro group. 4-Nitrostyrene was chemo-selectively transformed to 4-aminostyrene as major product with 92% selectivity (entry 10); in this case, the by-product of 4-ethylaniline was detected. The cause for the high chemo-selectivity might be explained in terms of high electrostatic interactions of polar nitro group with the catalyst surface as compared to non-polar $\text{C}=\text{C}$ bond.⁶⁹

Table 3 Transfer hydrogenation of various substituted nitro aromatic compounds over Pd/ZrP and FA^a

Entry	Reactant	Product	Time /h	Conv. /%	Yield /%	Sel. /%
1	 nitrobenzene	 aniline	2	>99	>99	100
2	 3-nitrotoluene	 3-aminotoluene	6	92	92	100
3 ^b	 4-chloronitrobenzene	 4-chloroaniline	18	94	93	99
4	 2-nitrobiphenyl	 2-aminobiphenyl	16	96	94	99
5	 1-nitronaphthalene	 1-aminonaphthalene	16	94	93	98
6	 2-nitroanisole	 2-aminidine	24	94	91	96
7	 methyl-3-nitrobenzoate	 methyl-3-aminobenzoate	12	>99	99	>99
8	 methyl-4-nitrobenzoate	 methyl-4-aminobenzoate	20	98	95	97
9	 4-nitrobenzonitrile	 4-aminobenzonitrile	18	93	91	97
10 ^c	 4-nitrostyrene	 4-aminostyrene	6	97	90	92

^a**Reaction Conditions:** Substrate (1 mmol), 2.1wt% Pd/ZrP (20 mg, ^c10 mg), FA (3mmol), Ethanol (5 mL), Temp. (313 K, ^b333 K), 500 rpm.

5.3.5 Hammett plot

The reactivity of substrates in heterogeneous catalysis mainly depends on the charge density at the reaction center and steric factor of substrates. Therefore, to study the reaction mechanism of CTH, the initial rate for various substituted nitroarenes with electron-withdrawing groups (EWG) like $-\text{COOCH}_3$, $-\text{Cl}$, $-\text{C}\equiv\text{N}$ at para position were measured. Initial rates and rate constants are shown in **Table 4**. The graph is plotted for $\log(K/K_0)$ against the Hammett substitution constants (σ)³⁰ in **Figure 6**, where K is an initial rate constant for substituted nitrobenzene and K_0 is an initial rate constant for nitrobenzene. The plot shows a linear relationship with a slope of -1.0. The negative slope with such a high value indicates that the present CTH proceeds via cationic intermediate and EWG hinders the rate of reduction of nitrobenzene.⁷¹

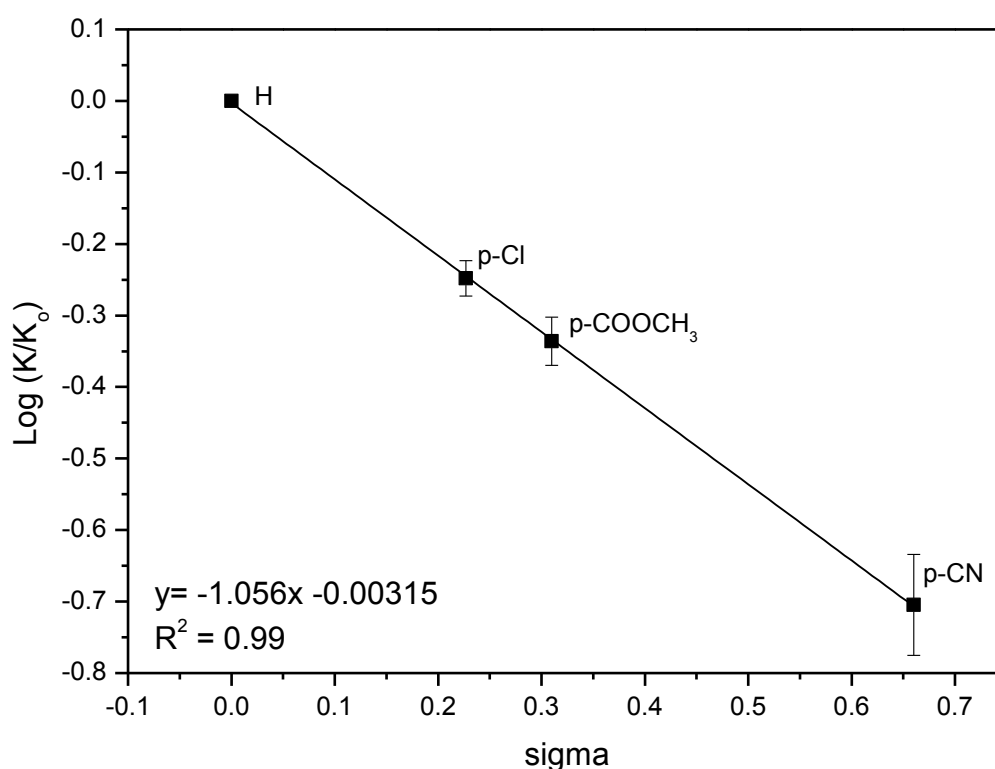


Figure 6: Hammett plot for reduction of *p*-substituted nitroarenes.

Table 4: Parameters for Kinetic study of *p*-substituted nitroarenes^a

Substrate	Initial Rate/ (min ⁻¹) ^b	log (initial rate)
Nitrobenzene	0.01250	-1.90
<i>p</i> -chloronitrobenzene	0.00560	-2.25
<i>p</i> -nitromethylbenzoate	0.00545	-2.26
<i>p</i> -nitrobenzonitrile	0.00196	-2.71

^a**Reaction Conditions:** Substrate (1 mmol), 2.1wt% Pd/ZrP (20 mg), FA (3 mmol), Ethanol (5 mL), 313 K, 30 min.

^bInitial rates of the each reaction were determined on the concentration of reactants as a function of time by GC.

5.3.6 XRD and TEM

Figure 7 shows the XRD pattern for fresh as well as used catalysts. The XRD pattern clearly demonstrates that there is no structural deterioration of catalyst after the reaction. However, an additional peak at 40 degree was observed for post reaction catalysts, which corresponds to Pd(0). This indicates that Pd(II) is reduced to Pd(0) during the reaction. While performing the reaction, it was also seen that the catalyst color changes to black from its initial brown color within a few minutes of the reaction. The high reusability of catalyst without any oxidation treatment of catalyst (shown in **Figure 5**) hints that the active site for transfer hydrogenation is in situ formed Pd(0) instead of Pd(II). From decades, it's known that the catalytic hydrogenation reaction requires metal (in reduced form).

FA has the ability and can convert Pd(II) from Pd(0).^{72,73} Very recently, Wang *et al.*, synthesised Pd nanoclusters from Pd(II) using FA as a reducing agent at room temperature.⁷⁴ From **Figure 6(b-e)**, I observed that the average particle size which was 3.5 nm for catalyst prior to reaction increases to 5.4 nm after the catalytic run. An increase

in particle size after reaction observed by TEM measurements may account the reduction of ionic Pd into Pd(0) nanoparticles in accordance with the XRD measurements.

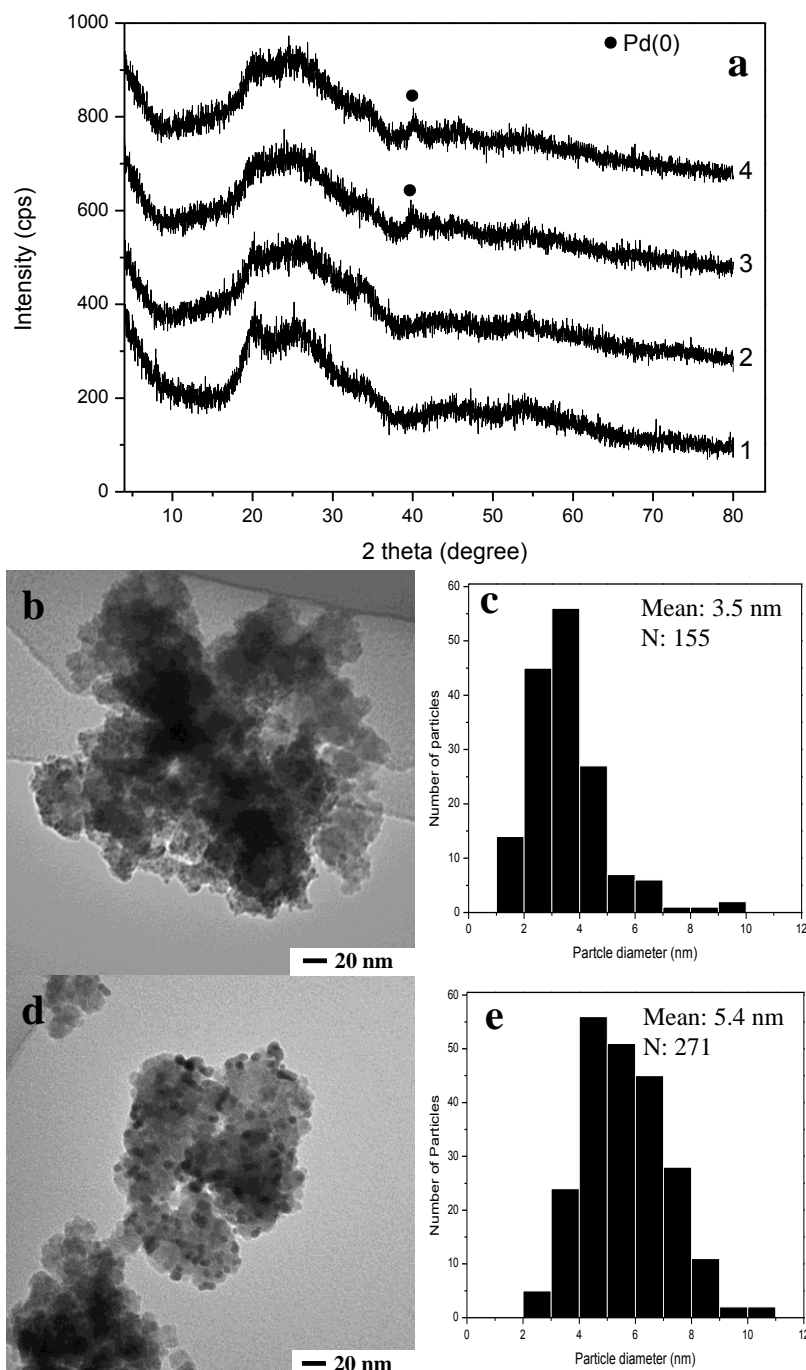


Figure 7: (a) XRD patterns for 1) ZrP support, 2) fresh Pd/ZrP, and Pd/ZrP after 3) first run and 4) fourth run. (b) & (d) are TEM images and (c) & (e) are particle size distribution for Pd/ZrP prior and after the reaction respectively.

5.3.7 Proposed Reaction Mechanism

A reaction mechanism is proposed for the CTH of nitroarenes with FA as a hydrogen source as shown in Figure 8 based on the experimental results mentioned above. At the initial stage, FA decomposes on the Pd/ZrP surface into CO_2 and H^+ , H^- (1 in **Figure 8**), CO_2 evolution is confirmed by GC-8A (TCD detector) of collected gas from the reaction.³² The H^- adsorbs on Pd surface to reduce Pd(II) into Pd(0) (2 in **Figure 8**). Since the nitro group attached to the benzene ring can pull electrons more strongly from benzene ring, and can easily be adsorbed on the surface of catalyst. Consequently, nitroarenes adsorbs on the catalyst surface by electrostatic interaction as shown in 3 (**Figure 8**). Thereafter, H^+ from Brønsted acid sites of ZrP and H^- (from FA) adsorbed on Pd are transferred to electron rich O and electron deficient N of nitro group, respectively, to form 4 (**Figure 8**).

One of the hydroxyl group in 4 attacks on the H^+ (from FA) to generate 5 eliminating a water molecule. Further protons are trapped and the free aniline is desorbed from catalytic surface as shown in 5 and 6 (**Figure 8**). A high value negative slope was observed in the Hammett plot signifies a well-developed positive charge on the transition state as discussed in **Figure 3**. Thus, in strong agreement to the Hammett plot a cationic intermediate was proposed for the transformation. The high activity of Pd/ZrP catalyst may be attributed to its high capacity of holding nitroarenes by electrostatic interactions between polar nitro group with H^+ and H^- on Pd/ZrP. This strong interaction leads to direct reduction of nitroarenes to anilines without the formation of any intermediates.

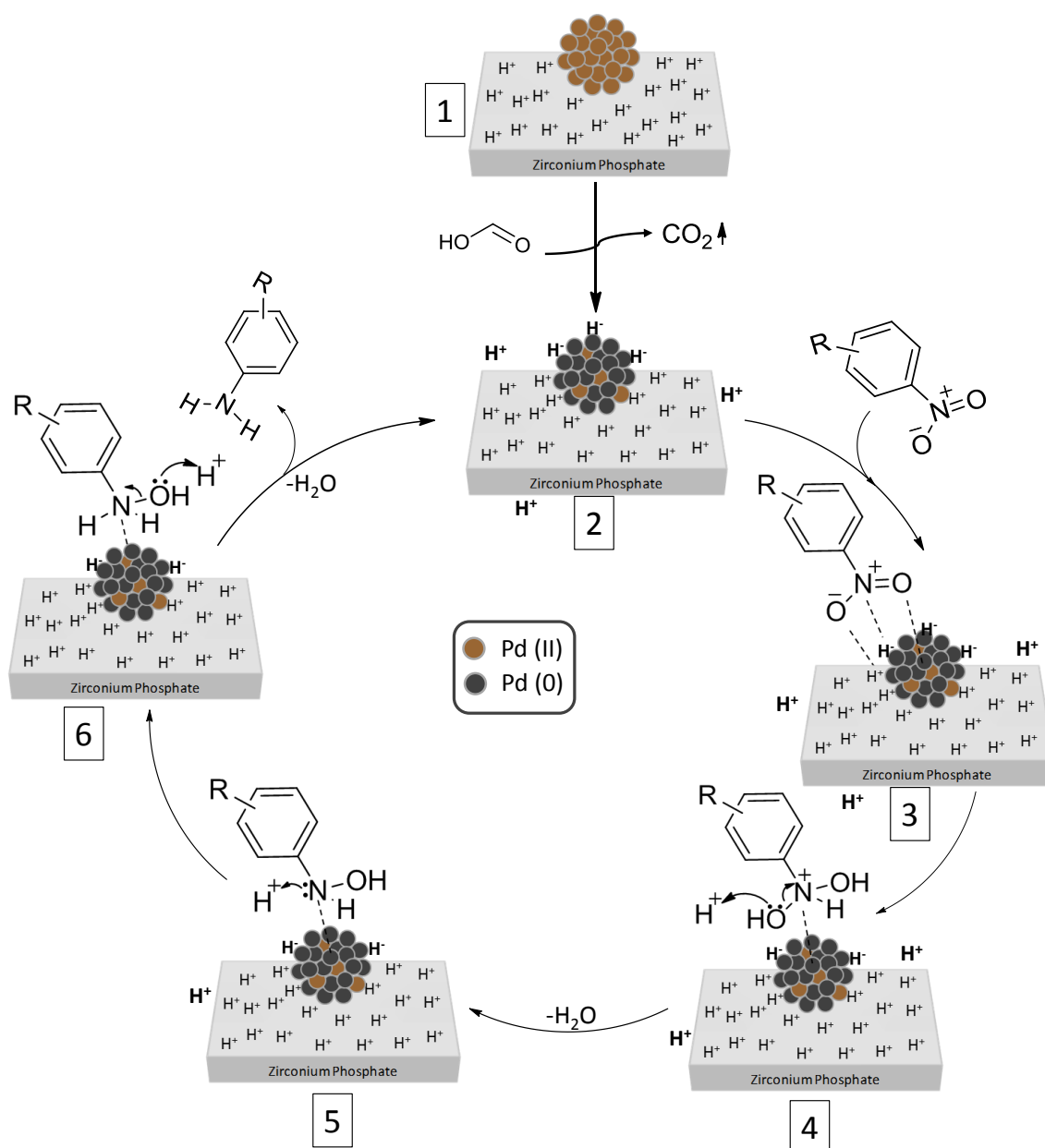


Figure 8: Proposed mechanism for transfer hydrogenation of nitroarenes over Pd/ZrP

5.4 Conclusions

In summary, a highly efficient, base-free, heterogeneously-catalyzed, and chemoselective CTH methodology is developed for the synthesis of industrially important anilines. The Pd/ZrP catalysis the selective transfer hydrogenation of various functionalized nitroarenes to the corresponding anilines with excellent yields at 313 K. Solid catalyst could be used repetitively without any obvious loss in activity. The reaction mechanism involving cationic intermediate has been proposed based on the above characterizations and the slope of Hammett plot. The presence of both high amount of Brønsted acid sites (of ZrP) and efficient reducing property (of Pd (0)) in Pd/ZrP forms the key factors for efficacious fixation of hydrogen species from FA in this study.

5.5 References

1. R. S. Downing, P. J. Kunkeler and H. Van Bekkum, *Catal. Today*, **1997**, 37, 121-136.
2. M. Suchy, P. Winternitz and M. Zeller, World (WO) Patent 91/00278, 1991.
3. N. Ono, *The Nitro Group in Organic Synthesis*, ed. François Terrier, Wiley-VCH, New York, 2001, pp. 126-158.
4. J. L. Klinkenberg and J. F. Hartwig, *Angew. Chem. Int. Ed.*, **2011**, 50, 86-95.
5. Y. Aubin, C. Fischmeister, C. M. Thomas and J.-L. Renaud, *Chem. Soc. Rev.*, **2010**, 39, 4130-4145.
6. T. Schulz, C. Torborg, S. Enthaler, B. Schaffner, A. Dumrath, A. Spannenberg, H. Neumann, A. Borner and M. Beller, *Chem.-Eur. J.*, **2009**, 15, 4528-4533.
7. Q. Shen and J. F. Hartwig, *J. Am. Chem. Soc.*, **2006**, 128, 10028-10029.
8. X. H. Huang and S. H. Buchwald, *Org. Lett.*, **2001**, 3, 3417-3419.

9. J. Yu, P.-I. Zhang, J. Wu and Z. Shang, *Tetrahedron Lett.*, **2013**, *54*, 3167-3170.
10. H.-H. Rao, H. Fu, Y.-Y. Jiang and H.-F. Zhao, *Angew. Chem. Int. Ed.*, **2009**, *48*, 1114-1116.
11. J. Pasek and M. Petrisko, EP 2471768 A1, 2012.
12. L. O. Winstrom, US Pat. 2822397 A, 1955.
13. H. U. Blaser, U. Siegrist, H. Steiner and M. Studer, in *Fine Chemicals through Heterogeneous Catalysis*, ed. R. A. Sheldon and H. van Bekkum, Wiley-VCH, Weinheim, 2001, pp. 389-406.
14. N. S. Sanjini and S. Velmathi, *RSC Adv.*, **2014**, *4*, 15381-15388.
15. Y. Xu, L. Wang, W. Jiang, H. Wang, J. Yao, Q. Guo, L. Yuan and H. Chen, *ChemCatChem*, **2013**, *5*, 3788- 3793.
16. D. He, X. Jiao, P. Jiang, J. Wang and B.-Q. Xu, *Green Chem.*, **2012**, *14*, 111-116.
17. T. Mitsudome, Y. Mikami, M. Matoba, T. Mizugaki, K. Jitsukawa and K. Kaneda, *Angew. Chem. Int. Ed.*, **2012**, *1*, 136-139.
18. A. Corma, P. Concepción and P. Serna, *Angew. Chem. Int. Ed.*, **2007**, *46*, 7266-7269.
19. A. Corma and P. Serna, *Science*, **2006**, *313*, 332-334.
20. F. Kovar and F. E. Armond, US Pat. 3,975,444, 1976.
21. J. Butera and J. Bagli, WIPO 91/09023, 1991.
22. A. Burawoy and J. P. Critchley, *Tetrahedron*, **1959**, *5*, 340-351.
23. K. Junge, B. Wendt, N. Shaikh and M. Beller, *Chem. Commun.*, **2010**, *46*, 1769-1771.
24. R. J. Rahaim and R. E. Maleczka, *Org. Lett.*, **2005**, *7*, 5087-5090.

25. J. W. Bae, Y. J. Cho, S. H. Lee and C. M. Yoon, *Tetrahedron Lett.*, **2004**, *41*, 175-177.
26. J. W. Bae, Y. J. Cho, S. H. Lee, C.-O. M. Yoon and C. M. Yoon, *Chem. Commun.*, **2000**, 1857-1858.
27. K. Abiraj Srinivasa, R. Gejjalagere and D. C. Gowda, *Can. J. Chem.*, **2005**, *83*, 517-520.
28. H. Berthold, T. Schotten and H. HSnig, *Synthesis*, **2002**, 1607-1610. (c) H. Imai and T. Nishiguchi, *Chem. Lett.*, **1976**, 655-656.
29. R. A. W. Johnstone, A. H. Wilby and I. D. Entwistle, *Chem. Rev.*, **1985**, *85*, 129-170.
30. R. E. Harmon, S. K. Gupta and D. J. Brown, *Chem. Rev.*, **1973**, *73*, 21-52.
31. S. U. Sonavane, M. B. Gawande, S. S. Deshpande, A. Venkataraman and R. V. Jayaram, *Catal. Commun.*, **2007**, *8*, 1803-1806.
32. A. S. Kulkarni and R. V. Jayaram, *Appl. Catal. A*, **2003**, *252*, 225-230.
33. D. S. Matharu, D. J. Moris, G. J. Clarkson and M. Wills, *Chem. Commun.*, **2006**, 3232-3234.
34. K. Prasad, X. Jiang, J. S. Slade, J. Clemens, O. Repič and T. J. Blacklock, *Adv. Synth. Catal.*, **2005**, *347*, 1769-1773.
35. T. T. Upadhyaya, S. P. Katdare, D. P. Sabde, V. Ramaswamy and A. Sudalai, *Chem. Commun.*, **1997**, 1119-1120.
36. J. Nemeth, A. Kiss and Z. Hell, *React. Kinet. Mech. Catal.*, **2014**, *111*, 115-121.
37. A. A. Vernekar, S. Patil, C. Bhat and S. G. Tilve, *RSC Adv.*, **2013**, *3*, 13243-13250.
38. M. Kumar, U. Sharma, S. Sharma, V. Kumar, B. Singh and N. Kumar, *RSC Adv.*, **2013**, *3*, 4894-4898.

39. D. Tavor, I. Gefen, C. Dlugy and A. Wolfson, *Synth. Commun.*, **2011**, *41*, 3409-3416.
40. L. Xu, X. Li, Y. Zhu and Y. Xiang, *New J. Chem.*, **2009**, *33*, 2051-2054.
41. P. W. Oxley, B. M. Adger, J. M. Sasse and M. A. Forth, *Org. Synth.*, **1989**, *67*, 187-192.
42. H. Imai, T. Nishiguchi and K. Fukuzumi, *J. Org. Chem.*, **1977**, *42*, 431-434.
43. R. Xing, W. Qi and G. W. Huber, *Energy Environ. Sci.*, **2011**, *4*, 2193-2205.
44. J. J. Bozell, *Science*, **2010**, *329*, 522-523.
45. A. Corma, S. Iborra and A. Velty, *Chem. Rev.*, **2007**, *107*, 2411-2502.
46. H. Choudhary, S. Nishimura and K. Ebitani, *Appl. Catal. B: Environ.*, **2015**, *162*, 1-10.
47. G. Wienhöfer, I. Sorribes, A. Boddien, F. Westerhaus, K. Junge, H. Junge, R. Llusar and M. Beller, *J. Am. Chem. Soc.*, **2011**, *133*, 12875-12879.
48. S. Fleischer, S. Zhou, S. Workmeister, K. Junge and M. Beller, *Chem.-Eur. J.*, **2013**, *19*, 4997-5003.
49. Z. Yu, W. Jin and Q. Jiang, *Angew. Chem. Int. Ed.*, **2012**, *51*, 6060-6072.
50. R. Weingarten, G. A. Tompsett, W. C. Conner Jr and G. W. Huber, *J. Catal.*, **2011**, *279*, 174-182.
51. J. Tuteja, H. Choudhary, S. Nishimura and K. Ebitani, *ChemSusChem*, **2014**, *7*, 96-100.
52. A. Ferry, J. Stemper, A. Marinetti, A. Voituriez and X. Guinchard, *Eur. J. Org. Chem.*, **2014**, 188-193.
53. M. Rueping and T. Theissmann, *Chem. Sci.*, **2010**, *1*, 473-476.

54. M. Rueping, A. P. Antonchick and T. Theissmann, *Angew. Chem. Int. Ed.*, **2006**, *45*, 6751-6755.
55. M. Rueping, E. Sugiono, C. Azap, T. Theissmann and M. Bolte, *Org. Lett.*, **2005**, *7*, 3781-3783.
56. M. V. Herrera, S. Werkmeister, K. Junge, A. Börner and M. Beller, *Catal. Sci. Technol.*, **2014**, *4*, 629-632.
57. Y.-F. Yang, G.-J. Cheng, P. Liu, D. Leow, T.-Y. Sun, P. Chen, X. Zhang, J.-Q. Yu, Y.-D. Wu and K. N. Houk, *J. Am. Chem. Soc.*, **2014**, *136*, 344-345.
58. C. Willocq, V. Dubois, Y. Z. Khimyak, M. Devillers and S. Hermans, *J. Mol. Catal. A: Chem.*, **2012**, *365*, 172-180.
59. H. Otsuka, E. Shirakawa and T. Hayashi, *Chem. Commun.*, **2007**, 1819-1821.
60. L. J. Gooben and K. Ghosh, *Chem. Commun.*, **2002**, 836-837.
61. S. Schallmayer, T. Ikuno, M. F. Wagenhofer, R. Kolvrnback, G. L. Haller, M. S. Sanchez and J. A. Lercher, *J. Catal.*, **2014**, *316*, 93-102.
62. S. M. T. Almutairi, B. Mezari, G. A. Filonenko, P. C. M. M. Magusin, M. S. Rigutto, E. A. Pidko and E. J. M. Hensen, *ChemCatChem*, **2013**, *5*, 452-466.
63. E. G. Derouane, J. Haber, F. Lemos, F. R. Ribeiro and M. Guisnet, Transformation of Alkanes on Solid Acid and Bifunctional Catalysts in Catalytic Activation and Functionalization of Light Alkanes, ed. E. G. Derouane, J. Haber, F. Lemos, F. R. Ribeiro and M. Guisnet, Nato ESI Series, 1998, pp. 65-68.
64. F. Omota, A. C. Dimian and A. Bliet, *Chem. Eng. Sci.*, **2003**, *58*, 3175-3185.
65. K. Suwannakarn, E. Lotero, J. G. Goodwin Jr and C. Lu, *J. Catal.*, **2008**, *255*, 279-286.
66. A. S. Kulkarni and R. S. Jayaram, *J. Mol. Catal. A: Chem.*, **2004**, *223*, 107-110.

67. J. Toubiana and Y. Sasson, *Catal. Sci. Technol.*, **2012**, 2, 1644-1653.
68. R. Vitali, G. Caccia and R. Gardi, *J. Org. Chem.*, **1972**, 37, 3745-3746.
69. M. Boronot, P. Concepci' on, A. Corma, S. Gonz'alez, F. Illas and P. Serna, *J. Am. Chem. Soc.*, **2007**, 129, 16230-16237.
70. L. P. Hammett, *J. Am. Chem. Soc.*, **1937**, 59, 96-103.
71. R. Sanjeev, V. Jagannathan and R. Veda Vratah, *Chemistry. Bulg. J. Chem. Educ.*, **2012**, 21, 71-77.
72. Q. Wang, Y. Wang, P. Guo, Q. Li, R. Ding, B. Wang, H. Li, J. Liu and X. S. Zhao, *Langmuir*, **2014**, 30, 440-446.
73. M. Zecca, *Metal Nanoclusters in Catalysis and Materials Science*, ed. B. Corain, G. Schmid and N. Toshima, Elsevier, 2008, pp. 216.
74. The gas was collected in a balloon and was subjected to GC analysis (Shimadzu, GC-8A, Activated C column, He carrier). The peak of CO₂ was observed which clearly demonstrates the decomposition of FA, which may illustrate that the FA is dissociated into CO₂, H⁺ and H⁻ under our reaction.

Chapter 6

Summary and Outlook

Summary

This thesis addressed the feasibility of producing important fuels and chemicals from biomass-derivatives, which can be accomplished using heterogeneous catalysis.

In **Chapter 2**, I concluded that combination of solid acid Amberlyst-15 and solid base Hydrotalcite (HT, Mg/Al = 3) catalysts was found to display the best activity for synthesis of furans from various sugars. The yield of furfural, MF and HMF from arabinose, rhamnose and lactose was observed to be 26, 39 and 34%, respectively. Only Amberlyst-15 or HT shows low activity in all cases (0-5 % yields of furans). The one-pot conversion of mixed-sugars was also demonstrated, and which serves the yields of 31% furfural, 32% HMF and 29% MF from the mixture of arabinose, rhamnose and lactose, respectively. The effective synthesis of furans from various saccharides are likely progressed by the aldose-ketose isomerization of sugars over solid base followed by successive dehydration to furans over solid acid. Both acid and base catalysts showed their characteristics features in a single-pot at the same time without neutralizing each other for the desired furans synthesis.

From the best of my knowledge, this is the first example of using rhamnose as a reactant for the catalytic synthesis of MF. The other sugars which I used (arabinose, galactose and lactose) for the synthesis of furans are also the one which were not used as commonly as glucose and xylose. The unique and special property about this process is that the catalysts pair is easily recoverable and could be reused upto three times without losing its catalytic activity for the synthesis of mixed-furans too. In overall conclusion, I can state that I have developed a catalytic system which has the ability to efficiently convert aldo-hexose, pentoses, disaccharides and multiple of sugars together in a single pot to produce furan derivatives.

In **Chapter 3**, a subsequent study was conducted in which 5-hydroxymethylfurfural (HMF) was selectively transformed into 1,6-hexanediol (HDO). The direct one-step ring opening hydrogenolysis of HMF in presence of formic acid (FA) as hydrogen source produces a range of products including 5-methylfurfural (MF), 2,5-hexanedione (HDN), HDO, tetrahydrofuran-2,5-dimethanol (THFDM) and 2,5-dimethylfuran (DMF). Initially, the hydrogenolysis reaction was screened over a variety of Pd supported catalysts to obtain a maximum of HDO yield. It was found that the selectivity of the product formation varied with the choice of support or the amount of Brønsted:Lewis acid sites. The support possessing high ratio of Lewis to Brønsted acid sites (Al_2O_3) favors ring hydrogenation and formed THFDM as major product. On the other side support with high ratio of Brønsted to Lewis acid sites (ZrP) selectively undergo C-O hydrogenolysis followed by hydrogenation to give HDO as major product.

In short, I have demonstrated for the first time the one-step direct conversion of HMF to HDO in high yields by deoxygenation/hydrogenation over Pd supported on ZrP as catalyst together with FA as hydrogen source. By optimizing the reaction time, temperature, FA amount and metal loading, the 7 wt% Pd/ZrP catalyst (50 mg) achieved 43% yield of HDO from HMF (1 mmol) in ethanol solvent (3 ml) using FA (22 mmol) at 413 K for 21 h. The Pd/ZrP catalyst was easily separated from the reaction mixture and was found to be reusable at least 5 times without any significant loss of activity and selectivity. Reaction mechanism was proposed based on the experimental data and product identification was done by NMR spectroscopy. The best part in this study is: it is the first report on the direct transformation of HMF to HDO with 43% yield under autogeneous pressure, which is more than 10 times higher than the reported 4% with high pressured-hydrogen. The key to the strategy was the use of high Brønsted acid sites

possessing ZrP as support and formic acid which has the potential to serve as an alternative hydrogen source and a deoxygenating agent.

Chapter 4 focussed on the selective oxidation of 1,6-hexanediol (HDO) using *N,N*-dimethyldodecylamine *N*-oxide (DDAO) stabilized AuPd-bimetallic nanoparticles (NPs) supported on hydrotalcite (HT) as heterogeneous catalyst in basic aqueous media with hydrogen peroxide as clean oxidizing agent. This selective oxidation of long chain aliphatic diol obtained from biomass to 6-hydroxycaproic acid (HCA) has been chosen because of its potential application in bio-renewable polycaprolactone production. This selective oxidation of HDO using hydrogen peroxide as oxidant gives a greener chemistry alternative over conventional petrochemical oxidation reaction with toxic and inorganic oxidants.

For this purpose, various capped AuPd bimetallic NPs supported on HT were prepared and catalytic activity was investigated with different metal ratios as well as for different capping agents. Firstly, A series of bimetallic Au- and Pd- containing heterogeneous catalysts were synthesized by a polyol reduction route and studied for their catalytic activity, structural and electronic properties. It was found that admixing of Pd to Au resulted in increased activity and selectivity of HCA reaching a maximum of 81% HCA yield at 87% HDO conversion with Au₄₀Pd₆₀-DDAO/HT at 353 K. The monometallic Au and Pd showed low activities, suggesting the importance of synergistic interaction between Au and Pd in reactivity. Spectroscopic analyses using UV-Vis, TEM, XPS and X-ray absorption (XAS) have been performed to explain the superior activity of the reusable Au₄₀Pd₆₀-DDAO/HT. In UV-Vis spectroscopy, the diminishment of SPR peak of Au in bimetallic catalysts hints the existence of Au-Pd interactions. The lower BEs in XPS for both Au 4f and Pd 3d in Au₄₀Pd₆₀-DDAO NPs as compared to their

monometallic counterparts are attributed to the electron exchanges among Au, Pd and/or DDAO. XAS analyses in Au-L₃, Pd-K and Pd-L₃ edge also supported the strong correlation between Au and Pd in Au₄₀Pd₆₀-DDAO/HT. It could be inferred that the Au-Pd alloy center plays crucial role in the significant catalytic performance for selective oxidation of HDO toward HCA. Further, the role of capping agent was explored by comparing the catalytic activity of Au₄₀Pd₆₀-DDAO/HT with Au₄₀Pd₆₀-PVP/HT and Au₄₀Pd₆₀-PVA/HT. The spectroscopic analysis informed that the electronegativity of Au and extent of Au-Pd metal bond formation (alloying between Au and Pd) can be tuned by changing capping agent. It was noticed that with DDAO as capping agent moderate electronegative Au species with a few Au-Pd metal bond formation occurs, which makes the highly active and selective catalytic sites for formation of mono-hydroxycarboxylic acid from oxidation of long chain aliphatic diols.

In **Chapter 5**, for establishing the scope of Pd/ZrP in other organic reactions, a convenient and highly chemoselective approach was developed for base-free catalytic transfer hydrogenation (CTH) reactions of nitroarenes under environmentally-benign conditions using FA and Pd/ZrP as a hydrogen source and a reusable heterogeneous catalyst, respectively, which account for the versatility of Pd/ZrP catalyst. It was found that 2 wt% Pd/ZrP catalyst (20 mg) with 3 eq. of FA provided >99% yield and selectivity of aniline at 313 K in ethanol (5 mL) for 2 h. Applicability of the Pd/ZrP catalyst was also explored for hydrogenations of various substituted nitroarenes. The Pd/ZrP catalyst showed the high specificity for hydrogenation of nitro group even in the presence of other reducible functional groups such as -C=C-, -COOCH₃, and -C≡N. This motivated me to investigate the reaction mechanism using Hammett plot of *p*-substituted nitroarenes. The ρ value which was found to be of -1, indicates that the reaction is sensitive to substituents

and positive charge is generated during the reaction *i.e.* cationic intermediate. Characterization of fresh and spent Pd/ZrP catalyst *via* XRD and TEM suggested that the active site is *in-situ* generated Pd(0) species. A plausible reaction mechanism has been proposed based on the experimental analysis and catalyst characterization. The Pd/ZrP catalyst was found to be reusable at least up to 4 times maintaining the same high activity and selectivity.

The overall summary of the thesis can be presented in pictorial form in **Figure 1**.

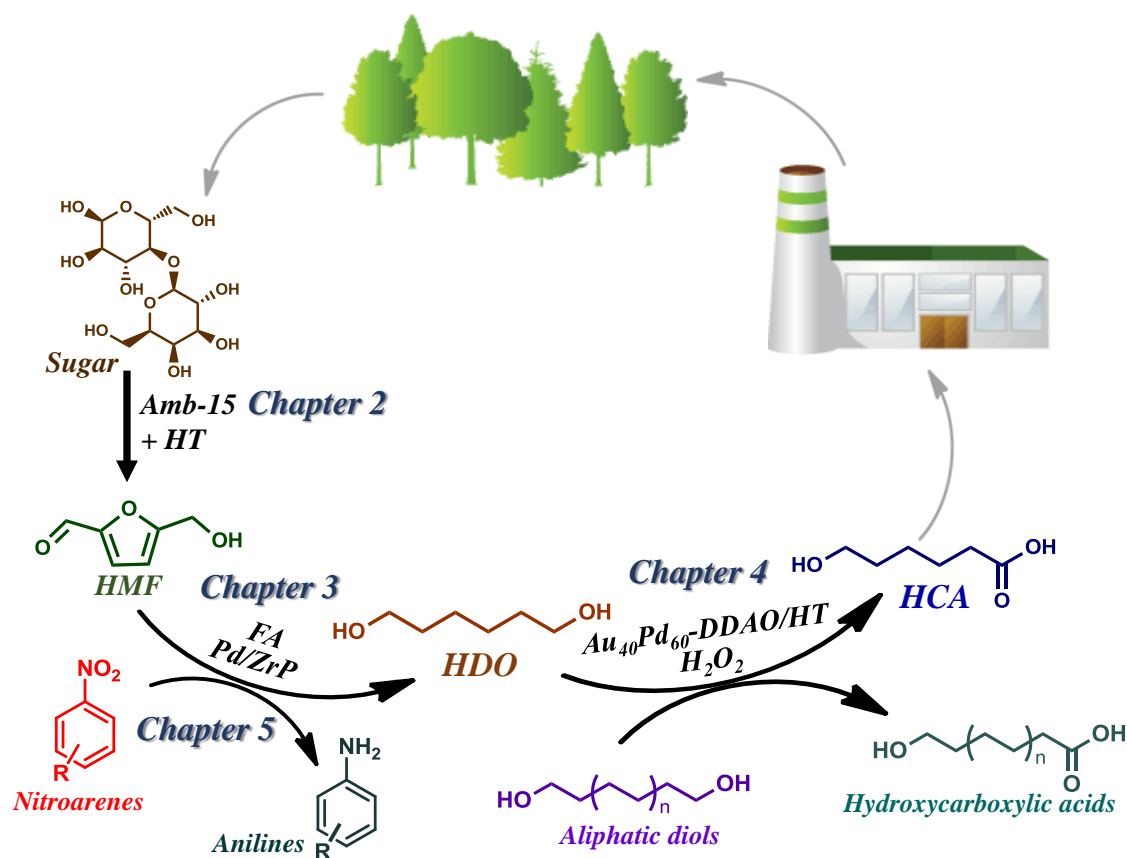


Figure 1: Summary of thesis

Outlook

Contribution to catalytic science and technology

Significant improvements or novel strategies have been developed in this thesis for the more efficient and economical utilization of woody biomass. These novel strategies will play a significant role in the implementation of biomass technology to replace fossil fuel energy sources. Four main approaches have been envisioned for the valorisation of biomass resources in this thesis. Firstly, “*one-pot synthesis*” used for converting sugar moieties to furan compounds, is proved to be highly attractive and viable approach. This pathway allows the application of all kinds of saccharides (mono- and di-) and mixture of saccharides.

The second approach involves the complete substitution of bulk chemicals by biomass based platform chemicals. Production of industrially 1,6-hexanediol (HDO) which was till date dependent of the fossil fuel resources, can now be produced from HMF by applying “*Brønsted acid mediated ring opening hydrogenolysis of HMF*”. This new reaction pathway for synthesis of HDO from renewable sources ultimately leads to process requiring fewer steps, in agreement with the principles of green chemistry. This particular process requires liquid hydrogen source instead of high pressured hydrogen which makes it economically more viable and easy to handle.

The third approach is “*selective oxidation of long chain aliphatic diols*” taking the advantage of the selective formation of 6-hydroxycaproic acid (HCA, monomer of polycaprolactone) in high yields from HDO over heterogeneous catalyst. So far, the existing catalytic systems typically focused on the selective oxidation of short carbon chain (C2-C5) diols. On the other side long chain aliphatic diol systems remained

untouched, on account of it is difficult in achieving high selectivity for mono-oxidation. In this respect, the novel catalytic system designed in this chapter *i.e.* *N,N*-dimethyldodecylamine *N*-oxide (DDAO) stabilized AuPd-bimetallic nanoparticles (NPs) supported on hydrotalcite (HT) as heterogeneous catalyst with aq H₂O₂ as greener oxidant represents a major advancement in the current catalytic technology.

The last approach which has been developed is “*base-free catalytic transfer hydrogenation (CTH) of nitroarenes*”. It is well understood that employment of liquid hydrogen source offers much advantages as compared to the gaseous hydrogen. The drawback which chemical industry facing till date is the use of homogeneous base as co-promoter while utilizing liquid hydrogen donor, which basically resulted in the waste generation and cost of the application. Thus keeping in mind the facts, an efficient methodology is developed for CTH using formic acid as reducing agent over Pd/ZrP as heterogeneous catalyst under base-free conditions.

Application of these newly investigated strategies in industrial production of polycaprolactone will be a great impact to the chemical industry. This is the first report on the synthesis of 6-hydroxycaproic acid from renewable source HMF in just two steps, whereas the current process needs six steps from fossil fuel-based benzene. The new process for polycaprolactone production will be economical, free from any kind of toxicity and dependent on completely renewable energy source based on these findings. Furthermore, a new catalytic CTH methodology will be developed using bio-based formic acid as hydrogen source over reusable Pd/ZrP catalyst. The chemoselective, eco-friendly, cost-effective methodology which can work under base-free conditions will give a new direction of CTH reactions.

Scope from thesis

In this thesis, new pathways have been developed to produce important industrial commodities directly from inedible biomass-resources employing novel heterogeneous catalytic systems. The rapidly growing field of furan synthesis from carbohydrates holds a great promise for the future. Current solid acid base pair of Amberlyst-15 and HT shows remarkable advantages for the batch reactor. Consequently, future research should target on the flow reactor for the realistic large scale processes.

In case of Pd/ZrP catalyzed hydrogenolytic ring opening of HMF to HDO, further studies could be investigated for the ring opening hydrogenolysis of fufural to 1,5-pentanediol and valerolactone to methyl-3-pentenoate.

The selective oxidation of HDO to HCA with DDAO stabilized AuPd NPs supported on HT opens a new general route for selective oxidation of long chain aliphatic diols. Thus, selective oxidation of >C6 diol system can be explored in near future with DDAO stabilized bimetallic NPs supported catalysts.

Zirconium phosphate (ZrP, heterogeneous acidic support) possessing high amount of Brønsted acid sites showed excellent activity for selective catalytic transfer hydrogenation (CTH) of nitroarenes. Further application of ZrP could be evaluated for other Brønsted acid catalyzed reactions such as HMF to levulinic acid, CTH of -C=C-, -C=O-, -C≡N and -C≡C moieties to develop noble route in modern organic synthesis.

List of Accomplishments

List of publications related to this thesis (peer-reviewed):

1. **Java Tuteja**, Shun Nishimura and Kohki Ebitani
“Effect of Capping Agent on Interaction of Au and Pd in AuPd- Bimetallic Catalysts for the Selective Oxidation of 1,6-hexanediol”
To be Submitted. (Chapter 4)
2. **Java Tuteja**, Shun Nishimura, Hemant Choudhary and Kohki Ebitani
“Selective Oxidation of 1,6-Hexanediol to 6-Hydroxycaproic acid over Reusable Hydrotalcite Supported AuPd Bimetallic Nanoparticle Catalysts”
ChemSusChem, *in Press*, DOI: 10.1002/cssc.201500255. (Chapter 4)
3. **Java Tuteja**, Shun Nishimura and Kohki Ebitani
“Base-free Chemoselective Transfer Hydrogenation of Nitroarenes to Anilines with Formic Acid as Hydrogen Source by Reusable Heterogeneous Pd/ZrP Catalysts”
RSC Advances, **2014**, 4, 38241-38249. (Chapter 5)
4. **Java Tuteja**, Hemant Choudhary, Shun Nishimura and Kohki Ebitani
“Direct Synthesis of 1,6-Hexanediol from HMF over a Heterogeneous Pd/ZrP Catalyst using Formic Acid as Hydrogen Source”
ChemSusChem, **2014**, 7, 96-100. (Chapter 3)
[\[Selected Top 25 for Most Accessed Article 11/2013-10/2014\]](#)
5. **Java Tuteja**, Shun Nishimura and Kohki Ebitani
“One-pot Synthesis of Furans from Various Saccharides using Combination of Solid Acid and Base Catalysts”
Bull. Chem. Soc. Jpn., **2012**, 85, 275-281. (Chapter 2)
[\[Selected as BCSJ Award Article\]](#)

Patent related to this thesis:

1. Kohki Ebitani, Shun Nishimura, **Jaya Tuteja**, Hemant Choudhary
"Reduction Catalyst, Synthesis of 1,6-hexanediol, synthesis of amino-benzene compounds"
JP patent Application No. 2013-215678.
2. Kohki Ebitani, Shun Nishimura, **Jaya Tuteja**, Hemant Choudhary
"Metal supported catalyst, Catalyst material and Synthesis method of hydroxy-fatty-acids"
JP Patent Application No. 2015-069723.

List of international conferences related to this thesis (peer-reviewed):

1. **Jaya Tuteja**, Shun Nishimura and Kohki Ebitani
"Effect of Capping Agent on AuPd Bimetallic Catalysts for the Selective Oxidation of 1,6-Hexanediol"
The 15th Korea - Japan Symposium on Catalysis, Busan, Republic of Korea, 2015.05.26. [[Young-Oral](#)]
2. **Jaya Tuteja**, Shun Nishimura and Kohki Ebitani
"Pd/ZrP-Catalyzed Transfer Hydrogenation Reactions using Formic Acid as Hydrogen Source"
22nd IUPAC Conference on Physical and Organic Chemistry (ICPOC 22), Ottawa, Canada, 2014.08.11. [[Oral](#)]
3. **Jaya Tuteja**, Shun Nishimura and Kohki Ebitani
"Convenient Pd/ZrP-Catalyzed Dissociation of Formic Acid for the Selective Hydrogenations"
JAIST Japan-India Symposium on Automotive Technologies (Energy, Fuel and Plastics), Nomi, Ishikawa, Japan, 2014.08.05. [[Oral](#)]

4. **Jaya Tuteja**, Shun Nishimura and Kohki Ebitani
“Selective Transfer Hydrogenations of HMF and Nitroarenes using Formic Acid as Reducing Agent over Heterogeneous Pd/ZrP Catalyst”
The Seventh Tokyo Conference on Advanced Catalytic Science and Technology (TOCAT7),
Kyoto, Japan, 2014.06.03. [\[Poster\]](#)
5. **Jaya Tuteja**, Hemant Choudhary, Shun Nishimura and Kohki Ebitani
“Ring opening of HMF to produce 1,6-hexanediol over Pd/zirconium phosphate catalyst using formic acid as hydrogenating agent”
247th ACS National Meeting & Exposition,
Dallas, Texas, USA, 2014.03.20. [\[Oral\]](#)
6. Kohki Ebitani, Hemant Choudhary, **Jaya Tuteja**, Pham Anh Son and Shun Nishimura
“Transformations of Biomass-derived Compounds into Useful Chemicals using Heterogeneous Catalytic Systems”
International Conference on Advances in Biotechnology and Bioinformatics (ICABB 2013),
Pune, India, 2013.11.25. [\[Oral-invited\]](#)
7. **Jaya Tuteja**, Hemant Choudhary, Shun Nishimura and Kohki Ebitani
“Pd/ZrP Catalyzed Hydrogenolytic Ring Opening of HMF to 1,6-Hexanediol Using Formic Acid as Hydrogen Donor” International Symposium on Advanced Materials 2013,
Nomi, Ishikawa, Japan, 2013.10.17. [\[Poster\]](#)
8. Kohki Ebitani, Saumya Dabral, **Jaya Tuteja** and Shun Nishimura
“One-Pot Conversions of Sugars into Furfurals and Sugar Alcohols Using Heterogeneous Catalysts”
7th International Symposium on Acid-Base Catalysis (ABC-7)
Tokyo, Japan, 2013.05.14. [\[Oral\]](#)

9. **Jaya Tuteja**, Shun Nishimura and Kohki Ebitani

“One-pot conversion of sugars to furans by combination of heterogeneous acid & base catalysts”

Pure and Applied Chemistry International Conference 2013 (PACCON 2013),
Chon Buri, Thailand, 2013.1.24. [\[Oral\]](#)

10. **Jaya Tuteja**, Shun Nishimura, Kohki Ebitani

“One-pot Conversion of Saccharides to Furfurals over Combination of Solid acid-base Catalysts”

The Asia-Pacific Interdisciplinary Research Conference 2011 (APIRC 2011),
Toyohashi University of Technology, Japan, 2011.11.17. [\[Poster\]](#)

Awards and Grants related to this thesis

1. 2014 JAIST Research Grant for Students (Ottawa, Canada, 462,000 JPY)
(Grant for a conference participation)
2. 2013 JAIST Research Grant for Students (Dallas, USA, 323,000 JPY)
(Grant for a conference participation)
3. 2012 JAIST Research Grant for Students (Chon Buri, Thailand, 180,000 JPY)
(Grant for a conference participation)
4. BCSJ (Bulletin of the Chemical Society of Japan) Award, The Chemical Society of Japan, 2012.
5. Graduate Research Program Scholarship from July 2012- June 2015. (2,700,000 JPY).
6. Selected for International Exchange Programme Scholarship 2011-2012.
(1,752,000 JPY)